

## INFORMATION TO USERS

This manuscript has been reproduced from the microfilm master. UMI films the text directly from the original or copy submitted. Thus, some thesis and dissertation copies are in typewriter face, while others may be from any type of computer printer.

**The quality of this reproduction is dependent upon the quality of the copy submitted.** Broken or indistinct print, colored or poor quality illustrations and photographs, print bleedthrough, substandard margins, and improper alignment can adversely affect reproduction.

In the unlikely event that the author did not send UMI a complete manuscript and there are missing pages, these will be noted. Also, if unauthorized copyright material had to be removed, a note will indicate the deletion.

Oversize materials (e.g., maps, drawings, charts) are reproduced by sectioning the original, beginning at the upper left-hand corner and continuing from left to right in equal sections with small overlaps. Each original is also photographed in one exposure and is included in reduced form at the back of the book.

Photographs included in the original manuscript have been reproduced xerographically in this copy. Higher quality 6" x 9" black and white photographic prints are available for any photographs or illustrations appearing in this copy for an additional charge. Contact UMI directly to order.

# UMI

A Bell & Howell Information Company  
300 North Zeeb Road, Ann Arbor MI 48106-1346 USA  
313/761-4700 800/521-0600



DEVELOPMENT OF A SPATIALLY DISTRIBUTED  
MODEL OF ARCTIC THERMAL AND HYDROLOGIC PROCESSES (MATH)

A  
DISSERTATION

Presented to the Faculty of the University of Alaska  
in Partial Fulfillment of the Requirements  
for the Degree of

DOCTOR OF PHILOSOPHY

By

Ziya Zhang, B.S., M.S.

Fairbanks, Alaska

May 1998

**UMI Number: 9838842**

---

**UMI Microform 9838842**  
**Copyright 1998, by UMI Company. All rights reserved.**

**This microform edition is protected against unauthorized  
copying under Title 17, United States Code.**

---

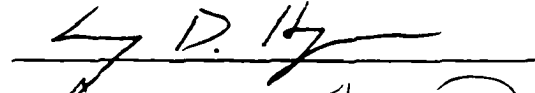
**UMI**  
**300 North Zeeb Road**  
**Ann Arbor, MI 48103**

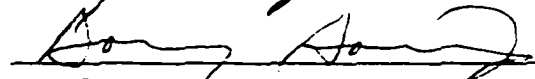
DEVELOPMENT OF A SPATIALLY DISTRIBUTED  
MODEL OF ARCTIC THERMAL AND HYDROLOGIC PROCESSES (MATH)

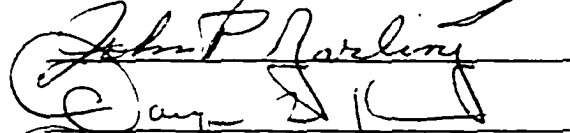
By

Ziya Zhang

RECOMMENDED:



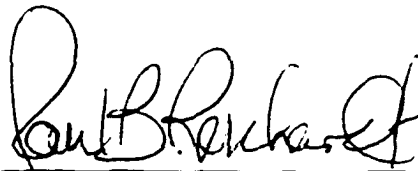




Advisory Committee Chair

  
Department Head

APPROVED:



Dean, College of Science, Engineering  
and Mathematics



Dean of the Graduate School

4-10-98

Date

## Abstract

A process based, spatially distributed hydrologic model with the acronym MATH (Model of Arctic Thermal and Hydrologic Processes) is constructed to quantitatively simulate the energy and mass transfer processes and their interactions within arctic regions. The impetus for development of this model was the need to have spatially distributed soil moisture data for use in models of trace gas fluxes (carbon dioxide and methane) generated from the carbon-rich soils of this region. The model is applied against the data from the Imnavait watershed (2.2 km<sup>2</sup>) and the Upper Kuparuk River basin (146 km<sup>2</sup>) located on the North Slope of Alaska. Both point and spatially distributed data such as precipitation, radiation, air temperature, and other meteorological data have been used as model inputs.

Based on the digital elevation data, one component of the model determines drainage area, channel networks, and the flow directions in a watershed that is divided into many triangular elements. Simulated physical processes include hydraulic routing of subsurface flow,

overland flow and channel flow, evapotranspiration (ET), snow ablation, and active layer thawing and freezing. This hydrologic model simulates the dynamic interactions of each of these processes and can predict spatially distributed snowmelt, soil moisture, and ET over a watershed at each time step as well as discharge at any point(s) of interest along a channel.

Modeled results of spatially distributed soil moisture content, discharge at gauging stations and other results yield very good agreement, both spatially and temporally, with independently derived data sets, such as Synthetic Aperture Radar (SAR) generated soil moisture data, field measurements of snow ablation, measured discharge data and water balance computations. The timing of simulated discharge results do not compare well to the measured data during snowmelt periods because the effect of snow damming on runoff generation is not considered in the model. It is concluded that this model can be used to simulate spatially distributed hydrologic processes within the arctic regions provided that suitable data sets for input are available. This

physically based model also has the potential to be coupled with atmospheric and biochemical models.



## Table of Contents

<u>Titles</u>	<u>Pages</u>
Abstract .....	3
List of Figures .....	10
List of Tables .....	16
Acknowledgments .....	17
Chapter I. Introduction .....	19
Chapter II. Literature Review .....	25
Chapter III. Site Description .....	55
3.1 Introduction .....	55
3.2 Kuparuk River Basin .....	55
3.3 Upper Kuparuk River Basin .....	59
3.4 Imnavait Watershed .....	61
3.5 Data Collection .....	65
Chapter IV. Model Development .....	68
4.1 Introduction .....	68
4.2 Topographic Delineation of a Watershed .....	72
4.2.1 Basic Unit/Element of Watershed .....	72

4.2.2	Flow Direction and Channel Networks	75
4.2.3	Flat Area Considerations	80
4.3	Results of Geometric Analysis	81
4.3.1	Channel Network and Analysis	81
4.3.2	Water Tracks	83
4.3.3	Drainage Area	87
4.4	Description of Physical Processes	88
4.4.1	Snowmelt	88
4.4.1.A.	Surface Energy Balance	91
4.4.1.B.	Degree-Day Method	98
4.4.2	Evapotranspiration	99
4.4.2.A.	Energy Balance Method	99
4.4.2.B.	Priestley-Taylor Method	101
4.4.3	Flow Routing	103
4.4.3.A.	Subsurface Flow Routing	103
4.4.3.B.	Overland Flow Routing	106
4.4.3.C.	Channel Flow Routing	110
4.5.	Discussions	112
4.6.	Conclusions	120

Chapter V.	Data Input for the Model	.....122
5.1.	Meteorological Data	.....122
5.2.	Parameters	.....135
5.3.	Model Execution/Computational Notes	.....135
Chapter VI.	Model Applications	.....142
6.1.	Introduction	.....142
6.2.	Study Area	.....144
6.2.1.	Imnavait Watershed	.....144
6.2.2.	Upper Kuparuk River Basin	.....146
6.3.	Results of Physical Processes	.....147
6.3.1.	Snowmelt	.....147
6.3.2.	Evapotranspiration (ET)	.....155
6.3.3.	Flow Routing and Moisture Content Simulation	.....160
6.3.3.A.	Subsurface Flow Routing	.....160
6.3.3.B.	Overland Flow Routing	.....163
6.3.3.C.	Channel Flow Routing	.....164
6.4.	Discussions	.....166
6.4.1.	Moisture Distribution and Hydrographs...	166

6.4.2. Data Input .....	177
6.4.3. Other Issues .....	180
6.4.4. Model Weaknesses .....	182
6.5. Conclusions .....	183
Chapter VII. Summary .....	186
7.1. About the Model .....	186
7.2. About the Results .....	193
7.3. Conclusions .....	201
References .....	206

## List of Figures

Figure 3-1. Kuparuk River Basin and major meteorological and gauging stations .....	56
Figure 3-2. Map of Upper Kupa-ruk River Basin with location of gauging stations and meteorological stations .....	60
Figure 3-3. Map of Imnavait watershed and Water Track 7 with location of gauging stations and a meteorological station .....	62
Figure 4-1. Triangular elements used in the model (a) and node notation (b) .....	74
Figure 4-2. Three possible flow cases for each element .....	77
Figure 4-3. Flow direction (a) and partitioning of flow through element boundaries (b) .....	78
Figure 4-4. Flow pattern for channel segments (a) and ridge (watershed) divides (b) .....	79
Figure 4-5. Channel network and stream orders of the Imnavait watershed, Alaska, generated by model .....	84

Figure 4-6. Channel network and stream orders of the Upper Kuparuk River basin, Alaska, generated by model .....	85
Figure 4-7. Hydrologic and thermal processes modeled for every element within an arctic watershed .....	89
Figure 4-8. Representation of active layer and permafrost in the model .....	104
Figure 4-9. Overland flow components within an element .....	108
Figure 4-10. Channel flow cross section .....	108
Figure 5-1. Measured radiation fluxes at a station within Imnavait watershed, 1993 .....	124
Figure 5-2. Seasonal variation of measured hourly air temperature at a station within Imnavait watershed, 1993 .....	125
Figure 5-3. Measured hourly wind speed at a station within Imnavait watershed, 1993 .....	127
Figure 5-4. Measured precipitation and relative humidity at a station within Imnavait watershed, 1993 .....	128

Figure 5-5. Hourly precipitation distribution (mm/hour) at June 24 (noon), 1996, at Upper Kuparuk River basin, Alaska .....	129
Figure 5-6. Hourly precipitation distribution (mm/hour) at August 15 (noon), 1996, at Upper Kuparuk River basin, Alaska .....	130
Figure 5-7. Wind speed distribution (m/s) June 24 (noon), 1996, at Upper Kuparuk River basin, Alaska .....	131
Figure 5-8. Wind speed distribution (m/s) August 15 (noon), 1996, at Upper Kuparuk River basin, Alaska .....	132
Figure 5-9. Air temperature distribution (°C) on June 24 (noon), 1996, at Upper Kuparuk River basin, Alaska .....	133
Figure 5-10. Air temperature distribution (°C) on August 15 (noon), 1996, at Upper Kuparuk River basin, Alaska .....	134

- Figure 6-1. Comparison of snowmelt between energy balance and degree-day methods and average measured data, Imnavait watershed, Alaska, 1993 .....152
- Figure 6-2. Initial snow distribution at May 10, 1994 (a) and modeled snow distribution after four days of melting (b) at Imnavait watershed, Alaska, 1994 .....154
- Figure 6-3. Initial snow distribution at May 21, 1996 (a) and modeled snow distribution after six days of melting (b) at Upper Kuparuk basin, Alaska, 1996 .....156
- Figure 6-4. Comparison between measured pan evaporation and calculated basin averaged evapotranspiration using energy balance model and Priestley-Taylor model, Imnavait watershed, Alaska, 1993 .....159
- Figure 6-5. Simulated evapotranspiration distribution for one hour at June 12, 1994, Imnavait watershed, Alaska .....161
- Figure 6-6. Modeled soil moisture content distribution (a) and SAR imagery of soil moisture content



distribution (b) of Imnavait watershed, Alaska, at noon, August 2, 1993 .....	168
Figure 6-7. Modeled soil moisture content distribution (a) and SAR imagery of soil moisture content distribution (b) of Upper Kuparuk basin, Alaska, at 13:00, August 15, 1996 .....	169
Figure 6-8. Comparison of simulated and measured discharges and cumulative volume of simulated and measured discharges at Imnavait Creek, Alaska, 1993 .....	171
Figure 6-9. Comparison of simulated and measured discharges and cumulative volume of simulated and measured discharges at Imnavait Creek, Alaska, 1994 .....	172
Figure 6-10. Comparison of simulated and measured discharges and cumulative volume of simulated and measured discharges at Upper Kuparuk River, Alaska, 1996 .....	173
Figure 6-11. Comparison of various hydrologic components that were measured and simulated for Imnavait and Upper Kuparuk watersheds .....	176

Figure 7-1. Classification of watershed models .....	187
Figure 7-2. Classification of models based on space and time scales .....	188
Figure 7-3. Classification of models based on solution techniques .....	189
Figure 7-4. Flow chart of the water flow computations in the hydrologic model .....	192
Figure 7-5. Comparison of soil moisture distribution along a transect within Imnavait watershed, Alaska, June 12, 1993 .....	196
Figure 7-6. Comparison of soil moisture distribution along a transect within Imnavait watershed, Alaska, July 25, 1994 .....	197

**List of Tables**

Table 5-1. Parameters used in the model .....136

Table 5-2. Definition of variables and units used in  
model .....137

## Acknowledgments

The success of this project is due in a large extend to the effort of two men who I feel fortunate and thankful to have as my advisors. Dr. Douglas L. Kane was the main driving force behind this dissertation. His experience, and expectation of excellence proved to be the key factor to my finishing this project. Dr. Larry D. Hinzman has spent countless effort to guide me during the research. His broad knowledge, and willingness to help were necessary for the completion and success of the project. Drs. Douglas J. Goering, and John P. Zarling served on my committee and significantly impacted the focus of my degree program and the quality of this manuscript. I would like to thank Drs. Douglas J. Goering, and Don Morton for their help and suggestions on the computer code optimization and management.

Because of the nature of this project, lots of different kinds of data were collected and analyzed. Many thanks to Elizabeth K. Lilly, Robert E. Gieck, and George "Bub" Mueller for their help and effort on these processes. I would also like to thank Yuwu Zhang, James

P. McNamara, Johnny Mendez, Neil Meade, Ronald Rovansek, David Robinson, Melissa Tendick and Jennifer Clark for their involvement in this project.

Special thanks go to a friend of mine, Huan V. Luong. His encouragement, sense of humor, and countless help both in my life and work will be remembered.

Finally, I would like to thank my wife, Jing, and my son, Jun Jun. Their patience, support and help throughout this study were invaluable.

This work was supported by the U.S. National Science Foundation under the Arctic System Science (ARCSS) Land Atmosphere Ice Interactions (LAI) Program (Grant Nos. OPP-9214927 and OPP-9318535).

## Chapter I. Introduction

In Arctic ecosystems, hydrologic and thermal processes differ from those in more temperate regions, primarily due to the influence of cold temperatures and large annual variation in solar radiation on the physical, biological and chemical systems. As a result, the water cycle is altered from the traditional perspective. In the Arctic, snow accumulation, redistribution of snow by wind, and snow ablation are important hydrologic events each winter. Perhaps the most unique characteristic of the Arctic is the existence of permafrost and the active layer on top of it. Continuous permafrost acts as an impermeable boundary to subsurface flow, restricting subsurface flow to the shallow active layer at the surface. The soil thermal and hydrologic properties change throughout most of the year because of the active layer's continual thawing and freezing, as well as changes in moisture content in the thawed portion of the soil profile. The long, severe cold winters and short summers with both low precipitation and temperature characterize this harsh arctic environment. All these special

characteristics that are unique to the Arctic need to be studied and quantified to truly understand the interactions between atmospheric and both terrestrial and aquatic systems.

Past interest in arctic hydrologic processes has been driven by resource development. However, there are more and more people interested in this environment for reasons other than resource development; such as, the fact that the arctic environment is fragile, more sensitive to climate change than more temperate environments [IPCC, 1992], and does play an important role in earth's climate [Alley, 1995]. Global climate models indicate that global warming induced by the greenhouse effect will be most acute in polar regions, likely resulting in changes in extent of sea ice, increased thawing of permafrost, and melting of polar ice masses, with profound societal impacts around the globe [IPCC, 1992]. A changing climate could induce numerous hydrologic and energy changes that could augment or retard global climate change and significantly impact arctic ecosystems [Kane and

*Hinzman, 1992; Manabe and Stouffer, 1980; Schlesinger and Mitchell, 1985; Roots, 1989*].

Hydrologic and thermal processes in the Arctic have a great influence on many global processes such as atmospheric and oceanic circulation [Alley, 1995]. It is believed that interactions among soil moisture, air temperature and vegetation type will impact future trace gas fluxes of CO<sub>2</sub> and CH<sub>4</sub> from the Arctic [Weller et al., 1995; Oechel et al., 1993; Burton et al., 1996]. So, the spatial information on water movement and soil moisture is very important for climate research. A quantitative understanding of the linkages between atmospheric, terrestrial and aquatic systems can improve our knowledge of regional and global climate change. Development of a process based, spatially distributed hydrologic model would provide a tool for doing this.

Researchers have developed models of different aspects of arctic hydrology [Kane et al., 1990, 1991a, 1993; Hinzman et al., 1991; Baracos et al., 1981; Ohmura 1982; Marsh and Woo, 1979; Woo 1982, 1983, 1986]. However until this point, a process based, spatially distributed hydrologic and thermal model for the Arctic



has not yet been developed. Such a model should cover all of the important aspects of arctic hydrologic processes and their interactions. Also, it should help us better understand the arctic system and provide crucial information for gas flux modeling as well as regional and global climate modeling.

In this dissertation, a process based, spatially distributed hydrologic model (acronym MATH model) is developed and verified against data from the North Slope of Alaska at different watershed scales. Two hypotheses of this study are: 1) a process based, spatially distributed hydrologic model can be developed that will accurately predict arctic hydrologic and thermal processes and their interactions, and 2) this spatially distributed model can be used to simulate hydrologic and thermal processes in watersheds at vary watershed scales. It is also suggested that this model will be designed such that it can produce distributed data that is relevant for other models and researchers.

A literature review of hydrologic modeling, with emphasis on applications in northern regions is presented in Chapter II. A nested watershed on the

North Slope of Alaska has been the subject of model applications. The site description, which includes geomorphology, meteorological characteristics and field projects within each watershed, are discussed in Chapter III.

Chapter IV details the model development. Watershed delineation including the determination of flow direction within each element, channel network structure over a watershed, and drainage area is addressed followed by simulations of physical processes in the watershed. These physical processes include snowmelt, active layer freezing and thawing, evapotranspiration (ET) and routing of subsurface flow, overland flow and channel flow.

Different data inputs and parameters are needed to drive the model. In Chapter V, a description of parameters used and how they were obtained is presented. Digital Elevation Model (DEM) data are used to define the watershed morphology. Finally a discussion of the massive amounts of input data, such as precipitation, radiation and meteorologic variables necessary for

conducting energy and mass balance computations in the model are discussed.

In Chapter VI, the results from applying the model to watersheds at two different scales are presented. Simulated modeling results from MATH are compared with field and remotely derived measurements such as stream flow, soil moisture (SAR satellite imagery), ablation, and water balance calculations.

In Chapter VII, MATH model performance and results are discussed and finally the conclusions are presented.

## Chapter II. Literature Review

Hydrological models are divided broadly into two groups, deterministic and stochastic. Deterministic models seek to simulate the physical processes for the catchment involved in the transformation of rainfall to streamflow, whereas stochastic models describe the hydrological time series of the several measured variables such as rainfall, evaporation and streamflow, utilizing probability distributions [Shaw, 1994]. Most models, both deterministic and stochastic, deal principally with movement, distribution, and storage of water as vapor, liquid and/or solid. General considerations in hydrologic modeling may include such specifications as governing equations, geometry, space-time structure of sources and sinks, initial and boundary conditions, scale in time, space, or frequency, availability of data, model complexity and detail in results, accuracy, economic constraints, and generalizations [Singh, 1989]. The significance of these considerations depends upon a particular problem and may vary from one situation to another.

Hydrological models can also be classified as lumped or distributed models according to spatial characteristics of system variables and parameters. A model is lumped if its variables and parameters are lumped, i.e., the spatial variability of them are ignored; it is distributed if the spatial variability of the variables and parameters are considered. *Becker* [1973] distinguished two classes of distributed models that account for spatial variability in input variables or system parameters. One is the probability-distributed model and the other is the geometrically distributed model. A probability-distributed model describes spatial variability without reference to the geometrical configuration of the points in the network at which an input variable such as rainfall is measured or estimated. Whereas, a geometrically distributed model considers spatial variability in terms of the relative location of the network points. It treats a watershed not as a random assembly of different parts but a system whose parts are related to each other by their common geomorphological history.

To accurately predict hydrologic processes is a long pursuit of hydrologists. Different hydrologic models have been developed in last two decades. Some models are event-based simulations models [Smith and Lumb, 1966; Huggins and Monke, 1968, 1970; Metcalf & Eddy, Inc. et al., 1971; Williams and Hann, 1972; Dawdy et al., 1972] and some are continuous streamflow models [Crawford et al., 1966; Cermak, 1979; Holtan et al., 1975; Bergström, 1976; Abbott et al., 1986; Charbonneau et al., 1977; Refsgaard, 1981; Beven and Kirkby, 1979; Grayson et al., 1992; Wigmosta et al., 1994; Jackson et al., 1996; Kite, 1989]. Some models were developed from the unit hydrograph theory [Nash, 1957; Maddaus and Eagleson, 1969]. Some models use conceptual modeling where the hydrological processes within are described mathematically and the storages are considered as reservoirs [Bergström, 1976]. Each model has its own characteristics, conditions, emphasis, and limitations.

The Hydrologic Engineering Center [1981] developed the HEC-1 flood hydrograph model to simulate the direct runoff hydrograph due to precipitation by representing the watershed with interconnected hydrologic and

hydraulic components. In addition, the model has options for multiplan-multiflood analysis, dam-break simulation, economic assessment of flood damage, and optimal sizing of flood control systems. This model has been extended to determining discharge-frequency relationships for ungauged watersheds [*Hydrologic Engineering Center, 1982*]. Many components of a simulation are modeled using different options [*Singh, 1989*]. Infiltration is estimated using options such as initial and uniform loss rate, exponential loss rate, SCS curve-number method, and Holtan's infiltration equation. The unit hydrograph and the kinematic wave methods are used to estimate the direct runoff hydrograph. The storage flow routing is conducted by the conic method, normal-depth storage and outflow, and modified Puls method. Whereas the channel flow routing is simulated by the lag and route and Muskingum methods. This model is one of the most commonly used models in the United States and can be used for hydrologic analyses under a wide variety of conditions [*Feldman, 1981*].

The SCS TR-20 model was developed by the Soil Conservation Service [1973] for inclusion of hydrologic processes in project formulation. The model uses the SCS dimensionless hydrograph method to estimate surface runoff resulting from synthetic or natural rainfall, which is then routed through stream channels using the convex method and through reservoirs using the storage indication method. It combines the routed hydrograph with the hydrographs from other tributaries and produces the flow rates, their times of occurrence, and their water-surface elevations at any desired cross section or hydraulic structure. The model provides for continuous analyses of nine different storms over a watershed under existing conditions and with various combinations of land-treatment floodwater-retarding structures and channel improvements. These routings can be performed for as many as 120 reaches and 60 structures in one continuous run. The model has the flexibility to accommodate other aspects of watershed planning, provision of input data and use of engineering judgment [Kent, 1966].



*Dawdy et al.* [1972] developed a parametric rainfall-runoff simulation model (USGS model) for estimation of flood volume and rates of runoff from small drainage basins. The model uses point rainfall and daily potential evapotranspiration data as its input. If more rain gauges are available, then their records can be combined by the Thiessen polygon method to produce mean distributed rainfall. A soil-moisture accounting is employed, considering infiltration, soil moisture accretion, and depletion, to determine the effect of antecedent conditions on infiltration. The flood-routing method developed by Clark [1945] is used to develop the basin unit hydrograph. The model has been modified to accommodate urban watersheds [*Dawdy et al.*, 1978; *Doyle and Miller*, 1980; *Doyle*, 1981].

A problem-oriented computer language for building hydrologic models was developed by *Williams and Hann* [1972]. The resulting model, HYMO, was designed for planning flood-prevention projects, forecasting floods, and research studies. The model transforms rainfall data into runoff hydrographs using a two-parameter gamma distribution like the Nash model [*Nash*, 1957], wherein

the parameters are estimated from their relationships with watershed area, slope and length-width ratio. Flows can be routed through both streams and/or reservoirs. Streamflow routing is conducted by using the variable storage coefficient method and reservoir flow routing is carried out by using the storage-indication method. Manning's equation is used to compute the normal flow-rating curve. The model is simple and flexible, but its scope is limited to flood routing.

The storm-water management model (SWMM), developed by *Metcalf & Eddy, Inc. et al.*, [1971], was originally designed to represent urban storm water runoff for purposes of assisting administrators and engineers in the planning, evaluation, and management of overflow abatement alternatives. The model has been modified to accommodate rural watersheds. It represents storm-water runoff from the onset of precipitation on the watershed, through collection, conveyance, storage, and treatment systems, to points downstream from outfalls that are significantly affected by storm discharges. The input data for the model include rainfall hyetograph,

watershed characteristics, land use, gutter and pipe characteristics, street cleaning, storage facilities, inlet characteristics, treatment devices, and indexes for costs of facilities. For large watersheds, this may not be a suitable model due to its excessive detail.

*Maddaus and Eagleson* [1969] developed a distributed linear reservoir MIT model of direct runoff. Cascades of linear reservoirs, connected by linear channels and each having lateral input, are used to represent the watershed. Separate submodels of overland flow and channel flow allow simulation of the watershed response to spatially variable effective rainfall. The model parameters are related to physical features of the watershed. This model has the capability to handle spatial variability of rainfall and can be used to evaluate errors due to lumping of rainfall and to investigate the importance of inclusion of non-uniform and anisotropy precipitation.

The watershed hydrology simulation (WAHS) model, developed by *Singh* [1983, 1987], is designed for prediction of the direct runoff hydrograph for a specified rainfall event from an ungauged watershed.

The rainfall hyetograph, observed at one or more points, constitutes input to the model. In addition, soil-vegetation-land use and geomorphic characteristics are needed to estimate model parameters. The model has been verified on more than 40 watersheds with errors of less than 30 percent in predicted direct runoff peak and its timing. The model is simple and is suitable for ungauged watersheds.

*Laurenson and Mein* [1983] developed an interactive streamflow-routing program called rainfall-runoff routing (RORB) model. It is used for flood estimation, design of spillways and detention basins, and flood routing. The model can be applied for rural, urban, or partly urban and partly rural watersheds. Floods can be routed with single and multiple reaches, networks of streams, and lateral inflow and outflow. The model simulates watershed losses and channel flow hydrographs resulting from rainfall events and/or other forms of inflow to channel networks [*Mein et al.*, 1974]. The model is areally distributed and nonlinear. It is relatively simple and efficient.

The flood hydrograph simulation model (FHSM) was developed by *Foroud and Broughton* [1981] to estimate the design hydrograph and peak discharge for watersheds smaller than 400 km<sup>2</sup>. The model takes into account storm and watershed characteristics. Antecedent moisture, rainfall loss, and runoff constitute the three main components of the FHSM. The model parameters are obtained by an optimization technique based on nonlinear least squares method. It was applied to several watersheds and yielded less than 25 percent prediction error.

*Zhao et al.* [1980] developed a conceptual Xinanjiang model (XJM) with distributed parameters corresponding to the various sub-watersheds. The concept of runoff formulation is introduced to estimate the rainfall loss due to infiltration and effective rainfall. The direct runoff hydrograph is computed by the lag and route model and routed through channels by the Muskingum method. This model has been widely used in humid and semiarid areas of China.

The Huggins-Monke (HM) model was developed by *Huggins and Monke* [1968, 1970]. This is a distributed model

using the concept of subdividing the watershed into a definite number of small independent elements [Huggins et al., 1975]. The elements are assumed to be sufficiently small so that hydrologically significant parameters are uniform within the element boundaries. The outflow from one element becomes the inflow for adjacent elements. Both interception and infiltration are subtracted from rainfall to determine the effective rainfall hyetograph. The effective rainfall satisfies depression storage or becomes surface runoff which is assumed to flow in the direction of each element's slope. Each element requires a definition of interception, six infiltration parameters, surface retention, hydraulic roughness, and slope direction and magnitude. Some of the model's parameters are determined from field measurements of watershed characteristics. The model has been applied to both gauged and ungauged watersheds.

*Smith and Lumb* [1966] developed the Kansas model for large watersheds in Kansas. Areal nonuniformity of rainfall is processed by subdividing the watershed into Thiessen polygons. When daily precipitation is less

than 0.1 inches, daily accounting is used; for greater precipitation amounts, hourly accounting is utilized. The subsurface component is modeled using a soil zone and a groundwater zone. The soil zone is divided into an upper zone and a lower zone. The groundwater zone is limited to the alluvial portion of the watershed. Subsurface drainage elsewhere in the watershed is treated as interflow in response to geologic and topographic considerations. Evapotranspiration is calculated at a potential rate based on mean daily temperature and discounted for moisture availability and depth. A lag and route procedure is used to develop the direct runoff hydrograph. Based on limited testing, the model appears to simulate streamflow reasonably well.

The Institute of Hydrology model (IHM) [Morris, 1980] is a physically based distributed model of watershed hydrology. The watershed is divided into hillslope areas represented by rectangular sloping planes and channel lengths represented by straight channels of constant cross section. Both channel and plane flows are modeled using one-dimensional form of the St. Venant equations for shallow water flow. Infiltration,

throughflow and groundwater flow are treated together as saturated-unsaturated flow in porous medium described by Richards' equation. Also included in the IHM are evapotranspiration, interception, and snowmelt. Potential evapotranspiration is determined using the Penman-Monteith equation and actual evapotranspiration in the root zone is calculated using the method of Feddes et al. [1976]. The model has been applied to rural as well as forested watersheds [Morris, 1980; Morris and Clarke, 1980]. Rogers et al. [1985] undertook a sensitivity analysis of the IHM parameters and found that the model results were most sensitive to Chezy's roughness coefficient and saturated hydraulic conductivity. The model is further improved as the Institute of Hydrology Distributed Model (IHDM) by Beven et al. [1987].

The models mentioned above are mainly event-based streamflow simulation models. Their emphasis is on modeling the direct runoff hydrograph or its peak flow. Some of the hydrologic processes are neglected, some are lumped, and some are considered with considerable approximation. The period of simulation is usually as



long as the duration of the direct runoff hydrograph. So, they are storm rainfall-runoff models.

Many models have been developed to simulate continuous streamflow for long periods of time and thus more fully utilize the capability of the digital computer. These models maintain a more or less continuous accounting of the water in storage in the watershed. Because of the long simulation period, such hydrologic processes as evaporation and transpiration infiltration, interception, depression storage, subsurface flow, and baseflow assume added significance. Truly, they model the entire hydrologic cycle. The building of such models involves simulating the various components of the hydrologic cycle and maintaining a continuous water balance involving these components. Following is a review of continuous streamflow simulation models.

The Stanford Watershed Model (SWM) has been developed and applied to many watersheds throughout the world [Crawford et al., 1966; Fleming, 1975; Llamas et al., 1980; Clarke, 1968; Cermak, 1979]. Its applications have encompassed data extension, flood forecasting,

flood-frequency analysis, estimation of peak discharge, sediment transport, and effect of urbanization and land use practices. Hourly and daily precipitation, daily temperature, radiation, wind, monthly or daily evaporation, and a variety of watershed parameters constitute input to the SWM. The model outputs hourly or daily streamflow at the watershed outlet and uses the time interval of 15 minutes for calculation. It is a lumped parameter representation with 34 parameters, of which most are physically based and evaluated from maps, surveys, or hydrometeorologic records and the rest are obtained by using an optimization scheme. Several other models have been developed or extended by modifying the SWM model to adapt local climatic and geographic characteristics [Liou, 1970; Ricca, 1972] or to fit specific purposes [Peck, 1976; Claborn and Moore, 1970]. The most comprehensive extension of SWM is the Hydrocomp simulation program (HSP) developed by Johansen et al. [1980, 1984]. Significant modifications of SWM are hydraulic reservoir routing and kinematic wave channel routing. The most significant extension of SWM is the addition of water-quality simulation capabilities. Input for water-quality simulation

includes the temperature, radiation, wind, and humidity. Output from HSP can be obtained for any desired point within the watershed. Because of its tremendous versatility, the HSP has been used for a wide variety of environmental and water resources problems [Singh, 1989].

The U.S. Dept. of Agriculture Hydrograph Laboratory (USDAHL) model was developed by *Holtan et al.* [1975] primarily for agricultural watersheds by including the effects of soil types, vegetation, pavements, and farming practices on infiltration and overland flow. The model is a lumped parameter representation and has been applied to several small watersheds in the United States. A watershed is divided into as many as four distinct land-use or soil-type zones. There can be as many as 41 parameters for each zone. Input to the model includes continuous records of precipitation, weekly averages of daily mean temperatures, weekly average pan-evaporation amounts, and data on soils, vegetation, land use, and agriculture practices. Runoff, return flow, and groundwater recharge form the model output. In addition to predicting streamflow, the model has been

applied to simulate soil erosion, transport of chemicals and environmental impact assessments [*Singh, 1989*].

*Bergström* [1976] developed the HBV model for flood forecasting, simulation of streamflow, and operational purposes [*Bergström et al., 1978*]. The model is a lumped parameter representation with 15 parameters: 4 for snow accumulation and ablation, 3 for soil moisture accounting, and 8 for runoff generation. Many of these parameters have to be obtained by calibration.

Streamflow simulation is performed in three steps: (1) snow accumulation and ablation, (2) soil moisture accounting, (3) generation of runoff and transformation of the hydrograph. Daily precipitation, temperature, and potential evaporation constitute input data, and daily discharge is the output data. The model has been applied to several Scandinavian watersheds and to some watersheds in other parts of the world [*Bhatia et al., 1984; Sand and Kane, 1986*]. *Hinzman and Kane* [1991] applied it to predict hydrological response of a watershed on North Slope of Alaska. The simulated stream flow had a good agreement with the measured one. This model does not consider spatial variability in

water storage and saturation profiles with depth. Furthermore, its resolution is too coarse to represent patterns relevant to many biological processes [Ostendorf et al., 1996]. The model is quite simple and is better suited for large watersheds.

Three European organizations (the British Institute of Hydrology, the Danish Hydraulic Institute, and the French consulting company SOGREAH) jointly developed the Système Hydrologique Europeen (SHE) model, which has been reported by Abbott et al. [1986], and Bathurst [1986]. The model is physically based and considers spatial distribution of watershed parameters, rainfall, and hydrologic response. Its primary components are interception, infiltration, soil moisture storage, evapotranspiration, surface runoff, snowmelt runoff, and groundwater runoff. They are modeled either by finite difference representations of the partial differential equations of mass, momentum and energy conservation, or by empirical equations derived from independent experimental research. The model has 18 parameters, of which soil characteristics and flow resistance coefficients are most important. Rainfall,

meteorological data, vegetation, and watershed characteristics are the main model inputs. The results from watersheds in Europe and elsewhere have been reported to be very promising [*Storm and Jensen, 1984*].

The CEQUEAU model was developed by *Charbonneau et al.* [1977] for a variety of applications besides streamflow simulation, such as flood-risk mapping, evaluating the effect of deforestation on floods produced by snowmelt, simulation of water quality, flood control, design of diversion and storage reservoirs, and the like. The model divides the watershed into grid squares for which calculations are carried out. This allows spatial variability of input and output data. The data types for the model include physiographic characteristics of each grid square (vegetal cover, slope, altitude, orientation, etc.), precipitation, minimum and maximum temperature, discharges of various gauged streams, and the storage levels of reservoirs.

The Susa catchment model (SCM), developed at the Technical University of Denmark [*Refsgaard, 1981; Stang, 1981; Refsgaard and Hanson, 1982*], is similar in concept to the CEQUEAU model, emphasizing integration of

surface water and groundwater components. The model is a distributed, physically based model, developed for the Susa catchment covering an area of about 1000 km<sup>2</sup>. The model operates with a time step of 1 day and requires as input only daily values of precipitation, potential evapotranspiration, and temperature. The model simulates the total annual streamflows and low flows reasonably well, but peak flows are simulated poorly. The model can be applied to ungauged watersheds and can predict hydrologic effects of land-use practices [Refsgaard and Stang, 1981].

TOPMODEL [Beven and Kirkby, 1979; Beven, 1986a, b] is a set of programs for rainfall-runoff modeling which use gridded elevation data for a catchment area. It has been applied in numerous watersheds [Ambroise et al., 1996; Iorgulescu and Jordan, 1994]. Band et al. [1993] have successfully linked the TOPMODEL with an ecosystem model. Ostendorf et al. [1996] also applied and modified the TOPMODEL and linked it with the GAS-FLUX model (it simulates short-term dynamics of canopy water and CO<sub>2</sub> exchange at the patch scale) to simulate landscape patterns of ecosystem gas exchange within the

Imnavait Creek watershed, the same watershed modeled by Hinzman and Kane with HBV model. The model is not fully distributed because lateral water flows are only implicitly computed [Ostendorf et al. 1996].

Grayson et al. [1992] developed a simple distributed parameter hydrologic model, THALES, and applied it to two catchments in Australia and the U.S. A contour-based method of terrain analysis, TAPES-C (Topographic Analysis Program for the Environmental Sciences: Contour [Moore et al., 1988; Moore and Grayson, 1991]) was used as a basis for structuring a dynamic hydrologic model. It divides a catchment into elements based on the way water flows over a surface, i.e., using streamlines and equipotential lines [Moore and Grayson, 1991]. For each element bounded by adjacent streamlines and contours, the following attributes are calculated: element area, total upslope contributing area, average slope of an element and the aspect or azimuth of the element, etc. The model was applied to simulate flow processes within a few days duration or a few continuous rain events and does not include snow simulation.



*Wigmosta et al.* [1994] presented a distributed hydrology-vegetation model that includes canopy interception, evaporation, transpiration, and snow accumulation and melting, as well as runoff generation via the saturation excess mechanism. The model was applied to a basin of 2900 km<sup>2</sup> in northwestern Montana. The AVHRR satellite data were used to monitor the distribution of snow in the watershed and compared this with simulated results during ablation.

*Jackson et al.* [1996] developed a spatially-distributed hydrologic model to simulate the snowmelt-driven hydrologic response of a small arid mountain watershed. Snow accumulation and drifting, evapotranspiration and subsurface mass balance were included.

*Kite* [1978, 1989] developed a simple lumped reservoir parametric (SLURP) model to simulate hydrologic responses of watersheds. It uses basin average input data and produces total basin streamflow. Later, *Kite and Kouwen* [1992] improved the same model by computing the rainfall-runoff and snowmelt processes separately for different land cover classes. A watershed in the

Rocky Mountains of British Columbia was divided into three contributing sub-basins, and each of these was further subdivided by land cover classification using Landsat images. A comparison was made between using the lumped hydrological model and using the updated version of the original model applied successively to different land uses within sub-basins. By relating the model parameters to vegetation type, Kite [1993] used the similar model SLURP\_GRU, to study the climate change and produce more realistic estimates of the resulting changes in streamflow. Kite [1994] also combined a hydrological model with a GCM for a macroscale watershed. The climatological outputs from the GCM were used as inputs to the hydrological model. The results show that using the hydrological model with the GCM data produces a better representation of the recorded flow regime.

Although some models described above have been used to evaluate arctic hydrological and ecological systems, most were developed to simulate hydrological processes in different settings other than the Arctic where the hydrological response is unique due to its physical

environment. One distinct difference between the Arctic and other areas is the existence of continuous permafrost. In the Arctic, the distribution, movement and storage of water are directly influenced by the presence of perennially permafrost. The frozen ground has limited permeability and it acts effectively as an aquitard [Dingman, 1975]; most hydrological activities are confined to the seasonally frozen and thawed zone above the permafrost table, known as the active layer. Many surface hydrological processes are inactive during the long, cold winters. Energy and water fluxes are closely linked as water storage and redistribution are impacted by freeze-thaw events. Snow and ice storage on a seasonal or multi-annual basis affects the temporal distribution of water, both liquid and solid, and the release of meltwater often has pronounced effects on other surface hydrological processes [Woo, 1990]. Because of the severe and harsh conditions and the limited accessibility, the hydrological and meteorological data, especially spatial data, are rare in the Arctic for hydrologic modeling of watersheds. Nevertheless, with the exploitation of resources and the Arctic's sensitivity to climate change, different

aspects of research (including permafrost hydrology) have been ongoing in the Alaskan Arctic since the 1970s.

Models have been applied to many facets of permafrost hydrology such as the soil moisture and ground temperature regimes [Harlan, 1973; Outcalt et al., 1975; Hinzman et al., 1991b; Hinzman and Kane, 1992; Goering and Zarling, 1985; Zarling et al., 1989]. An initial attempt at comprehensive modeling of small-basin runoff met with little success [Ambler, 1979]. The reasons were the lack of adequate input data, and more seriously, the use of a model developed for the temperate latitudes which did not include many of the processes relevant to the permafrost environment (e.g., a dynamic thawing zone in the active layer) [Woo, 1990]. Another approach was to treat the basin as a black box and predict design discharge from meteorological records using statistical methods [Ashton and Carlson, 1983; Baracos et al., 1981].

Kane and Hinzman [Kane et al. 1989, 1990, 1991; Kane and Hinzman, 1993; Hinzman et al., 1990, 1992; Hinzman and Kane, 1991] have been conducting extensive studies

on watersheds of the Kuparuk River in the North Slope of Alaska since 1985. Their studies covered many aspects of arctic hydrologic processes that encompass a basic understanding of arctic hydrology, data collection and analysis to simulate various processes and their interrelations, soil properties, biological and chemical processes, and model analyses ranging from lumped to distributed as presented in this paper. *Woo* [1982] has been a very active researcher in the arctic permafrost hydrology field. His studies include many aspects of mass and energy processes in the Canadian High Arctic [*Woo*, 1982, 1983, 1986; *Marsh and Woo*, 1979; *Woo and Heron*, 1987; *Woo and Sauriol*, 1980]. Many other researchers have contributed to arctic hydrology with studies addressing meteorological aspects and those concerning data collection methods and instrumentation [*Benson*, 1982; *Clagett*, 1988; *Weller and Holmgren*, 1974].

A one-dimensional model is proposed by *Woo and Drake* [1988] to simulate the daily hydrological and thermal processes of a permafrost site. The snow on the ground is accumulated when air temperature is below freezing on

a day with precipitation. Snowmelt is partitioned into radiation melt, rain-on-snow melt and turbulent-flux melt indexed by air temperature. Evaporation is computed using the *Priestley-Taylor* [1972] approach. Soil temperatures are calculated using a finite difference solution, with the solution predicting the position of the permafrost table. Daily water balance is performed and the water table is updated. When the water table rises above the ground to exceed the depression storage, lateral runoff is generated from the site. This algorithm can be used to generate runoff for different points in the basin or on a slope, but is not spatially distributed. In order to route the flow down the slopes and along the channels, further work is needed.

T-HYDRO is a spatially explicit watershed model that utilizes raster-based topographic information to generate a two-dimensional water flow field for the Imnavait Creek watershed [*Ostendorf and Reynolds, 1993*]. The watershed is divided into a grid of 21250 square pixels with 10 m side length and, for each pixel, the total discharge leaving a pixel per year based on the

difference between the sum of lateral flow into the element and precipitation minus evapotranspiration. It was used in vegetation typing and landscape models for nutrient availability and growth. The result is a 'drainage area' map that shows the total upslope area that 'drains' into a given pixel [Ostendorf et al., 1996]. It does not include the overland and channel flow routing because the time scale was one year.

Most modeling activities of ecosystems with a hydrologic aspect for the Arctic are related to:

1) Vegetation dynamics (effects of disturbance on vegetation) [Miller et al., 1979, 1984; Leadley and Reynolds, 1992; Chapin et al., 1979; Bliss, 1981],

2) Chemical and biological variables [Shaver et al., 1986, 1990; Shaver and Chapin, 1986], and

3) Gas flux exchange between the arctic terrestrial, atmospheric and aquatic systems [Reynolds et al, 1996; Tenhunen et al., 1992, 1994; Ostendorf et al., 1996; Oechel et al., 1993].

Studies [e.g., *Bliss et al.*, 1984; *Jasieniuk and Johnson*, 1982; *Jorgenson*, 1984; *Peterson and Billings*, 1980; *Webber*, 1978] have shown that the moisture gradients and patterns have a great impact on productivity of tussock tundra vegetation, and an array of chemical, physical and biological variables. So an improved hydrologic model that can predict spatial moisture distribution and water movement with time within a watershed is very important for other studies. Many studies have confirmed that a physically based, spatially distributed model is a proper way to accomplish this [*Goodrich*, 1990; *Woolhiser et al.*, 1990; *Grayson et al.* 1992; *Wigmosta et al.*, 1994; *Beven and Kirkby*, 1979; *Beven and O'Connell*, 1982; *Hirschi and Barfield*, 1988a, b; *Laramie and Schaake*, 1972; *Running*, 1991; *Flerchinger et al.*, 1996]. They can provide more detailed information within a desired area than lumped models. The key here is that these models can be used to generate distributed hydrologic data over a watershed and that these results can be used in various ecosystem models. The required hydrologic simulations are generally the distributed soil moisture contents.



The MATH model presented in this thesis is a process based, spatially distributed hydrologic model of mass and energy fluxes for application to arctic environments. It includes many hydrologic and thermal processes such as snowmelt, active layer thawing, evapotranspiration, subsurface flow, overland flow and channel flow routings. The model can be used for continuous simulations including distributed snowmelt, evapotranspiration and soil moisture contents. Hydrographs can be generated at any gauging station within a watershed. Because of its physical foundation, this model can, in the future, be coupled with chemical and biologic models.

## Chapter III. Site Description

### 3.1: Introduction

Since 1992, a field research study has been ongoing in the Alaskan Arctic in a nested watershed consisting of different scales of sub-basins. This work has been concentrated in Imnavait Creek watershed (2.2 km<sup>2</sup>), Upper Kuparuk River catchment (146 km<sup>2</sup>), and Kuparuk River basin (8140 km<sup>2</sup>). In addition, extensive physical process studies have been conducted at Imnavait Creek watershed since 1985. With seven major and five minor meteorological stations installed across the Kuparuk River watershed, spatially distributed and temporal data sets were available as inputs for the hydrologic modeling effort.

### 3.2: Kuparuk River Basin

The largest basin studied was that of the Kuparuk River that flows from the glaciated foothills just north of the Brooks Range through the low gradient coastal plain to the Arctic Ocean near Prudhoe Bay (Figure 3-1).

Kuparuk Watershed  
Area = 8140 km<sup>2</sup>

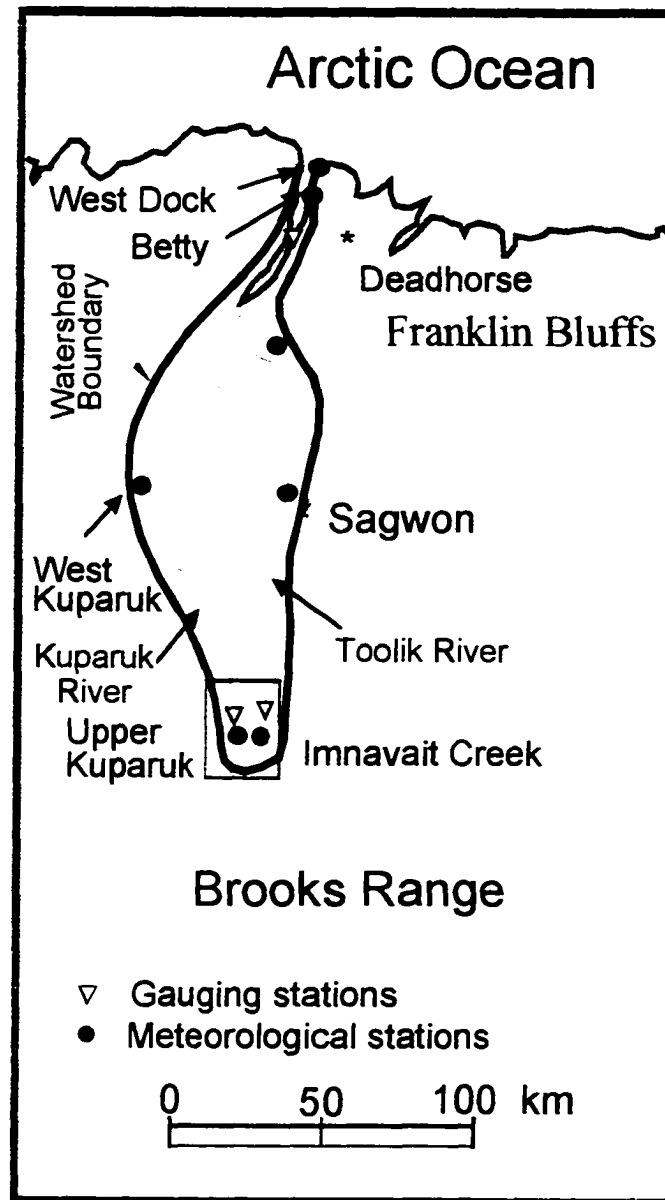


Figure 3-1. Kuparuk River Basin and major meteorological and gauging stations.

The drainage area at the U.S. Geological Survey gauging site near the coast is 8140 km<sup>2</sup>, with a basin length of nearly 250 km. The average elevation of the entire Kuparuk River basin is about 245 meters, ranging from 0 to 1500 meters.

The entire region lacks trees, is underlain by continuous permafrost, and is covered with snow for 7 to 9 months each year. The snowmelt event is generally the dominant hydrologic event each year, which typically occurs over a 7-10 day period between early May and early June [Kane et al., 1991a]. The average summer rainfall is around 18 cm in the foothills of the Brooks Range. The maximum snow water equivalent at winter's end typically averages from 8 to 14 cm of water, with less snow along the coast. The flow season typically begins in mid-May in the headwaters and late May to early June near the coast. Summer temperatures are typically between 6 °C and 18 °C, and winter temperatures are commonly around -15 °C to -25 °C. Freeze-up begins in mid-September, but the rivers and streams may not be completely frozen over until October. Permafrost thickness ranges from less than 300 meters in

the foothills to over 600 meters near the coast [Osterkamp and Payne, 1981]. Hence, the region is effectively isolated from deep groundwater. Subsurface flow occurs in a shallow zone above the permafrost. This shallow layer of soil is called the active layer, and undergoes annual freezing and thawing. The thawed active layer increases in depth throughout the short summer. Soils typically thaw to maximum depths of 25-40 cm, but can thaw to 1 m depending on several environmental factors including soil type, slope, aspect, and soil moisture [Hinzman et al., 1991b].

Although neighboring watersheds have active glaciers, there are no glaciers in the Kuparuk River basin. The coastal plain was never glaciated, and is characterized by abundant, wind-oriented thaw lakes [Walker et al. 1989]. There is, however, an aufeis field that develops annually and covers approximately 6-12 km<sup>2</sup> in the basin that may have a local moderating effect on streamflow. A small spring exists in the headwaters of the basin, but its source is believed to be from precipitation percolating through local gravel deposits [Kreit et al., 1992]. The dominant export of water from small basins

on the coastal plain is by evaporation, with little overland and channel flow due to the low gradients [Rovansek et al., 1996]. However, several large drainage channels originate in the foothill regions and subsequently cross the coastal plain.

The two smaller watersheds (described below) that have been modeled drain into this larger basin. To date, the MATH model has not been run at this larger scale, but it will be in the near future.

### **3.3: The Upper Kuparuk River Basin**

The Upper Kuparuk River basin is the next largest watershed studied (drainage area of 146 km<sup>2</sup>). It drains the northern foothills of the Brooks Range (Figure 3-2). The slopes in the Kuparuk River headwaters are covered with till from two glacial advances, Sagavanirktok and Itkillik, from the middle and late Pleistocene [Hamilton, 1986]. At the intersection with the Dalton Highway, the Upper Kuparuk River is a fourth order stream on a USGS 1:63360 map. However, the hillslopes and tributary valleys contain a complex network of water tracks, basins similar to Imnavait Creek, and rocky

## Upper Kuparuk Watershed Area = 146 km<sup>2</sup>

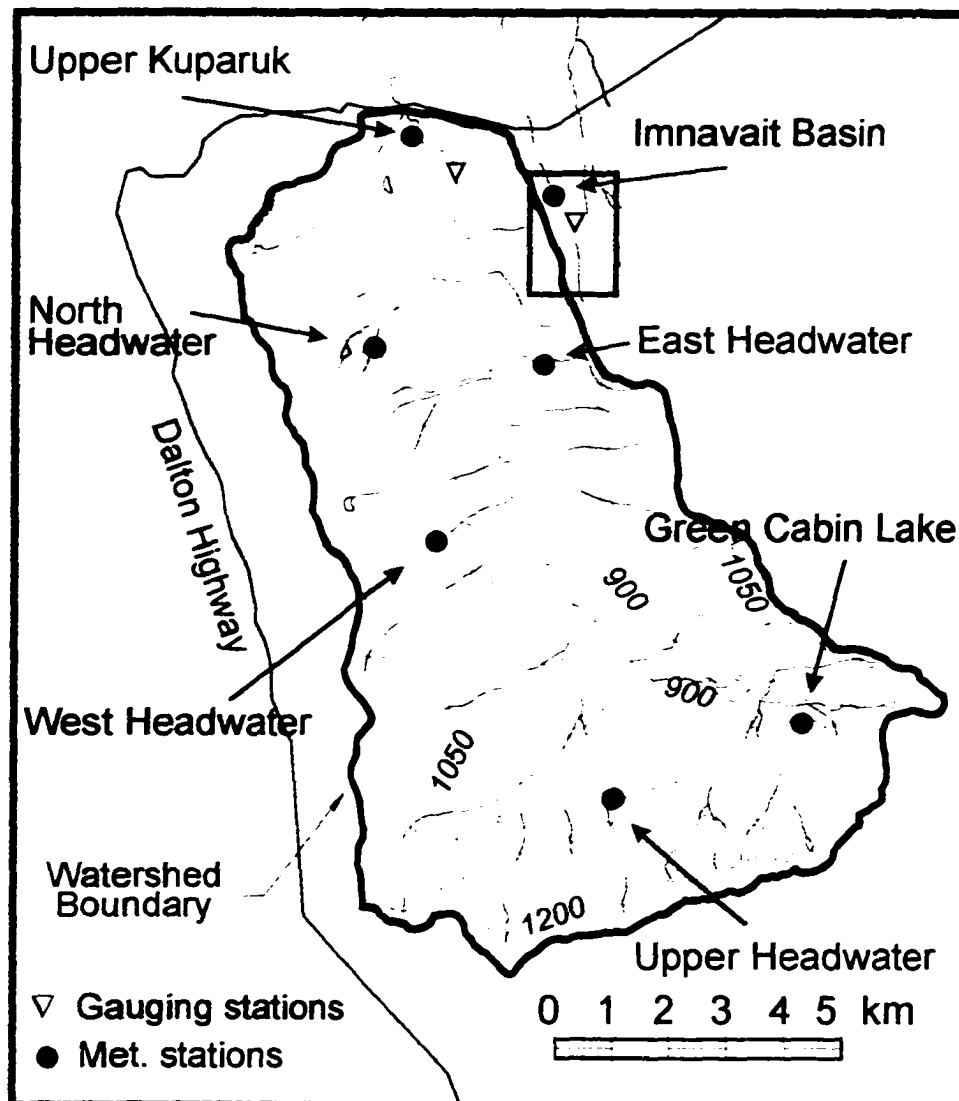


Figure 3-2. Map of Upper Kuparuk River Basin with location of gauging stations and meteorological stations shown. Upper Kuparuk and Imnavait are major stations while the remaining five are micro-stations (precipitation, wind speed and air temperature only).

headwater streams that do not appear on maps at that scale. At the headwaters, two dominant streams join together at the base of steep hills forming the main channel which occupies a north-northwest trending valley paralleling the Imnavait Creek basin. The average elevation of the basin is about 967 meters. The main basin length is 16 km, with a channel length of 25 km. Vegetation in the basin is varied, consisting of alpine communities at higher elevations and moist tundra communities, predominantly tussock sedge tundra, at lower elevations. Patches of dwarf willows and birches up to 1 m in height occupy a portion of the banks [Walker et al., 1989].

#### **3.4: Imnavait Watershed**

Imnavait Creek watershed, at 2.2 km<sup>2</sup>, is the smallest watershed studied. It is a north-northwest trending glacial valley with an average elevation of 904 meters (Figure 3-3) which was formed during the Sagavanirktok glaciation (Middle Pleistocene) [Hamilton, 1986]. The dominant vegetation in the Imnavait basin is tussock sedge tundra covering the hillslopes [Walker et al.



**Imnavait Creek Watershed**  
**Area = 2.2 km<sup>2</sup>**

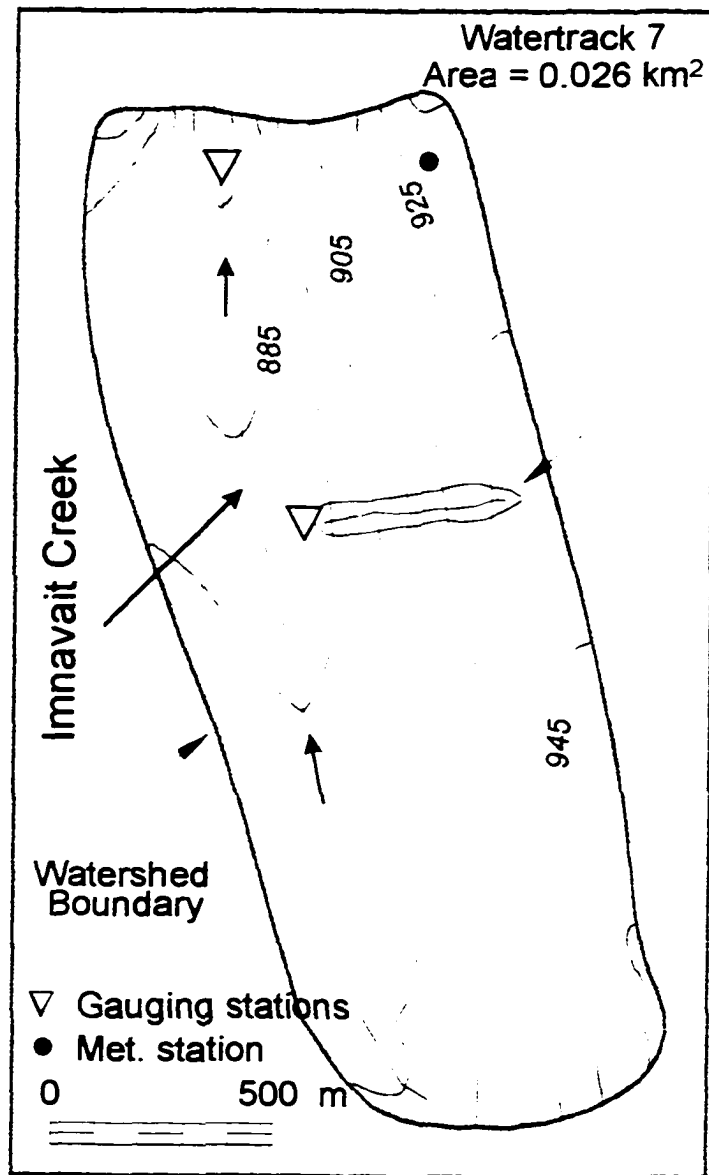


Figure 3-3. Map of Imnavait watershed and Water Track 7 with location of gauging stations and a meteorological station.

1989]. An organic layer typically near 10 centimeters thick, but up to 50 centimeters thick in the valley bottom, overlies glacial till [Hinzman et al., 1991b]. Approximately 1/3 of the annual precipitation falls as snow from September through May. Imnavait Creek is a beaded stream [Oswood et al., 1996], composed of a series of small pools connected by short water courses. The pools result from the thawing of ice masses that occur at ice-wedge polygon intersections, and the connecting drainage is commonly along the thawing ice wedges [Washburn, 1980]. The stream bottom rarely cuts through to mineral soil but maintains itself in the organic layer. Stream margins are predominantly peat, with occasional sections composed of stony banks. A gauging site was installed at a point draining 2.2 km<sup>2</sup>. Imnavait Creek flows another 12 kilometers beyond that station and joins the Kuparuk River.

The Imnavait Creek watershed is within a large region of tussock-tundra vegetation that covers much of northern Alaska, northwestern Canada, and northeastern Russia [Bliss and Matveyeva, 1992]. The hills near Imnavait Creek rise less than 100 m from the valley

bottoms to the crests, and are elongated in SSE to NNW trending ridges. The west-facing aspects of these ridges are much gentler and longer than the east-facing aspects. Hills in this region are covered with smoothly eroded mid-Pleistocene-age glacial deposits, fine colluvium, and tussock-tundra vegetation. Shallow peat deposits are found in the basins between the ridges [Walker and Walker, 1996]. Hillslope water tracks, shallow drainage channels spaced tens of meters apart, are common features on the mid-to-lower portions of most hills giving them a ribbed appearance [Hastings et al., 1989] (Figure 4-5). Most of the hillslope water tracks drain into a gently sloping valley bottom that forms the headwater of Imnavait Creek. Basins like Imnavait Creek consist of fine-grained, organic-rich deposits that appear to have moved into smaller basins from the surrounding slopes by solifluction, creep, and/or slope wash [Kreig and Reger, 1982]. The basins have a complex microtopography consisting of string bogs (peatlands characterized by low ridges of peat and vegetation interspersed with depressions that often contain shallow ponds [Washburn, 1980]), palsas (small ice-cored mounds), high-centered ice-wedge polygons, and wet areas

with lowland water-track patterns. Extensive alluvial and glaciofluvial deposits occur along the Kuparuk River.

### 3.5: Data Collection

The annual field programs begin in late April each year with extensive snow surveys throughout the Kuparuk basin to determine the pre-melt snow water equivalent (SWEQ) in each basin. SWEQ in the Imnavait Creek basin was estimated each year from approximately 90 water equivalent measurements in a 900 meter transect across the basin. The average water equivalent in the two larger basins was estimated by traveling throughout the basins on snow machines, helicopters, and vehicles where it had road access and by performing snow surveys in spots selected as representative of landscape units, based on slope, aspect, elevation, and latitude. At least ten measurements of water equivalent and 20 snow depth measurements were performed at each station according to the method described by *Rovansek et al.* [1996]. The weighted averages were calculated based on landscape units for each basin.

Streamflow was monitored at all three scales from the onset of snowmelt in the spring to near freeze-up in the fall. The U. S. Geological Survey provided hourly stage readings and daily flow averages at the mouth of the Kuparuk River. Stilling wells were installed at the Upper Kuparuk River basin, Imnavait Creek, and the water track outlets that recorded stream stage every minute, then averaged these 60 readings over one hour increments on Campbell Scientific CR10 data loggers. Chart recorders were used at each site as back up. A small weir was used at the water track, and an H-type flume was used at Imnavait Creek. Discharge measurements were made at several different stages to produce rating curves each year from which we calculated continuous records of discharge. At least two discharge measurements were taken daily during the spring snowmelt period until ice cleared from the channels and the stage-discharge relations became stable.

Seven meteorological stations recorded precipitation, wind speed and direction, air temperature, relative humidity, and various radiation terms between the headwaters in the foothills and the coast. Five micro

stations are located in the headwaters of the Upper Kuparuk watershed to capture rainfall, temperature and wind speed variability both spatially and temporally. Figures 3-1, 3-2 and 3-3 show the locations of the meteorological stations. Two neighboring stations near the coast capture the strong meteorological gradients from proximity to the ocean, and two neighboring stations in the foothills capture elevation gradients. Most analyses covered flow between snowmelt and September 7th each year because that is the latest date for which consistent data are available for most years.

## Chapter IV. Model Development

### 4.1: Introduction

The arctic ecosystem differs from those in more temperate regions, primarily due to the influence of cold temperatures and large annual variation in solar radiation on the physical, biological and chemical systems. This unique environment is thermally fragile when subjected to disturbance and more sensitive to climate change [IPCC, 1992; Manabe and Stouffer, 1980; Schlesinger and Mitchell, 1985].

Researchers believe that interactions among hydrological, meteorological and biological processes dictate the magnitude of green house gas fluxes in the Arctic [Weller et al., 1995]. Therefore, the spatial information simulated by MATH model on water movement and soil moisture is very important. It can be concluded that it is essential to have a quantitative understanding of coupled hydrologic and thermal processes in arctic regions when studying regional and global climatic change and its consequences. Many

researchers have developed models on different aspects of arctic hydrology [Kane et al., 1990, 1991a, 1993; Hinzman et al., 1991; Baracos et al., 1981; Ohmura, 1982; Marsh and Woo, 1979; Woo, 1982, 1983, 1986]. However, to have a better understanding of the interactive mass and energy dynamics of the arctic system, a process based, spatially distributed hydrologic model is needed that can provide more detailed spatial information for use in related research.

Numerous spatially distributed hydrologic models have been developed since early 1980s. The major modeling efforts of this kind are: the SHE model (Système Hydrologique Européen) [Jonch-Clausen, 1979; Abbott et al., 1986], the TOPMODEL [Beven and Kirkby, 1979], THALES model [Grayson et al., 1992], the model developed by Wigmosta et al. [1994], and other models [Beven and O'Connell, 1982; Hirschi and Barfield, 1988a,b; Running, 1991; Flerchinger et al., 1996; Jackson et al., 1996]. With the development of more sophisticated computers (faster CPU processor and bigger data storage ability), people are trying to develop more complex



component models which might provide more detailed information for different physical processes.

So far, most existing spatially distributed models deal with processes in temperate climates that have a different hydrologic regime compared to the Arctic. In the Arctic, the existence of continuous permafrost restricts subsurface flow within a shallow surface active layer which experiences thawing and freezing every year, and snow accumulation, redistribution of snow by wind, and snow ablation are important hydrologic events each year. Also, the soil thermal and hydraulic properties change with the active layer's thawing and freezing. All these special characteristics that are unique to the Arctic need to be quantified by a proper model which is not currently available. Many studies [Kane et al., 1989, 1990, 1991a,b, 1993; Kane and Hinzman, 1993; Hinzman et al., 1991a,b, 1993; Hinzman and Kane, 1991] which cover different aspects of arctic hydrologic processes have been ongoing in various watersheds in the North Slope of Alaska since 1985. Researchers in Canada have also done similar studies

[Woo, 1982, 1983, 1986; Marsh and Woo, 1979; Woo and Heron, 1987; Woo and Sauriol, 1980].

As far as the model development effort, most arctic hydrologic simulations rely on conceptual lumped models that produce average results that only reflect total response of a water basin. Since these conceptual lumped models do not consider the spatial characteristics of a watershed and physical processes, they can not supply spatial information on water movement and soil moisture which is very important in studying biological processes, trace gas fluxes, and other geochemical processes. There is no doubt that hydrologic models that examine spatially variability are useful as long as they adequately depict ongoing hydrologic processes and that there is a method to validate the spatial performance of such a model. This kind of model is presently not available for the arctic environment. In this chapter, the development of a spatially distributed model for use in the Arctic will be outlined.. Then, it will be tested and verified against data collected from the Kuparuk River basin in the Alaskan Arctic (see Chapter VI).

#### **4.2: Topographic Delineation of a Watershed**

Hydrologic response of a watershed is largely dependent upon its topography. The watershed topography serves as an important factor in determining the streamflow response of a basin to precipitation because it controls the movement of water within the basin and therefore it affects the spatial distribution of fluxes such as surface and subsurface water, sediment and dissolved chemicals (nutrients) in the watershed. It is essential to correctly depict slope, aspect and drainage characteristics of a watershed for use in spatially distributed models; following is a discussion of how we approached this problem.

##### **4.2.1. Basic Unit/Element of Watershed**

There are many articles that discuss the effect of topography on some aspects of hydrologic processes [Beven and Wood, 1983; Gary and Sen, 1994; Palacios and Cuevas, 1986; Wolock and Price, 1994]. In recent years, considerable work has been done on the representation of a watershed surface. Generally, terrain surfaces may be represented by a series of

discrete points which are characterized by their  $x$ ,  $y$  and  $z$  coordinates. Based on these known points, there are different ways to form elements. Triangular and rectangular elements are often used as the basic uniform areas when conducting hydrologic modeling [Gary and Sen, 1994; Jones et al., 1990; James and Kim, 1990; Paniconi and Wood, 1993]. Node based models are also used [Wigmosta et al., 1994]. In our model, the triangle element scheme (Figure 4-1a) is used to represent the watershed, and it is treated as a basic uniform unit for the calculation of mass and energy balances. Utilization of triangle elements has certain advantages over other types of elements [Jones et al., 1990]. Triangle elements are easy to conform to the three-dimensional geometry of an irregular watershed. It is more efficient to calculate the water flow directions using triangular elements as opposed to rectangular elements, because it is possible to fit a plane through the three points of the triangle while a rectangle must be fit with a non-planar surface. Having created a basic unit area, we can calculate flow area, slope, channel networks, ridges, drainage area and other

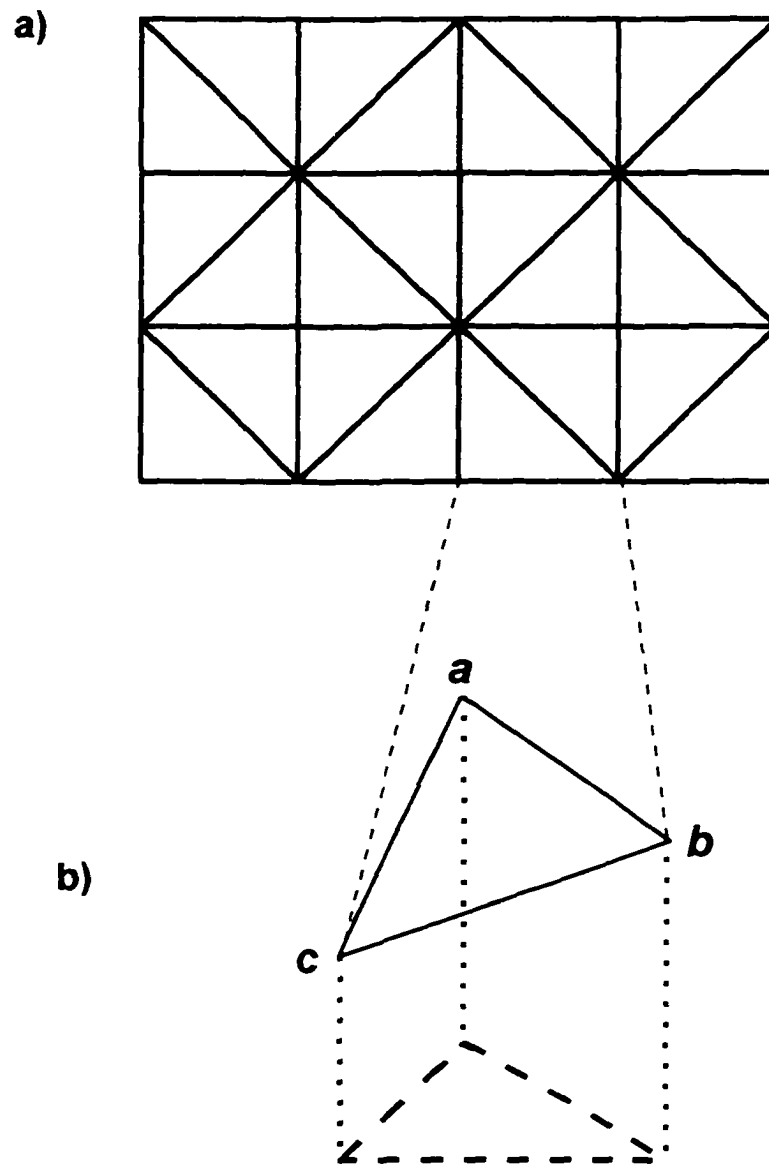


Figure 4-1. Triangular elements used in the model (a) and node notation (b).

related information needed when conducting physical simulations. It should be noted that the formation of triangular elements may be based upon a regularly or irregularly spaced grid.

#### **4.2.2. Flow Directions and Channel Networks**

This model simulates three different flow processes that include subsurface flow, overland flow and channel flow. Flow direction must be known before conducting flow routing. For subsurface flow and overland flow, the same flow direction is assumed for each element. This is based on the effect permafrost has on subsurface flow in the active layer. The determination of flow direction within each element is based on its gradient. For each element (Figure 4-1b), the three nodes are identified as *a*, *b* and *c* which refer to the highest, middle and lowest elevation point respectively. Two letters are used to indicate whether flow is leaving (*o*) or entering (*i*) the element across its boundaries. So for any element, three combinations of *i* and *o* can represent the possible flow patterns. For example, *ioi* means water flows into the element through boundaries

$\overline{ab}$  and  $\overline{ac}$  and flows out through boundary  $\overline{bc}$ . Figure 4-2 shows the three possible flow cases, which are *ioi*, *ioo* and *ioo*, noting that the flow is always into the element through the boundary  $\overline{ab}$  because *a* and *b* are the highest two points among the three nodes. By calculating the normal of the cross-product of the vectors from the lowest vertices,  $\vec{n} = \overline{bc} \times \overline{ac}$ , the gradient of the plane can be determined. Then the flow direction ( $\vec{f}$ ) is known for each element (Figure 4-3a) assuming that flow within each element is parallel to its plane gradient. In the case of *ioo* (Figure 4-3b), the partitioning of the areas that contribute flow through  $\overline{bc}$  and  $\overline{ac}$  are the triangular areas of *bcd* and *adc* respectively, where *d* is the intersection of  $\overline{ab}$  and  $\overline{cd}$ , which is parallel to flow direction  $\vec{f}$ . Once the flow direction of each element is determined, it is assumed not to change with time.

Channel segments can then be determined based on the determined flow direction in every element. If a boundary shared by two elements was an outflow boundary for both elements (Figure 4-4a), then that segment is

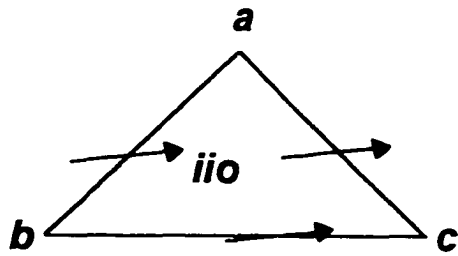
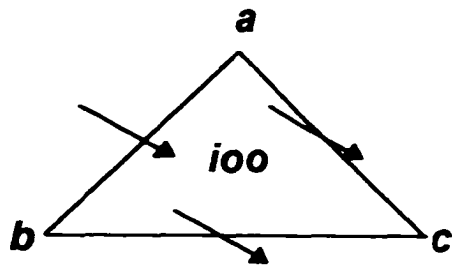
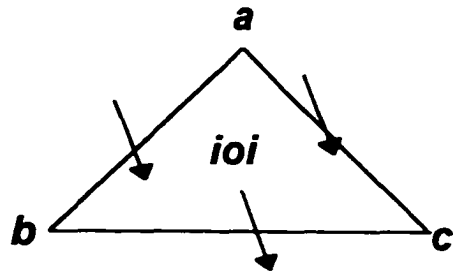


Figure 4-2. Three possible flow cases for each element.



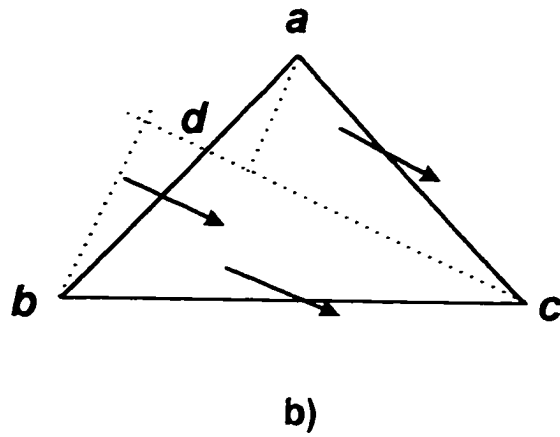
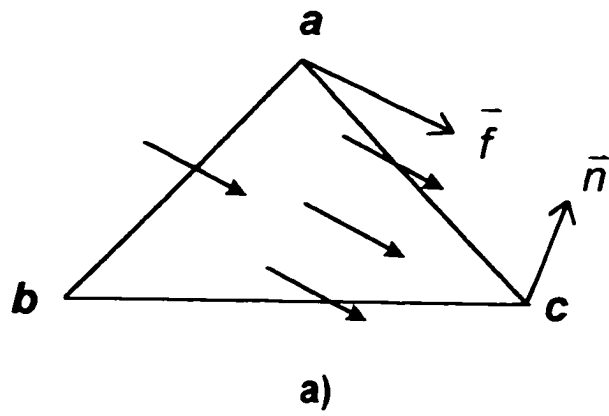


Figure 4-3. Flow direction (a) and partitioning of flow through element boundaries (b).

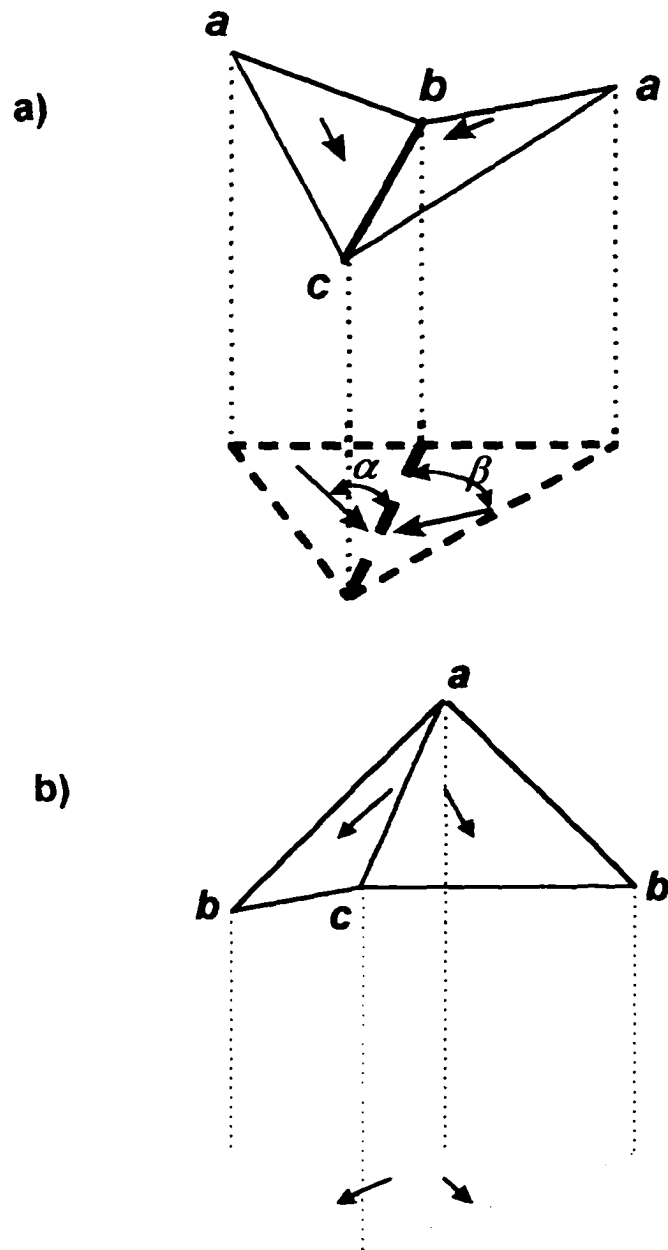


Figure 4-4. Flow pattern for channel segments (a) and ridge (watershed) divides (b).

considered as a channel reach. It is possible that the downstream reach of the created channel segment may not be a channel based on the definition described above (This can be anticipated because of the spacing of digital elevation data used.); however, once a channel reach is initiated, that channel must be continued until it meets another channel or reaches the boundary of the watershed. This can be accomplished by accepting the fact that the flow will follow the steepest path among the possible boundaries. Similar concepts can be applied to find ridges. If two adjacent elements share a common inflow boundary (flow pattern *i*), then that boundary becomes a single segment of ridge (Figure 4-4b). Ridges defining the outer watershed boundary will be continuous, but not necessarily ridges internal to the watershed.

#### **4.2.3. Flat Area Considerations**

Flow direction determination in flat areas needs special consideration [Jones et al., 1990; Lee and Schacter, 1980; Petrie and Kennie, 1987]. The method used for a non-flat element does not work mathematically

for a flat element. So, the direction must be defined before conducting flow routing. In our model, we accept the fact that water will flow from higher elevations to lower elevations by flooding flat areas. So, for each flat element, the elevations at the nodes are temporarily replaced by a new set of data that are taken by averaging the elevation values of its surrounding nodes. Once the directions are determined, the elevation values for those flat elements are set back to the original ones.

### **4.3: Results Of Geometric Analysis**

Since our model will be applied to two watersheds, Imnavait watershed and Upper Kuparuk River basin (Chapter VI), and since the drainage features of these watersheds only need to be simulated once from analysis of digital elevation data, results are presented below.

#### **4.3.1. Channel Network and Analyses**

An accurate simulation of hydrologic processes of a watershed depends on how well the topography is

represented, the channel network is delineated and flow directions within each element are determined. How an arctic watershed responds temporally and spatially to rain and snowmelt events depends upon the drainage network [McNamara, 1997]. Water tracks on the hillslopes and channels in the valley bottoms convey water much faster than both overland flow and subsurface flow [Kane and Hinzman, 1993]. If these hillslope drainage features, which are difficult to capture in digital elevation data sets, are not represented in the drainage network, hydrologic simulations are not realistic.

For Imnavait watershed, digital elevation data at a resolution of 50 m was used to delineate the channel network, whereas 300 meter resolution was used in the simulations for Upper Kuparuk River basin. Figures 4-5 and 4-6 show simulated channel networks over the Imnavait watershed and Upper Kuparuk River basin. The simulated channel networks are very compatible with actual channels and topography of the watershed.

Based on the simulated channels, this model also has the ability to analyze other quantitative

characteristics related to watershed delineation. One such descriptor is stream order, as depicted in Figures 4-5 and 4-6.

#### **4.3.2. Water Tracks**

The hillslopes in the Kuparuk River basin are drained by a network of water tracks. The smallest scale studied is hillslope Water Track #7 that drains 0.026 km<sup>2</sup> on a west facing slope in the headwater basin, Imnavait Creek [McNamara, 1997] (Figure 3-3). A water track is essentially a linear channel that drains an enhanced soil moisture zone that flows directly down a slope and is best detected by a change in vegetation from the surrounding hillslope [Hastings et al., 1989; Walker et al., 1989]. The Imnavait Creek basin contains numerous water tracks that are generally spaced tens of meters apart, although their density varies [Walker et al., 1989a, 1989b]. Only intermittently do incised channels exist in water tracks, but they are significant components of the hillslope hydrologic cycle. Some water tracks are well defined and have distinct channels; some are weakly defined and more subtle and do

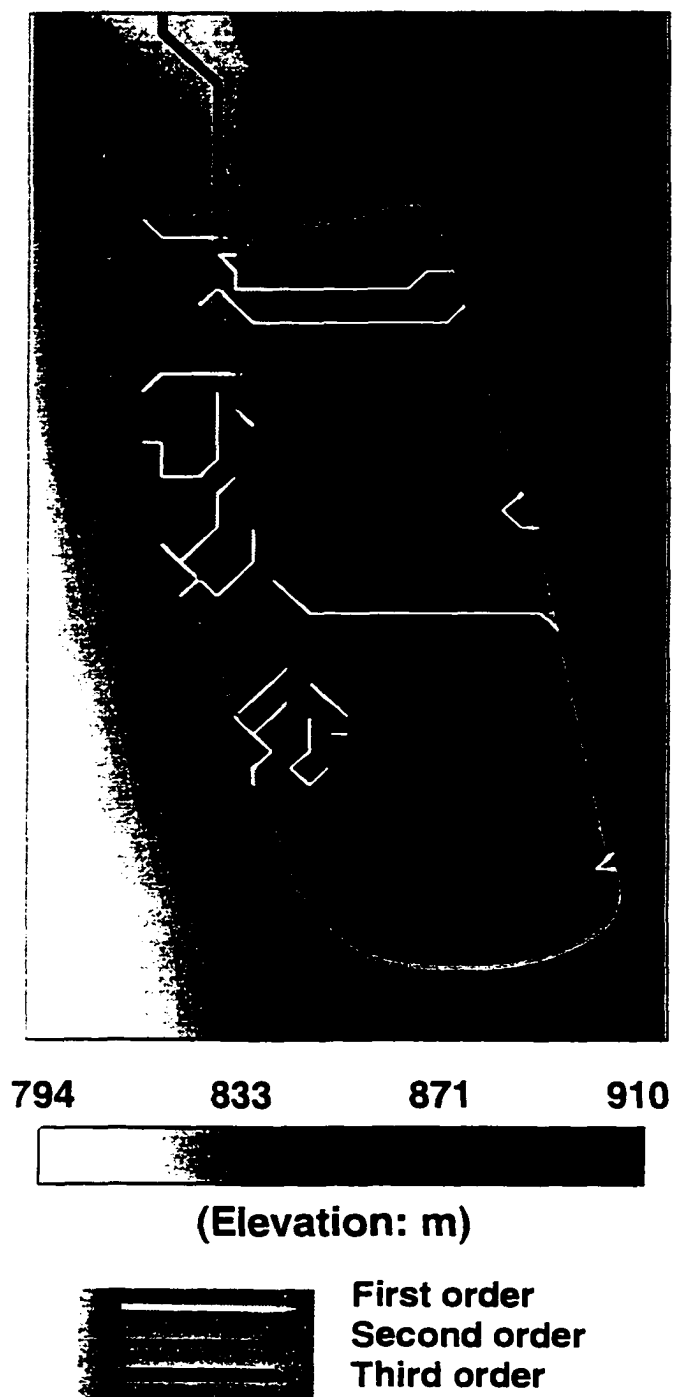


Figure 4-5. Channel network and stream orders of the Imnavait watershed, Alaska generated by model.

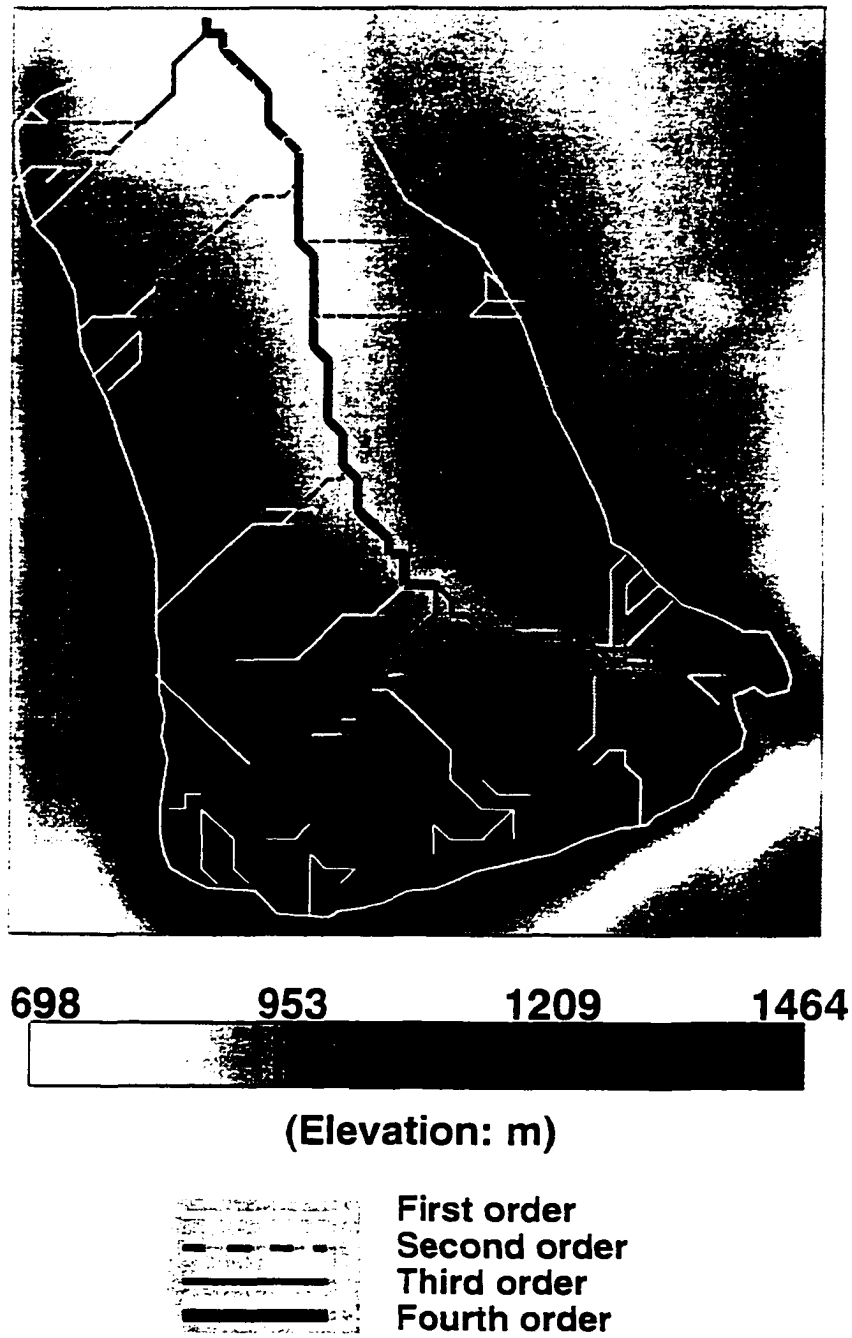


Figure 4-6. Channel network and stream orders of Upper Kuparuk River basin, Alaska generated by model.



not have incised channels. Well defined water tracks cover only about 1% of the watershed [Walker and Walker, 1996]. Vegetation in the water tracks varies with the degree of channel development. Weakly developed water tracks have communities that are scarcely distinguishable from tussock tundra, whereas well-developed tracks contain distinctive willow and dwarf-birch communities paralleling the water track. The water track ends in a peat covered valley bottom through which water travels to Imnavait Creek as diffuse subsurface flow through the active layer, or overland flow during extreme events. Figure 4-5 shows that most of the major water tracks are captured, particularly at the 50 m resolution. As the element size increases (Figure 4-6), the smallest order of channels may essentially become incised channels instead of water tracks. For example, in Figure 4-5 we have captured about 26 water tracks over 2.2 km<sup>2</sup>; for the Upper Kuparuk catchment we have captured around 52 water tracks in an area of 146 km<sup>2</sup>.

#### 4.3.3. *Drainage Area*

The flow paths and channel network are calculated in a rectangular area which completely encompasses the watershed. For the Imnavait watershed, the initial rectangular area is 5.25 km<sup>2</sup> consisting of 4200 triangular elements. Thus, it is clear that if all the physical process simulations are based on the rectangular area, it would not be an efficient approach since many calculations are outside the watershed of interest. In order to save computer resources and speed up the execution of the simulation, it is useful to determine the actual drainage area that contributes flow at the basin outlet before executing hydrologic simulations. By first determining channel segments that have flow contributions to the gauging site, those elements or drainage areas that contribute to the flow from the watershed can be obtained. Figure 4-5 shows the simulated drainage area of Imnavait Creek watershed. It is 1.9 km<sup>2</sup> and consists of 1512 elements. For the Upper Kuparuk River basin, the rectangular area has 6448 triangular elements that cover about 290 km<sup>2</sup>. The simulated drainage area (Figure 4-6) is about 145 km<sup>2</sup>.

and it consists of 3218 triangular elements. In both cases, the simulated drainage areas are very close to the drainage areas obtained from topographic maps (1:63,360) [McNamara, 1997].

#### **4.4: Description of Physical Processes**

The arctic system has its unique characteristics; the existence of permafrost and dynamic active layer development make it impossible to simulate hydrologic processes without coupling energy processes. In the model described here, all of the important components shown in Figure 4-7 have been considered. Following is a discussion of each hydrologic process that results in a mass flux and the relevant energy fluxes.

##### **4.4.1. Snowmelt**

The Arctic has an extended and cold winter. Snow accumulation and redistribution by wind (with some sublimation) are the major hydrologic activities during this time. About one-third of the annual precipitation for the Imnavait Creek watershed is contributed by snowfall [Hinzman and Kane, 1991]. Same is true for

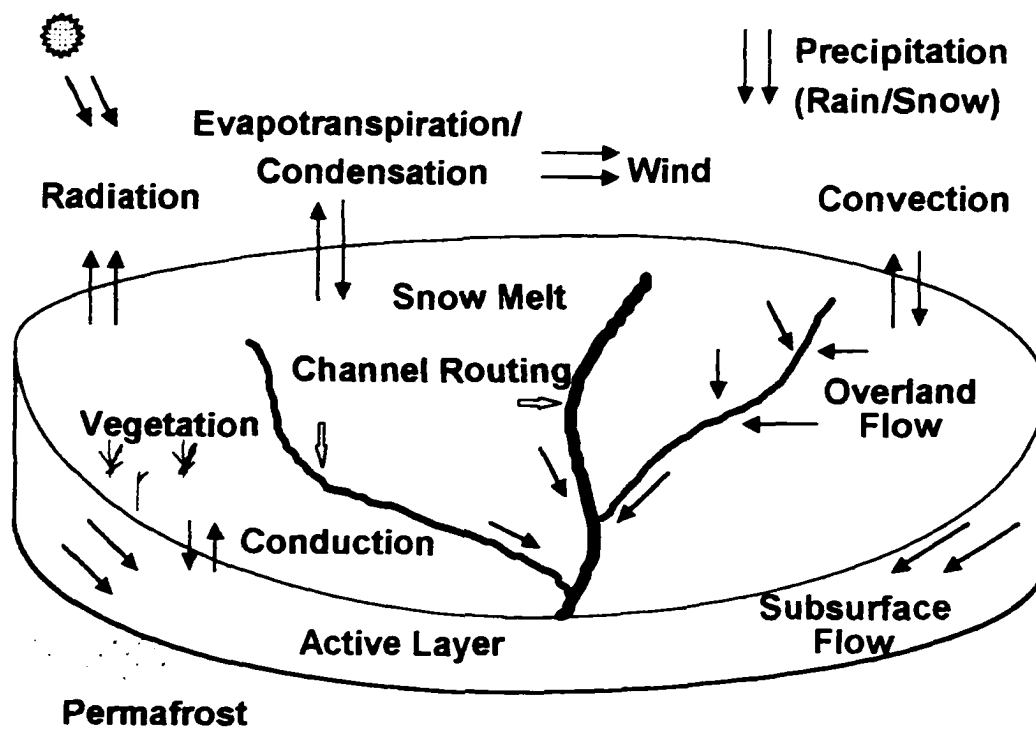


Figure 4-7. Hydrologic and thermal processes modeled for every element within an arctic watershed.

Upper Kuparuk River basin, which is confirmed by averaging five years of measured data [Lilly et al., 1998]. This is contrasted with the situation for the entire Kuparuk River basin where just less than one half of the annual precipitation is snowfall. This snow melts in a relatively short period and generally generates the highest stream flows of the year. Consequently, simulating snowmelt and predicting subsequent runoff from the watershed are very important components of arctic hydrologic modeling. Current snowmelt models either use the energy balance method or a simple temperature index method, depending on what type of data are available and how the results will be used [Laramie and Schaake, 1972; Kane et al., 1993, 1997; Hinzman et al., 1991a; Hinzman and Kane, 1991; Wigmosta et al., 1994; Bergström, 1986; Price and Dunne, 1976]. In our model, the surface energy balance method has been used as the primary choice. A simpler degree-day method has also been included as an option because in most arctic areas there are too little data available to do an adequate surface energy balance.

#### 4.4.1.A. *Surface Energy Balance*

The surface energy balance is physically-based since it is based on the total energy budget at the surface of snowpack. It can be expressed as:

$$Q_m = Q_{net} + Q_s + Q_e + Q_a + Q_c \quad (4-1)$$

where  $Q_m$  is the energy utilized for melting the snowpack. If  $Q_m$  is negative, it indicates a cooling of the snowpack. This is typical on nights when the temperature drops below freezing or when snowmelt is interrupted by a cold spell.  $Q_{net}$  is net radiation energy, either measured by a net radiometer or calculated as the sum of individual incoming and outgoing long and short wave fluxes (also measured).  $Q_s$  is sensible heat flux due to turbulent convection between the watershed snow surface and the air.  $Q_e$  is latent heat flux associated with evaporation/sublimation and condensation.  $Q_a$  is the energy advected by moving water (i.e. rainfall).  $Q_c$  is the energy flux via conduction through snow into the soil and is neglected here because the variation of temperature within the

snowpack during melt is negligible.  $Q_r$  has been measured with heat flux plates and found to be insignificant during snowmelt. In this surface energy balance approach, horizontal advection is not considered.

The two turbulent heat flow terms are determined in a manner similar to other researchers in equation (4-1) [Kane et al., 1991a, 1993 and 1997; Price and Dunne, 1976]. The following two equations were solved for sensible ( $Q_h$ ) and latent heat ( $Q_e$ ) fluxes:

$$Q_h = \rho_a C_{pa} D_{h(n,u, or s)} (T_a - T_s) \quad (4-2)$$

$$Q_e = L_v \rho_a D_{w(n,u, or s)} (0.622/p) (e_a - e_s) \quad (4-3)$$

where  $\rho_a$  = density of air, kg/m<sup>3</sup>;  $C_{pa}$  = specific heat of air, J/kg°C;  $D_h$  = heat exchange coefficient, m/s, with atmospheric conditions being  $n$  = neutral,  $s$  = stable, and  $u$  = unstable;  $T_a$  = temperature of air at elevation  $z$ , °C;  $T_s$  = effective surface temperature, °C;  $L_v$  = latent heat of vaporization, kJ/kg;  $D_w$  = vapor exchange coefficient and is assumed =  $D_h$ , m/s;  $p$  = atmospheric pressure, millibars;  $e_a$  = vapor pressure at height  $z$ ,

millibars; and  $e_s$  = surface saturated vapor pressure, millibars.

$$D_{r,n} = k^2 (u_z) / [\ln(z - h/z_0)]^2 \quad (4-4)$$

where  $k$  = von Karman's constant, 0.41;  $u_z$  = wind speed at height  $z$ , m/s;  $z$  = height of measurements, m;  $z_0$  = roughness length, m; and  $h$  = snow depth, m.

When calculating both the sensible and latent heat fluxes, the stability of the air just above the snow surface must be considered because the mixing in the lower atmosphere can occur due to wind and density gradients. This can be corrected by adjusting the convective heat transfer coefficient ( $D_{r,n}$  in equation (4-4)) for non-neutral (stable and unstable) conditions ( $D_{r,s}$ ,  $D_{r,u}$ ). When the air density at the surface is greater than the air above, then stable condition exists and

$$D_{r,s} = D_{r,n} / [1 + \sigma \cdot R] \quad (4-5)$$

In the case where the air is unstable, the density of the air at the surface is less than above and the heat transfer coefficient is modified as:



$$D_{hu} = D_{hn} / [1 - \sigma \cdot R] \quad (4-6)$$

where  $D_{hn}$  = neutral convective heat transfer coefficient, m/s;  $D_{hs}$  = stable convective heat transfer coefficient, m/s;  $D_{hu}$  = unstable convective heat transfer coefficient, m/s;  $\sigma$  = empirical constant = 10; and  $R$  = Richardson number.

$$R = [g \cdot z \cdot (T_a - T_s)] / [(u_z^2 (T_a + 273.2))] \quad (4-7)$$

where  $g$  = gravitational constant, 9.81 m/s<sup>2</sup>.

Once the energy available for snowmelt is determined from equation (4-1), the water equivalent of snowmelt can be determined as:

$$M = Q_m / (\rho_w \cdot L_f) \quad (4-8)$$

where  $\rho_w$  is density of water,  $L_f$  is latent heat of fusion, and  $M$  is the water equivalent of snowmelt.

The calculation can be started at any time. No melting of the snowpack is allowed until the net energy overcomes the cold content of the snowpack and it is isothermal. The energy supplied by the right side of

equation (4-1) will be first used to reduce the cold content or warm up the snowpack until it is ripe. After that, the energy will be used to melt snow. If the energy obtained by adding  $Q_{net}$ ,  $Q_h$ ,  $Q_s$  and  $Q_c$  is negative during calculation for each time step, then it is added to the cold content. The initial cold content of the snowpack, when starting the calculation, can be evaluated by:

$$Q_{cc} = h \cdot \rho \cdot C_p \cdot (T_0 - T) \quad (4-9)$$

where  $h$ ,  $\rho$  and  $C_p$  are depth, density and heat capacity of snow, respectively.  $T$  is snow temperature.  $T_0$  is the temperature of snow when it reaches isothermal condition of melting, usually 0 °C. We also do a similar calculation for upper part of soil column where snowmelt water can easily infiltrate organic soils and refreeze.

Studies in the Imnavait watershed [*Hinzman and Kane, 1991; Kane et al., 1990; Kane and Hinzman, 1993*] have consistently shown that the rates of snowpack ablation and the total time required for complete ablation are

greater on the east facing slope than the west facing slope. The deeper snowpack on the east-facing slope, caused by wind redistribution, will have a greater cold content, thus requiring more energy input before the snowpack becomes ripe. A deeper snowpack will also delay ripening by decreasing the amount of energy absorbed by the vegetation and soil surface. Also, east facing slopes receive the most direct radiation in the morning when it is cool, while west facing slopes receive the most direct radiation in the afternoon when air temperatures are at a maximum. Thus, topography has a major influence on snowpack distribution and rates of ablation. We introduce a slope correction adjustment to radiation measured on a horizontal plane to partially account for this effect [Hinzman et al., 1993].

The amount of solar energy received at the top of the atmosphere is a function of latitude, time of year, and time of day. At a given location on the surface of the earth, it is also influenced by the topography and the atmospheric conditions. The atmosphere exerts its influence through the thickness of the optical air mass which the radiation must penetrate (it is a function of

sun angle), the amount of water vapor, cloud cover, and turbidity. The primary topographic effects are slope, aspect and elevation [Coulson, 1975; Monteith, 1973]. The total shortwave irradiance,  $Q_{SW1}$ , on a horizontal surface is the sum of the direct irradiance,  $Q_{SWE}$  on a horizontal surface and the diffuse irradiance,  $Q_{SW2}$  [Campbell, 1977]:

$$Q_{SW1} = Q_{SWE} + Q_{SW2} \quad (4-10)$$

A simplified estimation described by *Hinzman et al.* [1993] is adopted here to apply a slope correction adjustment to shortwave irradiance measured on a horizontal plane. After determining slope effect on  $Q_{SWE}$  to get  $Q'_{SWE}$ , corrected shortwave radiation estimates of spatial  $Q'_{SW1}$ , can be obtained as:

$$Q'_{SW1} = Q'_{SWE} + Q_{SW2} \quad (4-11)$$

Other factors such as cloud cover and elevation were accounted for from our radiometer measurements at the ground surface.

#### 4.4.1.B. Degree-Day Method

For many areas in the Arctic, we do not have the required data for an energy balance. So, a simple degree-day method [Kane et al., 1993, 1997; Hinzman and Kane, 1991], which requires less data, has been added in the program as an option. This algorithm can be written as:

$$M = C_s(T_a - T_s)/s \quad \text{when } T_a > T_s \quad (4-12)$$

where  $M$  is melt-water equivalent of snow in depth,  $C_s$  is degree-day melt factor,  $T_a$  is air temperature,  $T_s$  is threshold value of air temperature, and  $s$  is time steps per day (1 day or 24 hours). Equation (4-12) is valid only when  $T_a > T_s$ . If  $T_a < T_s$ , then simply let  $M = 0$ .

In order to apply degree-day method, the model should be started when the snow is isothermal. This simplified approach does not lend itself to handling cooling of the snowpack [Kane et al., 1997; Kuusisto, 1984]. Bengtsson [1982] presented a method to account for diurnal refreezing in the degree-day method.

#### 4.4.2. *Evapotranspiration*

Evapotranspiration (ET) is one of the major components that affect energy and water balances in the Arctic. A study shows that ET represents 30% to 60% of annual precipitation in Imnavait watershed [Kane et al., 1990]. In the summer with almost 24 hours of sunshine daily, about 40% to 65% of net radiation is consumed by the ET process in the Arctic [Kane et al., 1990]. In this model, both energy balance method and the Priestley-Taylor method [Priestley and Taylor, 1972] have been used to evaluate ET. The Priestley-Taylor method is included because like the degree-day method for snowmelt, it requires substantially less input data.

##### 4.4.2.A. *Energy Balance Method*

The energy balance technique is a widely used method in determining evaporation and/or transpiration [Kane et al., 1990]. It can be expressed as:

$$Q_{et} = Q_{net} + Q_s + Q_c \quad (4-13)$$

where  $Q_{et}$  is the energy utilized for evapotranspiration from the surface.  $Q_{net}$  is net radiation transferred at the surface.  $Q_c$  is sensible heat flux between the watershed surface and air and is determined in the same way as it is discussed in snowmelt section.  $Q_s$  is conductive energy between surface and subsurface and can be obtained from Fourier's Law:

$$Q_s = K_s \cdot \frac{T_x - T_s}{x} \quad (4-14)$$

where  $K_s$  is the thermal conductivity of soil,  $T_x$  is soil temperature at depth  $x$  below the surface, and  $T_s$  is soil surface temperature. The horizontal advection is not considered.

The amount of water that is lost through evapotranspiration then can be evaluated as:

$$M_{et} = \frac{Q_{et}}{\rho_w \cdot L_v} \quad (4-15)$$

where  $M_{et}$  is the water loss.  $\rho_w$  is density of water.  $L_v$  is latent heat of vaporization.

#### 4.4.2.B. Priestley-Taylor Method

The Priestley-Taylor method [Priestley and Taylor, 1972] is an alternate technique for ET calculation. In the energy balance method, some components like sensible and latent heat fluxes are difficult to accurately quantify and the technique requires large data sets. By using a technique similar to the Bowen Ratio method [Bowen, 1926], the Priestley-Taylor equation was derived in the following form:

$$Q_{\text{net}} = \alpha \left( \frac{s}{s + \gamma} \right) (Q_{\text{net}} - Q_s) \quad (4-16)$$

where  $\alpha$  is an evaporability parameter relating to actual equilibrium evaporation,  $s$  is the slope of the specific humidity and temperature curve and  $\gamma$  is a psychometric constant in terms of specific humidity. After conducting studies at a well drained, upland lichen heath area in a subarctic region, Rouse and Stewart [1972; Stewart and Rouse, 1976] found that  $\alpha$  has an average value of 0.95 and that  $s/(s + \gamma)$  could be



simplified to a linear function of the screen air temperature as:

$$\frac{s}{s + \gamma} = 0.406 + 0.011 T_s \quad (4-17)$$

*Kane et al.* [1990] used a similar value of  $\alpha$  when evaluate ET from a small watershed in Northern Alaska. *Rouse et al.* [1977] found that the evaporability parameter  $\alpha$  varies with vegetation type and soil moisture content. In the model developed here, evaporation and transpiration were not evaluated separately, instead they were combined into a single algorithm. Since the soil moisture content can be predicted at each time step in our model, an empirical relationship has been used to evaluate the  $\alpha$  value expressed as:

$$\alpha = R \cdot \alpha_1 + \alpha_2 \quad (4-18)$$

where  $R$  is the degree of saturation of the soil and is defined as the ratio of actual soil moisture content by

volume to the saturated moisture content by volume.  $\alpha_1$  is a parameter that accounts for the moisture condition of the soil.  $\alpha_2$  is a parameter that accounts for vegetation effect. The vegetation distribution is assumed uniform for the arctic watersheds discussed here and  $\alpha_2$  is assumed constant. The amount of ET can be calculated by using equation (4-15) as shown above. When the soil is saturated ( $R = 1$ ), the ET reaches its potential value. This is an indirect method to address the combined effect of evaporation and transpiration [Waelbroeck, 1993].

#### **4.4.3. Flow Routing**

##### **4.4.3.A. Subsurface Flow Routing**

In the Arctic, continuous ice-rich permafrost acts like an impermeable boundary to water flow. So the subsurface hydrologic processes are limited to the shallow active layer [Kane et al., 1989]. We have defined three layers within the soil profile as shown in Figure 4-8. Each layer has its own characteristics such

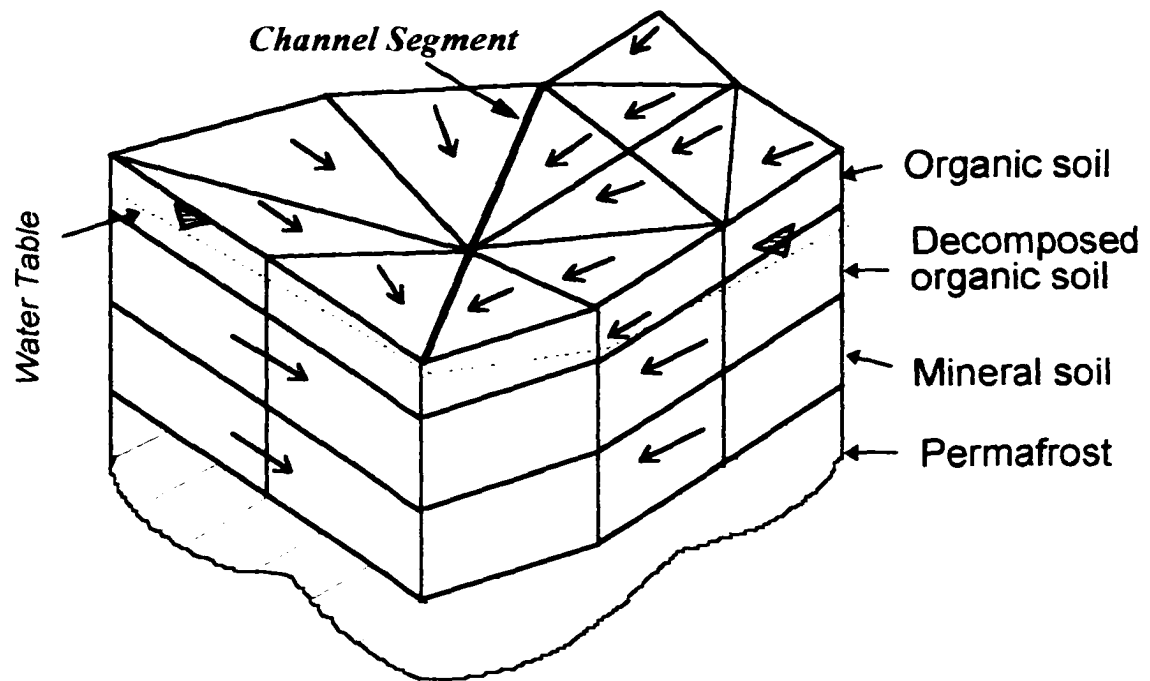


Figure 4-8. Representation of active layer and permafrost in the model.

as thickness, hydraulic conductivity and moisture holding capacity. The organic soils are highly porous and can absorb moisture quickly in response to spring snowmelt and summer precipitation. The mineral layer, however, is generally saturated throughout the summer, has a lower hydraulic conductivity and maintains the water table near the top of the mineral soil. It is reasonable to assume then that infiltration is a very rapid process as compared to lateral flow. Infiltrating water typically only has to travel about 20 to 30 cm or less vertically through porous organic soil to reach the water table in the active layer. Therefore, the time required for infiltration is neglected. For each layer  $i$  at any element  $j$ , the lateral flow rate is calculated by Darcy's Law (See Chapter VI for validation):

$$q = K_i \cdot s_j \cdot A_i \quad (4-19)$$

where  $K_i$  is hydraulic conductivity of layer  $i$ ;  $s_j$  is the slope of element  $j$ , which initially is the geographic slope, and later on is modified by considering the water table in surrounding elements, and then it becomes a hydraulic gradient;  $A_i$  is the flow

cross section of each layer, which varies depending on how flow from an element is partitioned to neighboring elements (Figure 4-3) and the depth of thaw. The total amount of subsurface flow within a time step  $\Delta T$  from an element  $j$  is:

$$Q_j = \sum_i K_i \cdot s_i \cdot A_i \cdot \Delta T \quad (4-20)$$

After each time step calculation, the storage of an element is compared with its level of saturation to determine if there is subsurface flow downslope. The time step  $\Delta T$  for subsurface flow should be such that water will not flow past the whole element within one time period.

#### **4.4.3.B. Overland Flow Routing**

*Anderson and Burt* [1990] discussed various aspects of overland flow. As we mentioned earlier, the topsoils in the arctic watershed are highly porous organics where infiltration rates are very high. The soils become saturated up to the surface, by a rising water table

from below [Kane et al., 1991a]. In our model, we use the flow mechanism that overland flow exists when the soil moisture in each element exceeds saturation.

Although overland flow could be represented completely by the Saint-Venant equations [e.g. Chow et al., 1988; Bedient and Huber, 1992], the kinematic wave solution has been shown to be an excellent tool for most cases of overland flow [Anderson and Burt, 1990; Ciriani et al., 1977; Eagleson, 1970]. Under the kinematic wave assumption, the friction slope ( $S_f$ ) and the bed slope ( $S_b$ ) are equal, and Manning's equation can be used to express the relationship between flow rate and depth:

$$q = v \cdot A = \frac{C}{N} AR^{2/3} \sqrt{S_b} \quad (4-21)$$

where  $q$  is the rate of lateral flow per unit length,  $v$  is fluid velocity,  $R = A/P$ , the hydraulic radius,  $P =$  wetted perimeter,  $N =$  roughness coefficient,  $C =$  unit factor. For a sheet flow as has been considered in this model,  $R \approx y$ . So the cross sectional area  $A = B \cdot y$ , as shown in Figure 4-9, where the width  $B$  depends upon the

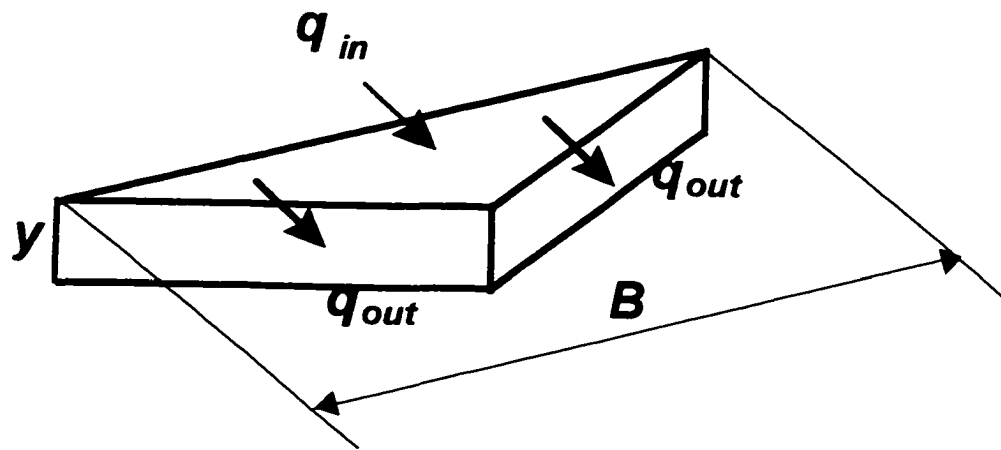


Figure 4-9. Overland flow components within an element.

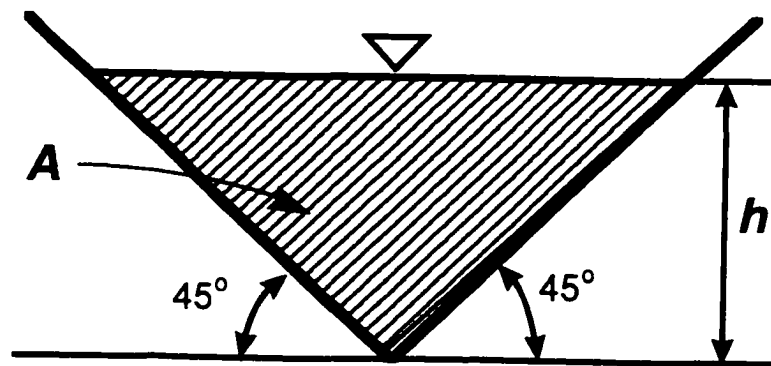


Figure 4-10. Channel flow cross section.

length projected on the plane perpendicular to flow direction. The overland flow of each element in each time step  $\Delta t$  can be explicitly written as:

$$(\Sigma q_{i,t} - \Sigma q_{i,t-\Delta t}) \cdot \Delta t = \Delta s \quad (4-22)$$

and

$$q = \frac{C}{N} B \sqrt{S_0} Y^{3/2} \quad (4-23)$$

where  $\Delta s$  is the change of storage in each element within  $\Delta t$  which is limited by the Courant condition,  $\Delta t \leq \Delta x/c$  [Bedient and Huber, 1992; Ciriani et al., 1977], where  $c = v \pm \sqrt{gy}$ ,  $\Delta x$  is the smallest grid scale of an element,  $v$  is overland flow velocity, and  $g$  is the gravitational constant.

After each time step, a new soil moisture content for each element can be obtained and then the uniform water depth of each element,  $y$ , can be determined by comparing the new soil moisture content and the storage capacity. This new  $y$  is used to calculate flow rate



leaving/entering each element based on equation (4-23). It should be noted that, when conducting mass balance for each element using equation (4-22), precipitation input, evapotranspiration and contribution from subsurface flow should be included. The subsurface flow contribution to equation (4-22) has been equally distributed over  $\Delta T$ . This is based on the fact that subsurface flow is far slower than overland flow. So, within each  $\Delta T$ , overland flow routing is carried out for many relative shorter time steps than  $\Delta T$ . The variation of subsurface flow over these shorter time steps is neglected within each  $\Delta T$ .

#### **4.4.3.C. Channel Flow Routing**

The same method as overland flow has been applied to channel flow routing. Within each reach of a channel, Manning's formula shown in equation (4-21) can be applied. A triangular cross section has been assumed for channel flow as shown in Figure 4-10. So,

$$R = A/P = h^2 / (2\sqrt{2}h) = h / (2\sqrt{2}) \quad (4-24)$$

where  $R$  is hydraulic radius,  $A$  is the flow cross section area,  $P$  is wetted perimeter, and  $h$  is the flow depth. The mass balance and flow calculation for each channel can be characterized as:

$$(\Sigma q_{in} - \Sigma q_{out}) \cdot \Delta \tau = \Delta s \quad (4-25)$$

$$q = \frac{C}{2n} \sqrt{S_e} h^{8/3} \quad (4-26)$$

where  $\Sigma q_{in}$  is the sum of flow rate that is entering a channel segment,  $\Sigma q_{out}$  is the sum of flow rate that is leaving the same channel segment,  $\Delta \tau$  is the time step for channel flow,  $\Delta s$  is change of water storage in the channel segment,  $h$  is the flow depth,  $C$  is a unit factor,  $n$  is roughness coefficient, and  $S_e$  is the energy slope which is equal to the slope of bed plus a modification by considering the upstream and downstream depths. After each time step  $\Delta \tau$ , the mass balance is conducted based on equation (4-25) by considering the amount of flow going into each channel reach from upstream, the overland flow from its adjacent elements,

and the flow leaving each channel reach. A new water depth  $h$  then can be obtained and is used to determine how much flow is going out during the next time step based on equation (4-26). The choice of time step  $\Delta t$  follows the same condition, the Courant condition [Bedient and Huber, 1992; Ciriani et al., 1977], as described before. But the channel flow velocity will be considerably higher than the velocity in overland flow. Again, by accepting the fact that channel flow is much faster than overland flow, the contribution from overland flow to the channel segment is averaged over  $\Delta t$ .

#### 4.5: Discussions

Most of the recent distributed hydrologic models have been developed for temperate regions where the hydrologic regime is dissimilar to the Arctic. This fact encouraged us to develop a process based, spatially distributed hydrologic model to accommodate this unique environment.

*Hinzman and Kane* [1991] have modeled hydrologic processes during snowmelt using the reservoir based HBV model [*Bergström*, 1976] for Imnavait Creek and have demonstrated that such a model can be used for arctic watersheds. The degree day approach for snowmelt adequately predicted ablation and simulated flows that compared favorably with measured discharges. However, we are now faced with the problem of predicting spatially distributed soil moisture levels for use in trace gas flux models of methane and carbon dioxide from the abundant carbon-rich soils of the Arctic or predicting nutrient fluxes within a watershed. Deriving spatially distributed soil moisture at a relatively large watershed scale was the stimulus for developing the process-based model described here.

The concept of developing and utilizing physical based hydrologic models has been questioned by both *Grayson et al.* [1992] and *Beven* [1989]. Both groups have considerable experience with developing and utilizing such models and are well versed in the spectrum of problems associated with these models. *Grayson et al.* [1992] question both the perception of

model capabilities and the appropriateness of algorithms with their inherent assumptions. Still, we are faced with the task of making predictions on various hydrologic processes such as nutrient, sediment or contaminate transport, soil moisture distribution or runoff response at various points within a watershed. Numerous reasons exist why such models perform badly and most of these reasons are raised by *Grayson et al.* [1992]. *Beven* [1989] presents limitations associated with physically based models and expresses his concern that their use can be abused if a user does not have a realistic attitude. Both groups concede that the development of physically-based models will proceed and that there are existing problems that can only be solved by physically-based models.

The simpler the physical structure of the catchment to be studied, the better the chances of the model performing adequately. Uniformity of topography, soils, and vegetation, along with a simple subsurface groundwater system will enhance model performance. Complex subsurface flow systems in temperate regions are difficult to model because hydraulic properties are

highly variable and it is extremely costly to instrument and monitor groundwater systems. The task of modeling subsurface flow in the Arctic is made simpler by the presence of continuous permafrost that effectively limits subsurface flow to the upper 50 cm of the soil column. The residence time for the active layer, that layer that freezes and thaws each year, is on the order of one year. The thin active layer has such a limited moisture storage capacity that the annual precipitation (snowpack water equivalent and rain) volume is about equal to the maximum amount of water stored in the active layer at maximum depth of thaw. For temperate watersheds, the residence time is generally several orders of magnitude higher than this.

The quality of output from models is closely aligned with the quality of the parameters and input data used to drive them; physically-based, spatially distributed models are no exception to this rule. To adequately evaluate a spatially distributed model, it is necessary to have independent spatial data sets. Remotely sensed data is the most appropriate mechanism for this purpose. For example, *Wigmosta et al.* [1994] used AVHRR satellite

data to monitor the distribution of snow in the watershed and compared this with simulated results during ablation. We are attempting to measure near surface soil moistures with synthetic aperture radar (SAR) and use this as a check on the spatial performance of the model [Kane et al., 1996]. This technique shows promise in this region of the world because of the limited height of vegetation and the high level of wetness due to the close proximity of permafrost to the surface.

Grayson et al. [1992] also raised the issue that model development was not in concert with field programs designed to test the models, and therefore the linkage to reality is lost. In this study, we were fortunate to have the resources to carry out a field program in parallel with the model development. It would have been futile to proceed ahead with the model without a field program in the Arctic; the data to test the MATH model does not presently exist for most catchments in the circumpolar countries. Our approach was to collect data at three watershed scales (2.2, 146 and 8140 km<sup>2</sup>) and apply the model to each, starting with the smallest.

Several watershed attributes in the Arctic are conducive to the development and success of a spatially distributed, physical based hydrologic model. The existence of permafrost and how it limits the depth of the subsurface system has already been discussed. The lack of both trees and diversity of arctic plants restricts the variability in vegetation cover. This watershed is completely undeveloped, therefore the number of land surface classifications are reduced. On the negative side, the lack of hydrologic and meteorologic data in the Arctic limits the application of such models to other areas.

We entertained the thought of using an existing spatially distributed, physically based hydrologic model for the watersheds being studied in the Alaskan Arctic. For several reasons, we decided to develop our own model. First, vegetation in the Arctic is limited in size and plant diversity compared to most ecosystems. This does not mean that transpiration is not important; transpiration coupled with evaporation is the main mechanism of water export out of low gradient arctic watersheds during the summer months. Second, the surface soils are usually organic with very high



infiltration rates and hydraulic conductivities. Third, permafrost is continuous with a very shallow active layer that results in a water table that is quite close to the ground surface. The time period for water to enter the ground surface and reach the water table is quite short relative to the time to move downslope. Downslope water movement is parallel to the ground surface with the gradient being approximately the ground surface slope. The active layer is continually freezing or thawing throughout the year and none of the existing models address this issue. Finally, surface drainage features, i.e. water tracks, are an integral component of the drainage network and must be included to properly simulate hillslope hydrologic processes.

We have two aspects of our modeling exercise that we feel could be improved upon. It is important to capture the essence of the drainage network before one proceeds ahead with running the model. The scale of the digital elevation data will determine the detail one generates with a drainage model. In the Arctic, very subtle features called water tracks efficiently drain hillslopes. The existence of these drainage features is best observed during snow melt or significant rainfall

events. Vegetation can also be used as an identifier for water tracks. Water movement in the water tracks is more efficient than overland flow, which is more efficient than subsurface flow; so it is important to model these features correctly.

Snow damming of melt water retards the runoff event. In the headwater basins, melt water collects in the valley bottom until a dramatic slush flow cuts a channel through the snowpack. We do not understand the controlling processes well enough to incorporate snow damming into the model at this time.

For the three routing routines in the model, subsurface ( $\Delta T$ ), overland ( $\Delta \tau$ ) and channel ( $\Delta \tau$ ) flow, calculations were performed using different time steps with subsurface being the longest and channel the shortest time period. Finally, parameter values used in this model were taken from complementary field research and related published papers. There was no attempt to vary parameter values to improve simulated output or do any type of sensitivity analyses.

#### 4.6: Conclusions

A process based, spatially distributed hydrologic model has been developed for arctic regions; the first of its kind for arctic environments. The model consists of two parts. The first part is watershed drainage delineation based on the DEM data. By dividing the watershed into triangular elements, the area, aspect, and the slope of each element can be determined. The drainage area for above any point in a basin and the channel network for a watershed can be simulated. The model also has the ability to analyze the stream orders and drainage density based on a given scale of DEM data.

The second part of the model deals with hydrologic processes and their interactions within the arctic environment. The model is capable of simulating distributed processes such as snowmelt, subsurface flow, overland flow, channel flow, and evapotranspiration; output can be obtained on moisture content distribution, snow distribution, and other distributed results for each time step. Because of the existence of permafrost which limits the subsurface flow within a relative shallow active layer and the fact that we neglect the

infiltration process due to the high porosity of organic soils, subsurface routing is easier compared to other non-permafrost regions. Another factor that makes subsurface modeling easier than areas with deep aquifers is the limited subsurface storage within active layer.

Some process algorithms discussed in this paper have room for improvement in the future. The soil thawing/freezing process is not fully incorporated as a physically based, spatially distributed subroutine. Instead, it is currently simulated as a simple function of air temperature (degree-hour method). Evaporation and transpiration were not simulated separately, instead they were coupled into one process, evapotranspiration. The snow damming process, as often seen during the snowmelt season in the headwater basins, has not been incorporated in this model yet. This causes hydrograph discrepancies during the snowmelt season. Like all other spatially distributed models, very large data sets are required to utilize MATH model fully. The performance of each component in this model and the integrated response of this model on two arctic watersheds of different sizes are discussed in Chapter VI.

## Chapter V: Data Input for the Model

### 5.1: Meteorological Data

One of the characteristics in spatially distributed hydrologic modeling is a usage of extensive data input to drive the model. For distributed simulations, spatially varied data are essential not only for the model input but also for the model verifications. Obtaining good quality data is not always easy, especially for an arctic environment where severe weather and limited road access prevents routine instrumentation and operation checkups. Nevertheless, considerable instrumentation has been installed with great effort and logistical costs in the Kuparuk River Basin (Figures 3-1, 3-2 and 3-3) since 1993. Three gauging stations were installed to monitor the continuous discharge for two streams and one water track. In addition, the U.S. Geological Survey operates a gauging station on the Kuparuk River near the coast.

Seven major meteorological stations were set up for measurement of many climatic variables such as wind speed and direction, air temperature, relative humidity,

precipitation, and various radiation fluxes at sites extending from the foothills of Brooks Range to the coast of the Arctic Ocean (Figure 3-1). Some soil temperature measurements are made at those sites also. In addition, five additional micro-sites were installed in 1996 in the Upper Kuparuk basin for the measurement of air temperature, wind speed and relative humidity.

Radiation fluxes play a major role in the thermal related processes. Figure 5-1 shows the measured radiation fluxes at a site within Imnavait watershed. Before the snowpack has melted, the albedo is high, producing higher reflected shortwave radiation. Right after the snow melt, incoming net radiation increases because of the lower albedo of vegetated soil surface than that of snow. Air temperature has a significant impact during the snowmelt since the net radiation and convective heat flux are the two main driving forces [Kane et al., 1991a]. Figure 5-2 shows the hourly temperature variation at Imnavait watershed in 1993. It is clear from this data that the air temperature varied seasonally (Figure 5-2) and diurnally. Wind speed, like air temperature, also influences the surface energy

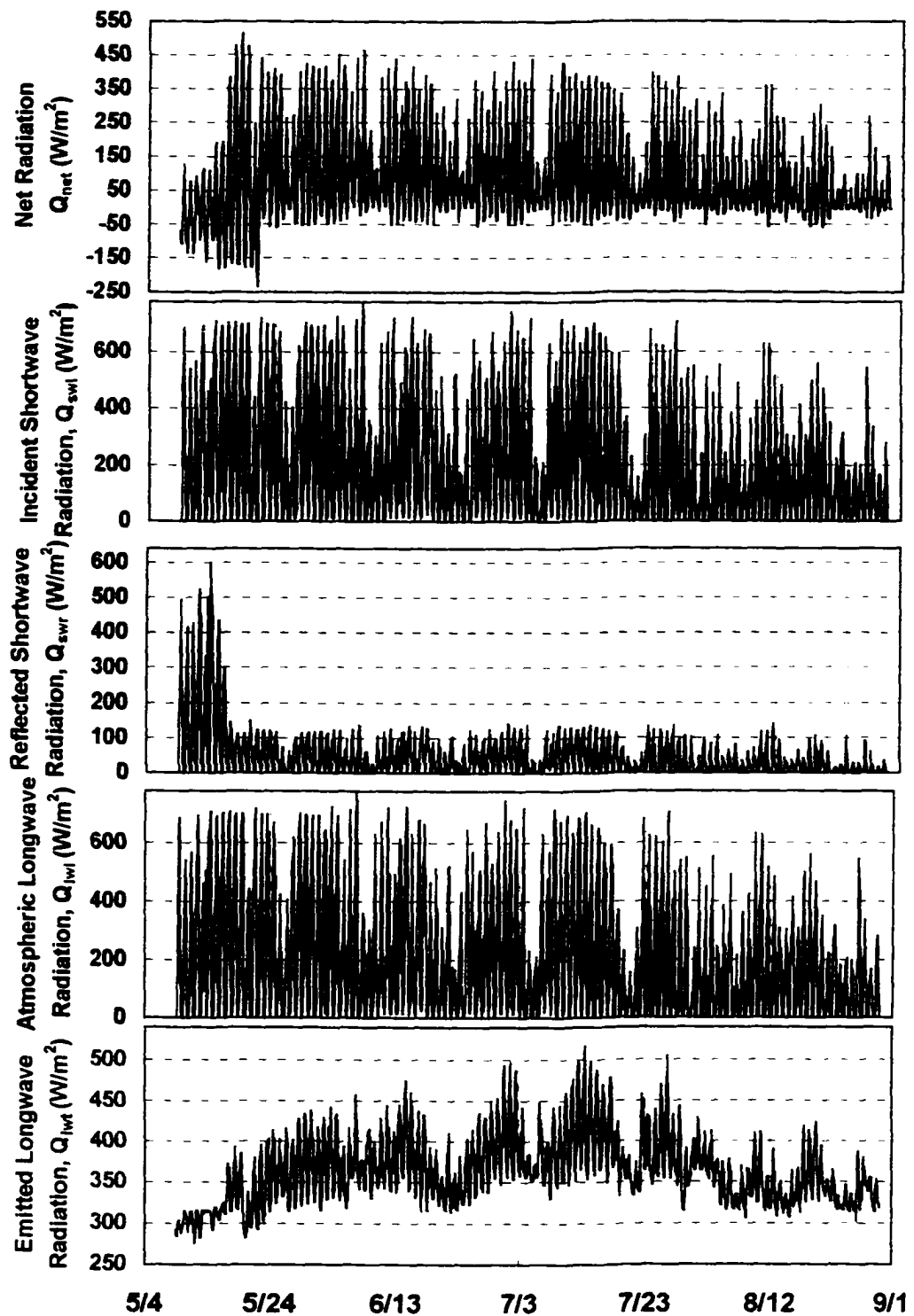


Figure 5-1. Measured radiation fluxes at a station within Innavait watershed, 1993

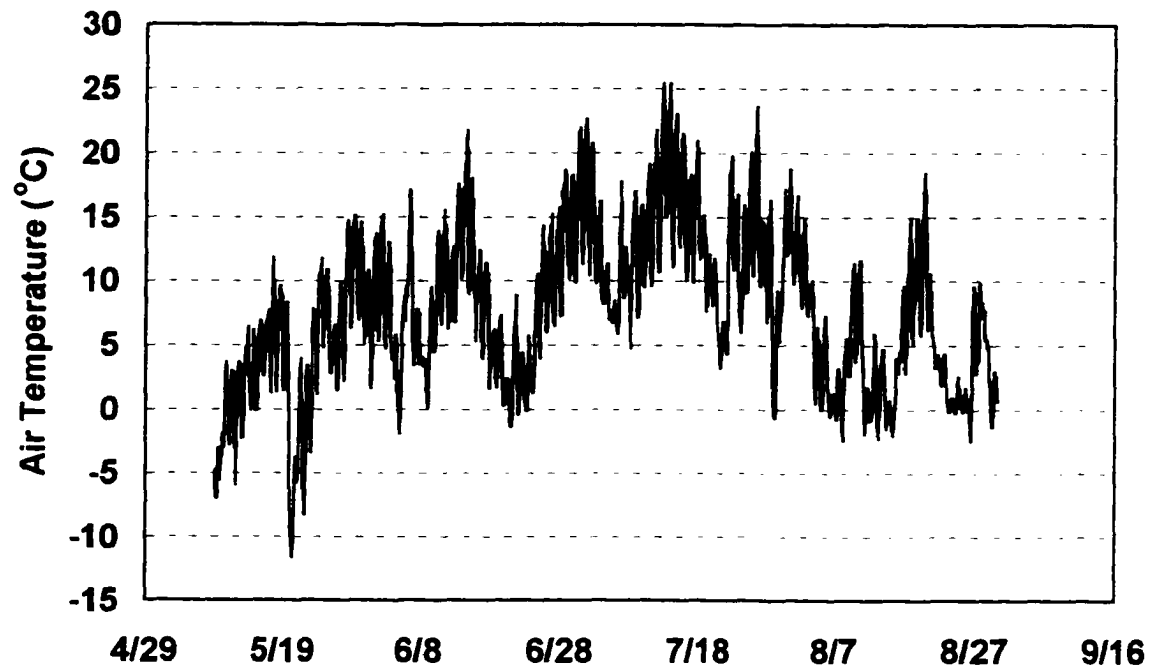


Figure 5-2. Seasonal variation of measured hourly air temperature at a station within Innavait watershed, 1993



balance processes (in both latent heat and sensible heat flux calculations). From Figure 5-3, the hourly wind speed varies within the range between 0.7 m/s and 8 m/s. Relative humidity changes compatibly with precipitation events as shown in Figure 5-4.

Imnavait watershed is relatively small area where most input variables can be approximately treated as uniformly distributed. For the Upper Kuparuk River basin, however, this assumption of uniformity is no longer valid. Spatially distributed input data should be used, especially for those important variables like precipitation and air temperature. Figures 5-5 and 5-6 show precipitation distribution maps of one hour at two different times. Different precipitation distribution exists across the watershed. Distributions of wind speed and air temperature over the watershed at two different times are shown in Figures 5-7, 5-8, 5-9, and 5-10. These figures show that the distributions of wind speed and air temperature, like the case for precipitation, are greatly varied spatially and temporarily. So, it is necessary to use distributed data sets over time for Upper Kuparuk River basin.

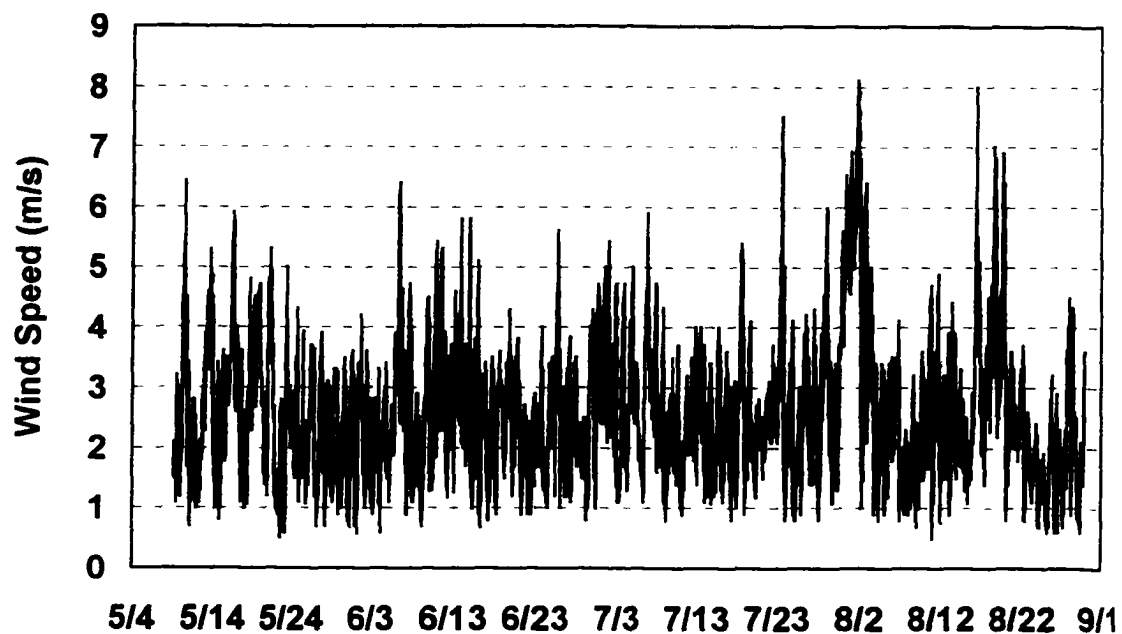


Figure 5-3. Measured hourly wind speed at a station within Imnavait watershed, 1993.

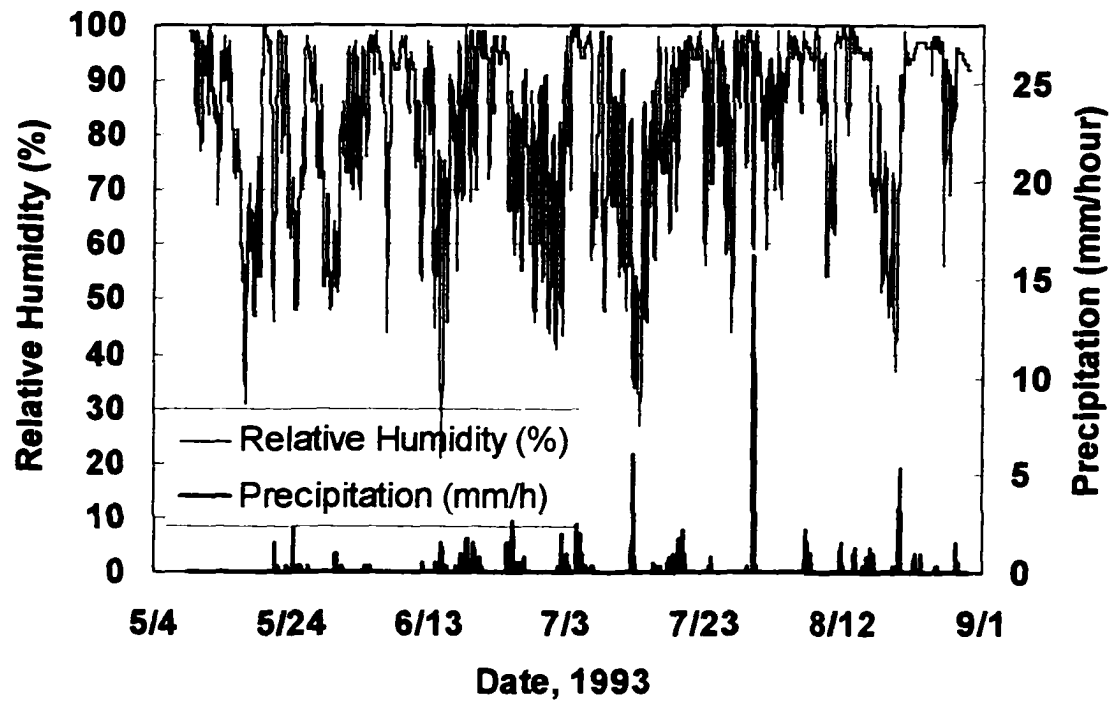


Figure 5-4. Measured precipitation and relative humidity at a station within Imnavait watershed, 1993.

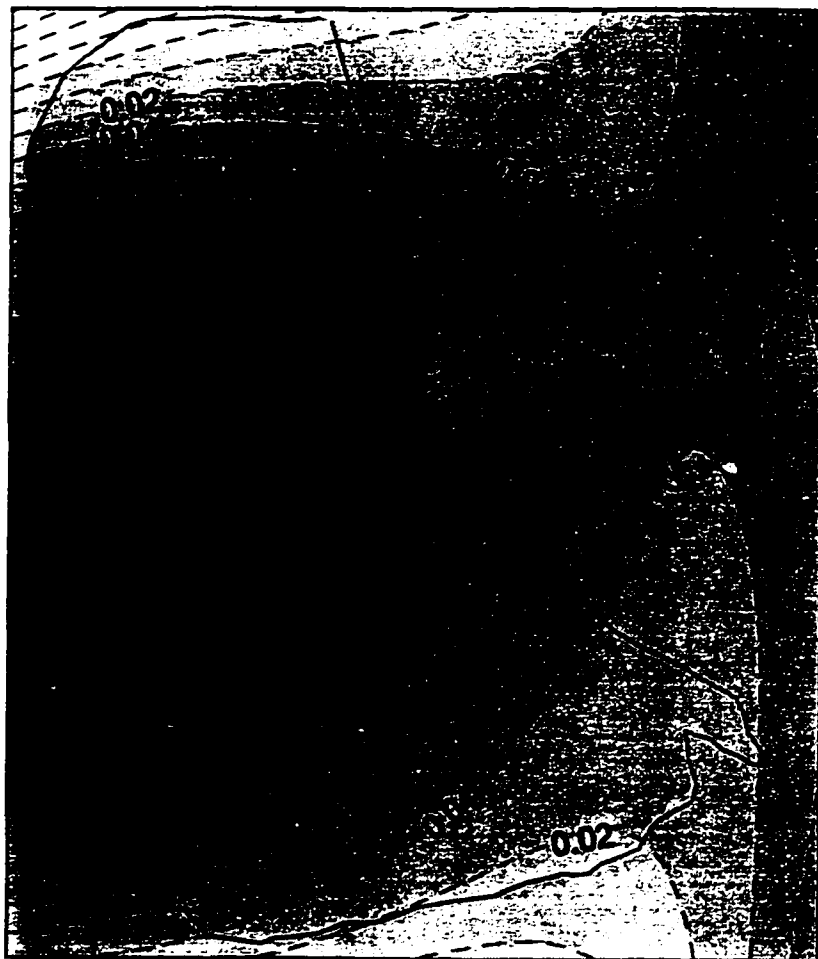


Figure 5-5. Hourly precipitation distribution (mm/hour) on June 24 (noon), 1996, at Upper Kuparuk River Basin, Alaska.

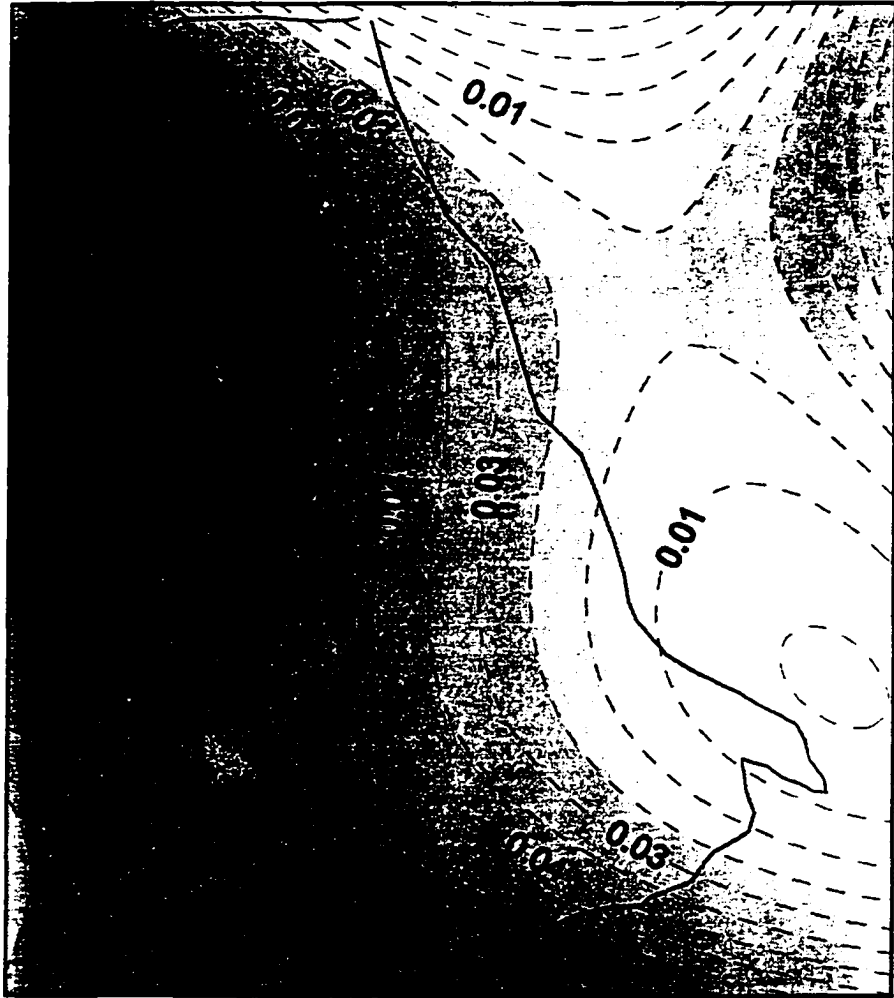


Figure 5-6. Hourly Precipitation distribution (mm/hour) on August 15 (noon), 1996, at Upper Kuparuk River basin, Alaska.

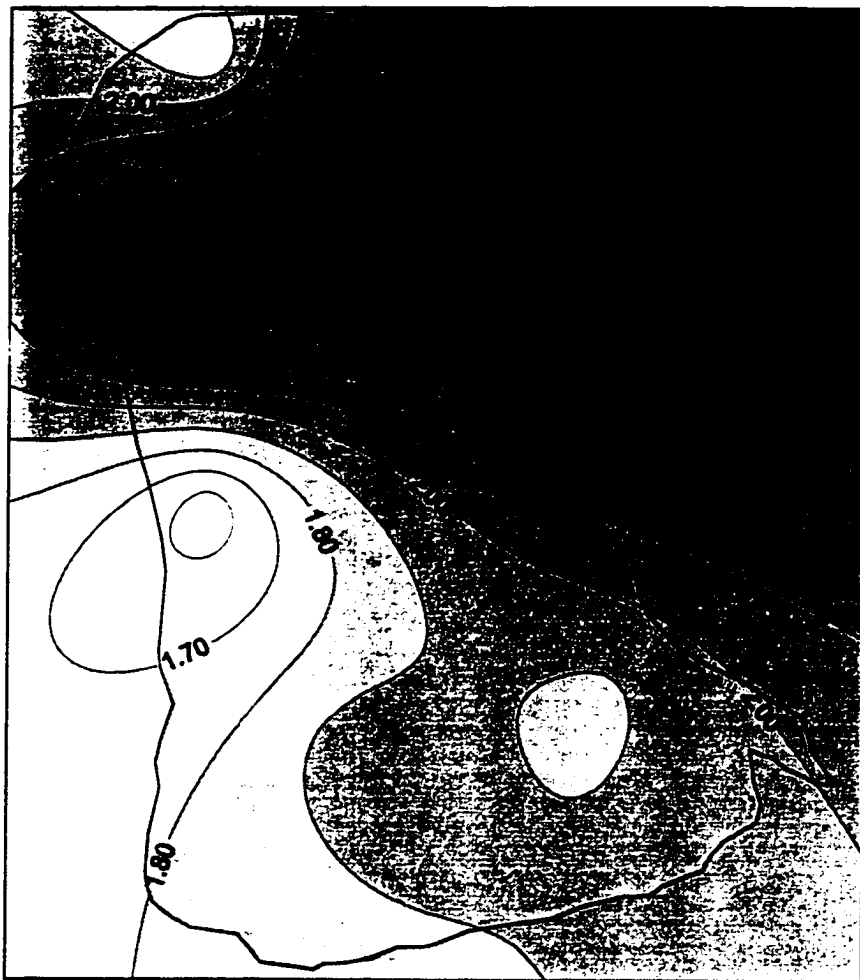


Figure 5-7. Wind speed distribution (m/s) on June 24 (noon), 1996, at Upper Kuparuk River basin, Alaska.

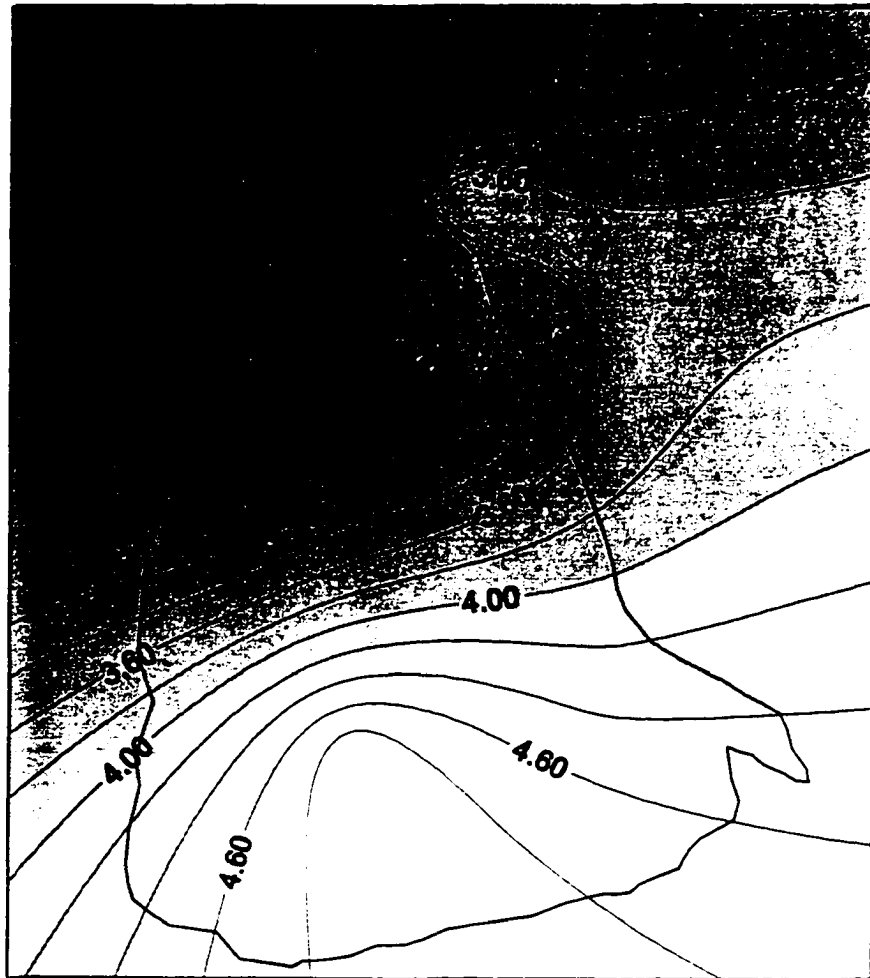


Figure 5-8. Wind speed distribution (m/s) on August 15 (noon), 1996, at Upper Kuparuk River basin, Alaska.

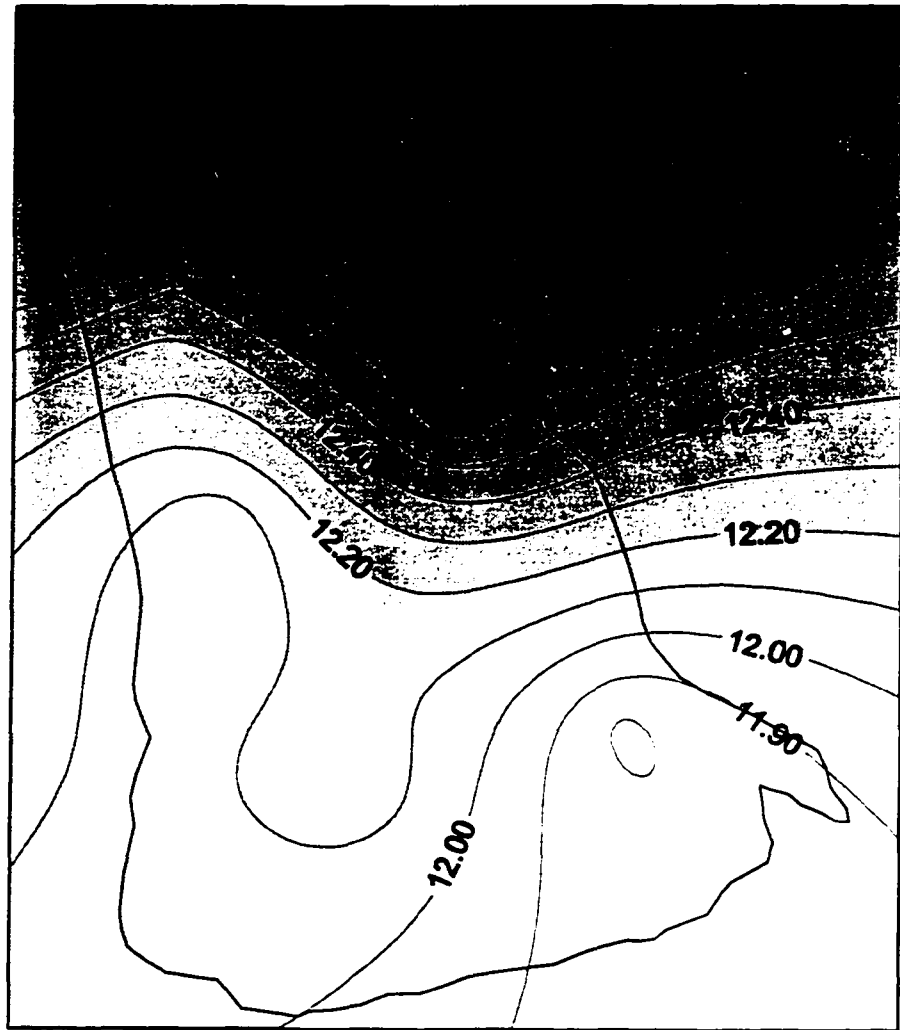


Figure 5-9. Air temperature distribution ( $^{\circ}\text{C}$ ) on June 24 (noon), 1996, at Upper Kuparuk River basin, Alaska.



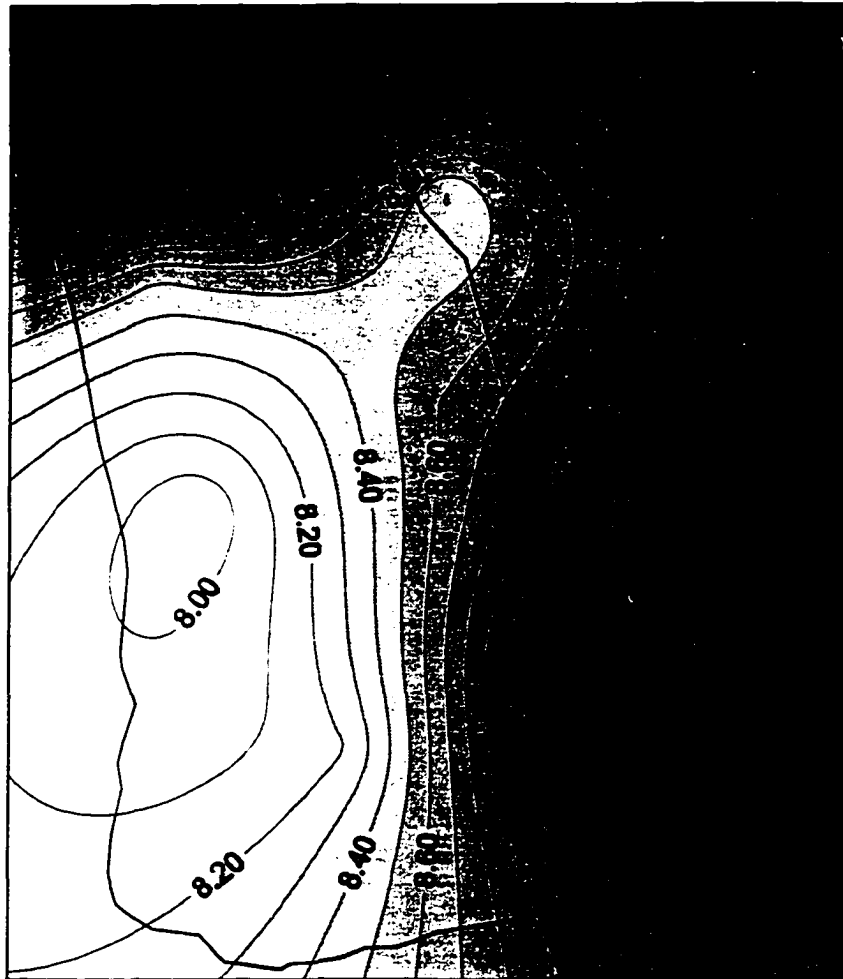


Figure 5-10. Air temperature distribution ( $^{\circ}\text{C}$ ) on August 15 (noon), 1996, at Upper Kuparuk River basin, Alaska.

Spatially distributed input data were based on the measured data obtained at several meteorological stations spread over the watershed. By using a Kriging routine, visually informative contour and surface plots can be shown from the irregularly spaced data. After selecting a compatible scale and other options within the software [Keckler, 1995], distributed data sets can be generated into digital files.

## **5.2: Parameters**

Certain parameters need to be defined before running the model. The parameters used in the model and their values are summarized in Table 5-1. Detailed descriptions of these parameters can be found in Chapter VI. Table 5-2 is a list of all variables and their units used in this model.

## **5.3: Model Execution/Computational Notes**

The program codes contains two main parts. The first part deals with watershed delineation. The program first reads in a file containing digital elevation data for each node and element number with corresponding node

## **NOTE TO USERS**

**The original manuscript filmed by the school contained missing page(s).**

**136-139**

**This reproduction is the best available copy.**

**UMI**

numbers. Then the model determines those elements that are located at watershed boundaries and the relationship between elements. Several subroutines are designed to carry out different calculations including area, flow direction, slope, aspect for each element, drainage area, and channel orders. The geometric processes only need to be simulated once before physical process simulations. During and at the end of the calculations, some desired information such as the number of channel segments, the number of flat elements, how many channel segments for each order, and drainage area for the desired gauging station is retained in a file. An algorithm examines the calculated drainage network to ensure there are no loops within the channel pattern.

The algorithm for the physical processes is executed under the time loop. The simulation starts at a specific date when required data are available. Within the time loop, the input data are read in first, then the subroutines to simulate the soil thaw, snowmelt, evapotranspiration, subsurface flow, overland flow, and channel flow follow, but not always with the same time increment. The time increment for channel flow ( $\Delta t$ ) is

smaller than that for overland flow ( $\Delta t$ ) and both are smaller than that for subsurface flow ( $\Delta T$ ).

## Chapter VI: Model Applications

### 6.1: Introduction

A physically based, spatially distributed hydrologic model offers several advantages [Goodrich, 1990; Woolhiser et al., 1990; Wigmosta et al., 1994; Beven, 1996]. Such a model is more broadly applicable, requiring less calibration than conceptual or empirical models. A spatially distributed model provides greater amounts of detailed information over the entire basin rather than just lumped basin averages. Currently existing physically based, spatially distributed hydrologic models have been developed for temperate regions where the hydrological regime is different from the arctic regions. Extreme temperatures, a long winter with limited solar radiation, a short growing season, the accumulation and redistribution of snow by wind, the freezing and thawing of the active layer, the existence of permafrost, and low, sparse vegetation cover are some of the characteristics of the extreme arctic environment. Arctic energy and mass processes play a key role in many global processes such as atmospheric

and oceanic circulation [Alley, 1995]. Arctic regions represent potentially important sources and/or sinks of greenhouse gases. There is evidence that the arctic tundra is currently a net source of CO<sub>2</sub> and CH<sub>4</sub> to the atmosphere and the interactions among moisture, temperature and vegetation type will impact future trace gas fluxes from the Arctic [Oechel et al., 1993; Burton et al., 1996]. Some research suggests [Roots, 1989; Kane et al., 1991b; Hinzman and Kane, 1992] that arctic regions are more sensitive to climate change. As hydrology is the main linkage between atmospheric and terrestrial/aquatic systems, it is important to scientifically improve our knowledge of hydrology of this region.

One tool for doing this is a physically based, spatially distributed hydrologic model. We refer to the MATH model as a process based, spatially distributed hydrologic model. Most processes in the model are simulated with equations that are physically rooted. However, the use of Manning's equation in routing and a mass transfer function in the calculations of the

sensible and latent heat fluxes cannot be derived from fundamental equations of mass, momentum and energy.

In this paper, results from such a model are presented using spatially distributed data collected over several years from Imnavait Creek and the Upper Kuparuk River basin on the North Slope of Alaska. Details on model construction are discussed in Chapter IV.

## 6.2: Study Area

### 6.2.1. *Imnavait Watershed*

Imnavait Creek is a small (2.2 km<sup>2</sup>) headwater basin located between the Toolik and Kuparuk Rivers in the northern foothills of the Brooks Range (latitude 68°30', longitude 149°15'). This northern draining basin is a combination of areas in which 78% west-facing slope, 17% of east-facing slope and 5% of valley riparian area. At the headwater, the hillslopes are around 10% on the west-facing slope and slightly greater than 1% on the east-facing slope. This is in contrast with the greater than 13% west-facing slope and greater than 7% east-facing slope at the outlet. The average elevation is



about 900 meters (Figure 3-3). Most of the field measurements were conducted in the center of the basin on the west-facing slope where the slope averaged 10% and on the ridge just east of the gauging site. Continuous permafrost (>250 m) [Osterkamp et al., 1985] exists with an active layer depth of usually 40 to 60 cm, which typically has about 10 cm of organic soil, 10cm of highly decomposed organic soil that overlays a mineral soil of glacial till. There is more organic material in the valley bottom than on the ridges. Tussock tundra is the dominant vegetation type [Kane et al., 1989]. Numerous water tracks are distributed over the hillslopes and are very efficient at conveying water off the slopes. Although quite obvious in aerial photography, most of these water tracks are difficult to detect on the ground, except when flowing with water during snowmelt and major rainfall events. Climatic data are collected at a meteorological station within the basin. These data include precipitation, wind direction, longwave and shortwave radiation fluxes, and profiles between the surface and 10 m of wind speed, relative humidity, and air temperature. Streamflow is measured in an H-flume at the basin outlet. Imnavait

Creek, located east of the Upper Kugaruk River, flows parallel about 12 kilometers before it joins the Kugaruk River.

### **6.2.2. Upper Kugaruk River Basin**

Upper Kugaruk River basin drains 146 km<sup>2</sup> in the northern foothills of the Brooks Range and has many of the same attributes as Imnavait Creek. Five micro-meteorological stations are installed within the Upper Kugaruk River basin (Figure 3-2); they measure precipitation, air temperature, and wind speed. There is a complete meteorological station near the gauging site on the Upper Kugaruk River identical to the meteorological station on Imnavait Creek. The main channel, which occupies a north-northwest trending valley, is formed at the base of steep hills. Patches of dwarf willows and birch up to 1 meter in height occupy portions of the banks and water tracks. Vegetation in the basin is varied from alpine at the higher elevations to moist tussock tundra at the lower elevations [Walker et al., 1989].

### 6.3: Results Of Physical Processes

#### 6.3.1. Snowmelt

Snow is a major component in the precipitation process of the arctic hydrologic cycle. The annual snow cycle is characterized by a relatively long accumulation period followed by a short melt season [van Everdingen, 1987]. In Imnavait watershed, for example, snow precipitation constitutes about 1/3 of annual precipitation [Kane et al., 1991a] and about 2/3 of the snowpack water equivalent leaves the basin as runoff [Lilly, et al., 1998]. So the snowmelt process and subsequent runoff are very important in arctic hydrologic modeling. The start of spring snowmelt varies greatly depending on the initial depth of the snowpack and the meteorological conditions at the time of melting [Hinzman et al., 1996]. The energy balance approach and degree-day method have been used to compute rates of snowmelt. A discussion of parameters used in the MATH model follows.

The average surface roughness length used in energy balance computations,  $z_0$ , is a constant value of 0.0013

m during the spring melt period when snow cover exists. *Hinzman et al.* [1993] determined this constant from wind-speed profiles between 1.5 and 10 m as

$$z_0 = \exp\left[\frac{u_2 \ln(z_1) - u_1 \ln(z_2)}{u_2 - u_1}\right] \quad (6-1)$$

where

$z_1$  and  $z_2$  are two heights at which measurements are made, m,

$u_1$  and  $u_2$  are wind speeds at the two heights  $z_1$  and  $z_2$ , m/s.

As the snow melts, the surface roughness increases as the vegetation protrudes through the snowpack. *Price and Dunne* [1976] concluded, from field work in Schefferville, Quebec, Canada, that protruding small vegetation will increase the  $z_0$  from 0.005 to 0.015 m as the melt progresses. *Braun* [1985] used optimal values between 0.00015 m and 0.007 m; he found that these values changed from one melt period to another.

Anderson [1976] used a constant value of  $z_0$  equal to 0.0005 m.

The melt factor in the degree day method,  $C_s$ , is the amount of melting which occurs per degree of positive air temperature within one time step (one degree hour in our model).  $T_s$  is the threshold value of air temperature, and it therefore specifies at what temperature snow will begin to melt. Kane et al. [1993, 1997], after analyzing several years' data, gave the optimized values of  $C_s = 2.7 \text{ mm}/(\text{day } ^\circ\text{C})$  and  $T_s = -0.2 \text{ } ^\circ\text{C}$ . The values of the threshold temperature are usually less than  $0 \text{ } ^\circ\text{C}$  because some ablation can occur through radiative melt when the air temperature is below freezing. Hinzman and Kane [1991] utilized values of  $C_s$  of  $3.5 \text{ mm}/(\text{day } ^\circ\text{C})$  and  $T_s$  between  $-1.9 \text{ } ^\circ\text{C}$  and  $0.5 \text{ } ^\circ\text{C}$ . However, in this case they were predicting runoff in the HBV model, not ablation over a small area. In our model simulation,  $2.7 \text{ mm}/(\text{day } ^\circ\text{C})$  and  $-0.2 \text{ } ^\circ\text{C}$  have been used for  $C_s$  and  $T_s$  respectively.

Hinzman et al. [1991] used a guarded hot plate to determine the effective thermal conductivities of

organic and mineral soils sampled at Imnavait watershed. The conductivities were determined as a function of temperature (both when frozen and unfrozen) and moisture content. It was found that when the organic soil is thawed with moisture content near field capacity the effective thermal conductivity is about  $0.45 \text{ W/m}\cdot^{\circ}\text{C}$ . The same soil when frozen has an effective thermal conductivity of around  $1.0 \text{ W/m}\cdot^{\circ}\text{C}$ . Therefore the soil has more resistance to heat flow in the summer than it does in the winter. The mineral soil, when saturated and thawed, has an effective thermal conductivity of about  $1.3 \text{ W/m}\cdot^{\circ}\text{C}$ ; the same soil when frozen has a thermal conductivity of about  $1.9 \text{ W/m}\cdot^{\circ}\text{C}$ . These values compare well with other published data [Farouki, 1981].

In our model, when determining the surface energy balance, only conductive heat flux through organic soil in the active layer is considered (convective energy is assumed to be zero). Standard values were used for latent heat of fusion and vaporization, water density and specific heat of air. Field measurements of net radiation, wind speed, air temperature, atmospheric pressure, and relative humidity were kriged from the

stations in each basin to create distributed input files.

Figure 6-1 shows similar basin averaged snowmelt simulation results for Imnavait watershed in 1993 using the energy balance and degree day methods. A good agreement between simulated and observed data was obtained in both cases. Kane et al. [1997] showed that snowmelt rates from both of these methods were comparable in performance as long as  $C_s$  and  $T_s$  could be obtained for a variety of conditions.

The snow distribution at the end of the accumulation season is not uniform. Snow drifting and redistribution occurs throughout the winter, and the distribution is largely a function of precipitation amount, wind speed and direction, and topography. The depths of snow before melting can range from a few centimeters on windswept ridge tops to more than one meter in the valley bottom [Hinzman et al., 1996]. This region has primarily north-trending katabatic winds that result from downslope drainage of denser air from the Brooks Range; however major wind events from both the east and west are common for short periods of time. Large wind

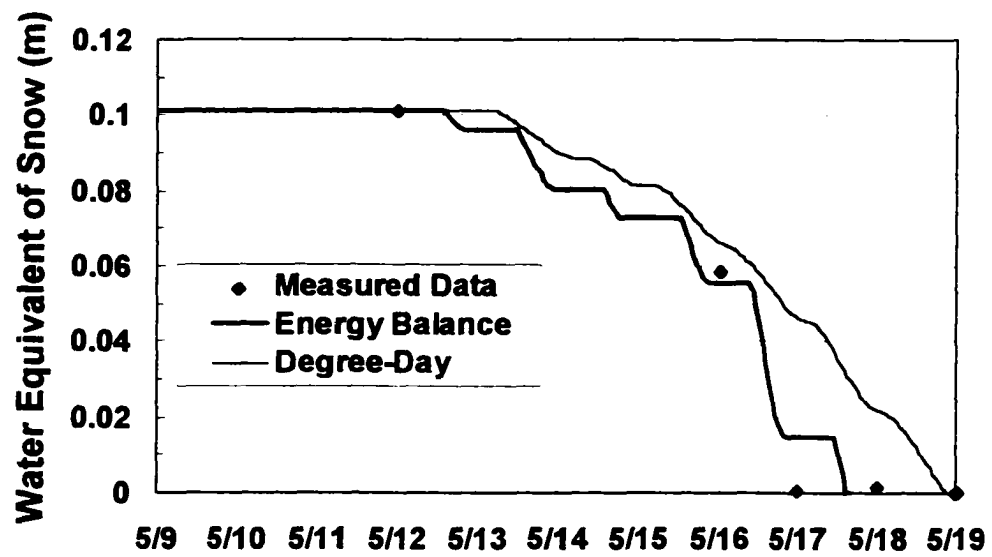


Figure 6-1. Comparison of snowmelt between energy balance and degree-day methods and average measured data, Imnavait watershed, Alaska, 1993.



events can cause extensive drifts and wind slabs throughout the watershed with orientation of slabs depending on wind direction. The density of the drift depends on the magnitude of the wind events. Nevertheless, the consistency of the predominantly southeast wind yields a similar snow distribution each year, i.e., deposition in valley bottoms and on the lee side of slopes. Index map that represents the initial snow distribution as a function of basin average snow depth over actual snow depth were compiled based on several years of field measurements [Hinzman et al., 1996]. Once the index map is compiled, the actual snow distribution over a watershed can be obtained if an estimation of basin-averaged snow depth is known. Figures 6-2a and 6-2b show the initial snow distribution and the distribution after four days of melting for Imnavait watershed in 1994. From Figure 6-2b, we can see that most of the snow in the watershed was gone after a few days except on the east-facing slope. The sun shines directly on the east-facing slope in the morning when the air temperature is low; it shines directly on the west-facing slope in the afternoon when the air temperature is warmer. This causes melting to

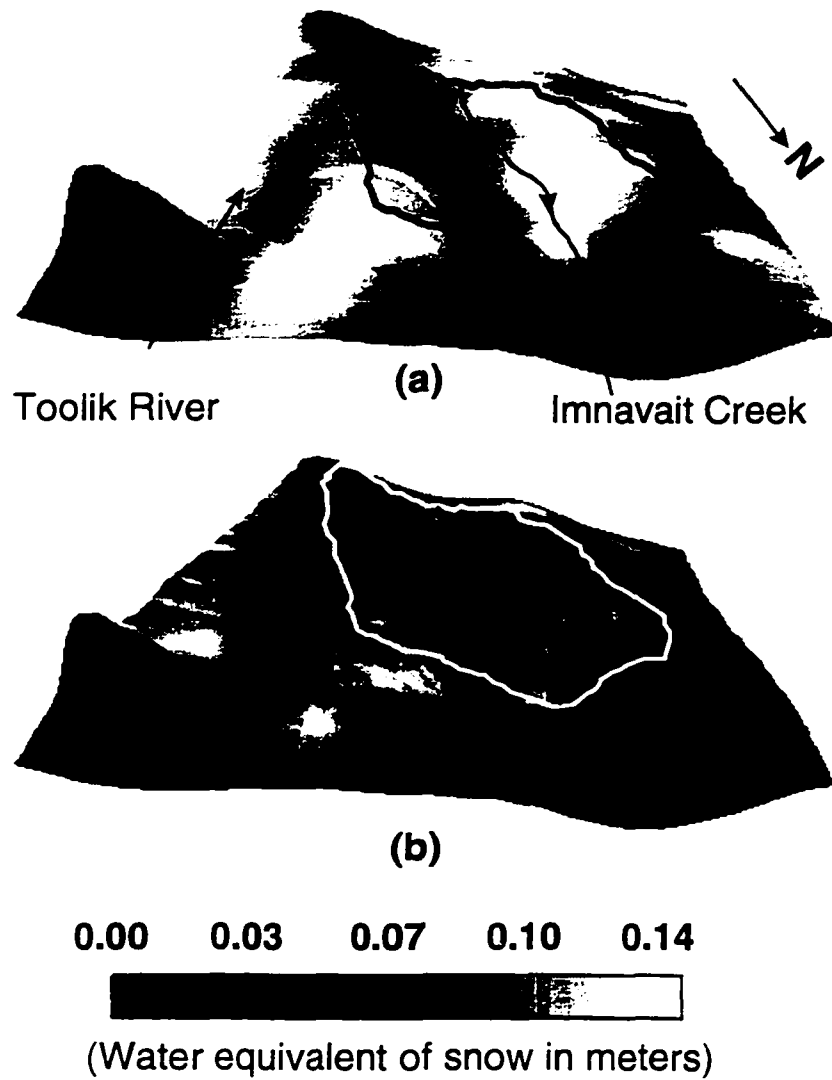


Figure 6-2. Initial snow distribution at May 10, 1994 (a) and modeled snow distribution after four days of melting (b) at Imnavait watershed, Alaska.

occur on the west-facing slopes faster than on the east-facing slopes. Another reason is that initial snow depth was deeper on the east-facing slopes than on the west-facing slopes. This maintains a high albedo on east-facing slope as this prevents vegetation from protruding through the snowpack. This is consistent with what was observed in the field every year from 1985 to 1997.

The initial snow distribution for the Upper Kupa-ruk watershed was developed from extensive snow surveys in the basin. The rugged topography and winds result in a very heterogeneous snowpack with no discernible trends. Figures 6-3a and 6-3b show the initial snow distribution and the distribution after six days of melting for the Upper Kupa-ruk basin in 1996. Those areas with the highest snowpack water contents are the last to melt in the simulation.

### **6.3.2. *Evapotranspiration (ET)***

Two separate routines have been included in our model to simulate evapotranspiration, surface energy balance and the Priestley-Taylor method. For the surface energy

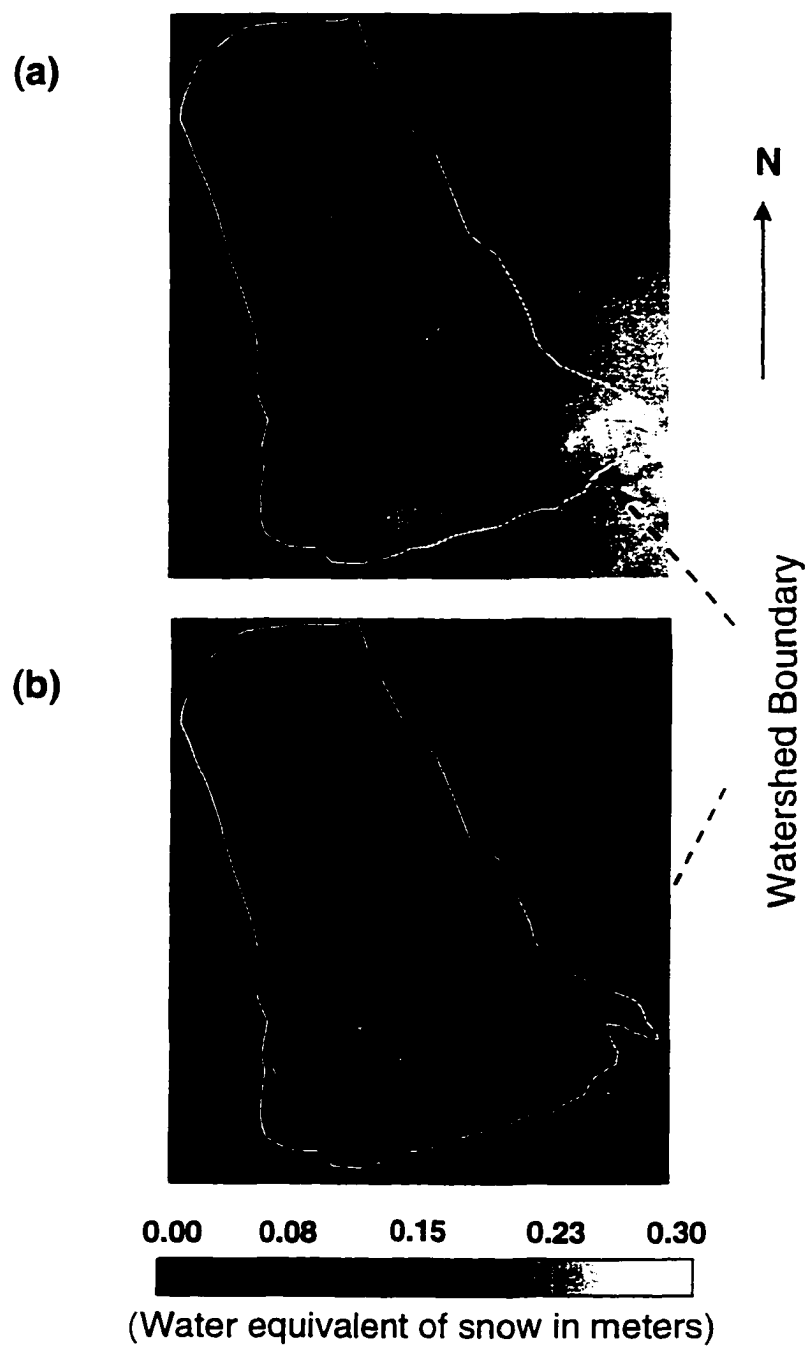


Figure 6-3. Initial snow distribution at May 21, 1996 (a) and modeled snow distribution after six days of melting (b) at Upper Kugaruk basin, Alaska.

balance, heat conduction between surface and subsurface is considered in the top 5 centimeters of soil when calculating surface energy balance. The thermal conductivity of a thawed organic soil of  $0.6 \text{ W/m}\cdot\text{C}$  is used. A constant value of  $0.02 \text{ m}$  for surface roughness length was evaluated by averaging several hundred wind profile measurements [Hinzman et al., 1993]; there were no clear seasonal trends of surface roughness observed for the Imnavait watershed after snowmelt. This is partially because the vegetation type and height do not change much through the summer.

The evaporability parameter  $\alpha$  in the Priestley-Taylor method is modified as:

$$\alpha = \alpha_1 R + \alpha_2 \quad (6-2)$$

where  $\alpha_1$  counts for the moisture condition of the soil and  $\alpha_2$  for vegetation effect. A value of  $1.0$  for  $\alpha_1$  and  $0.2$  for  $\alpha_2$  is used in the model. If  $R = 1$  for saturation, then  $\alpha = \alpha_1 + \alpha_2 = 1.2$ , this will predict the highest combined total of surface evaporation and

transpiration from the vegetation. Jackson et al. [1996] used the evaporability parameter  $\alpha$  of 1.26 when the soil moisture deficit becomes zero (saturation). When  $R$  is very small,  $\alpha \cong \alpha_z$ , transpiration will be the main contributor to ET. Plant transpiration is also a function of soil moisture. In our model, we only use the parameter  $\alpha$  discussed above to account for the effect of soil moisture changes on evaporation. Evapotranspiration is calculated in each time step the same as subsurface flow and is one of the mass balance components.

Figure 6-4 shows a comparison between the measured pan evaporation and the simulated basin average evapotranspiration in Imnavait watershed during the summer of 1993 by the energy balance method and the Priestley-Taylor method. The comparison between the two modeled estimates is relatively close through the summer. The ratio of total simulated ET over pan evaporation is 0.35 for Priestley-Taylor and 0.39 for energy balance for 1993. The average value over eleven years (from 1986 to 1996) of data in Imnavait Creek watershed is about 0.52, its range is between 0.34 to

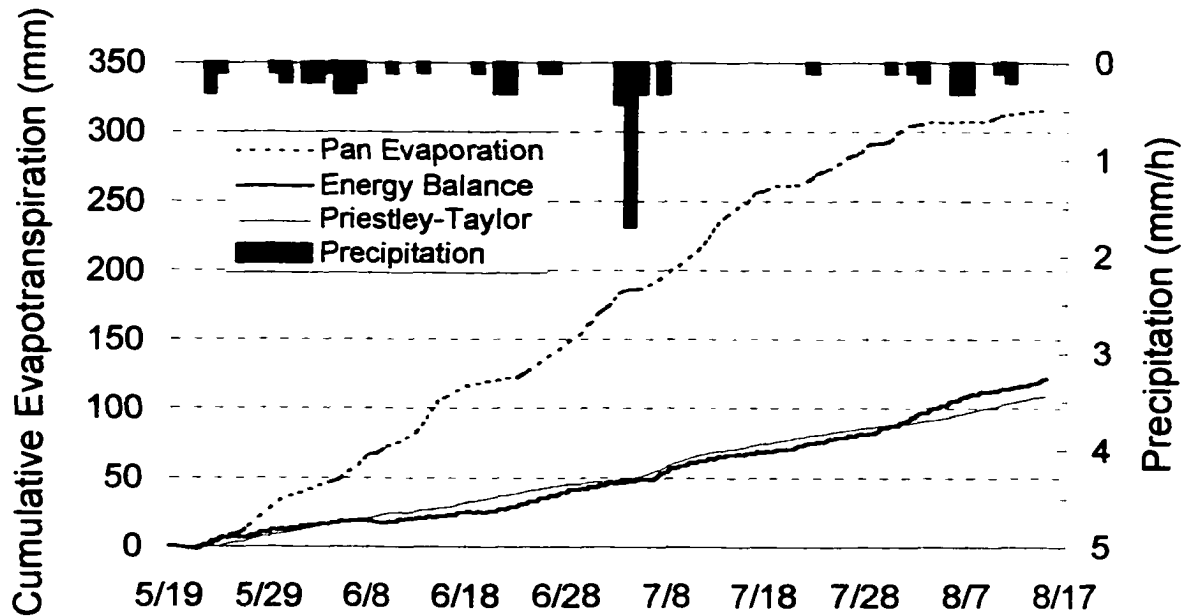


Figure 6-4. Comparison between measured pan evaporation and calculated basin averaged evapotranspiration using energy balance model and Priestley-Taylor model, Imnavait watershed, Alaska, 1993.

0.66. For 1993, the water balance value from field measurements is 0.34 and compares quite well with modeled results above.

Figure 6-5 shows the distributed ET for one hour for Imnavait watershed in 1994 and shows that ET is greater in the valley bottom where moisture content is higher and lowest on the drier ridges. The pattern is very similar to soil moisture distribution.

### ***6.3.3. Flow Routing and Moisture Content Simulation***

#### ***6.3.3.A. Subsurface Flow Routing***

Darcy's law was applied to simulate subsurface flow. The validation of using Darcy's law was confirmed by the fact that the Reynolds number is much less than one. This is true even when we use the highest soil hydraulic conductivity values that correspond to soils with the largest pores. There are three different soil types within the active layer of Imnavait watershed. The top layer is a mixture of organic and live vegetation and the bottom layer is mineral soil with a highly decomposed organic layer in between. The layered system



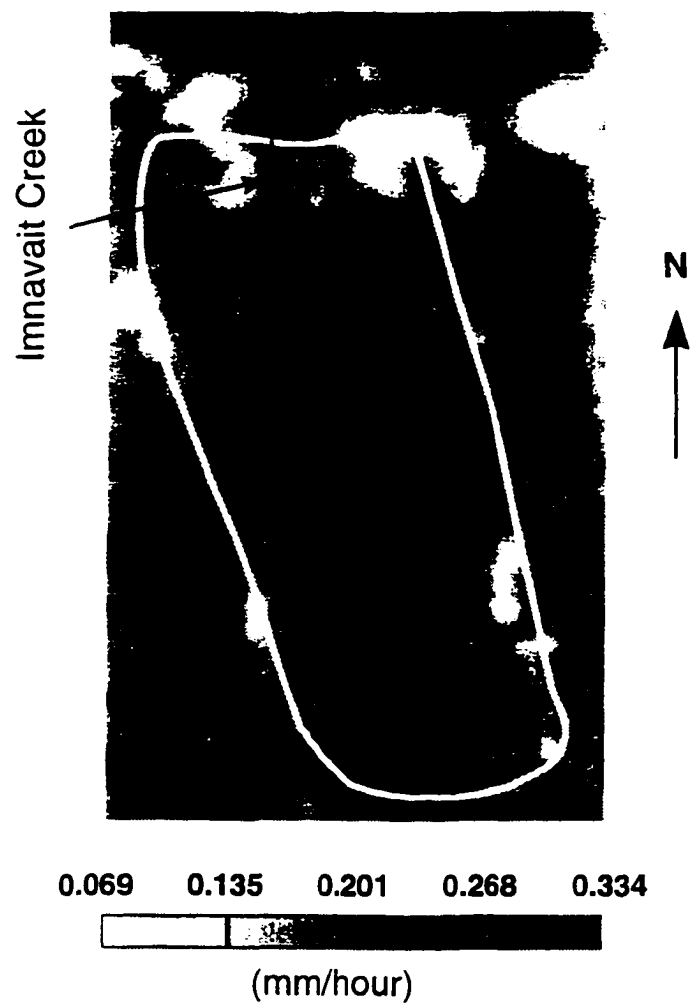


Figure 6-5. Simulated evapotranspiration distribution for one hour at June 12, 1994, Imnavait watershed, Alaska.

of soil horizons regulates moisture movement into and through the active layer. *Hinzman et al.* [1991b] analyzed soil samples taken from Imnavait watershed and found that the hydraulic conductivity of top 10 cm is about  $15 \times 10^{-5}$  m/s and the next 10 cm of highly decomposed organic soil is about  $3.5 \times 10^{-5}$  m/s. The rest of the active layer is mineral soil and it has a conductivity of about  $1 \times 10^{-5}$  m/s. Soil water characteristic curves were developed for different soil layers. A one-hour time step  $\Delta T$  was used in calculation of subsurface flow through soils. Based on the hydraulic conductivity of surface organic soils and maximum slope of watershed, the distance of subsurface water movement within one hour is approximately 0.25 m, which is smaller than the grid scale for each element. The same time step was used for the calculation of subsurface flow in the Upper Kuparuk River basin. It should be pointed out that the active layer starts thawing after snowmelt and continues to thaw during the summer and reaches its maximum depth in the fall. So the soil depth in the Darcy's equation can change with each time step. Soil moisture capacities for each layer

of soil can also change, since they are related to the soil depth. The same soil properties have been used for the Upper Kuparuk basin as Imnavait Creek. In the Upper Kuparuk River basin, on some steep slopes there is no vegetation and bedrock is exposed; however, these site specific features were not incorporated into the model partially because they occupy less than 5% of total watershed area.

#### **6.3.3.B. Overland Flow Routing**

The kinematic wave equation was used to route the overland flow, which is treated as sheet flow. The parameters related to this method are time step and roughness coefficient. Since the overland flow velocities are higher than those for subsurface flow, a smaller time step was used in the model. According to the Courant condition [Bedient and Huber, 1992; Ciriani et al., 1977], time step  $\Delta t$  for overland flow should satisfy  $\Delta t \leq \Delta x / (v \pm \sqrt{gy})$  where  $\Delta x$  is the grid scale and equals 50 m for the Imnavait watershed and 300 meters for the Upper Kuparuk River basin,  $v$  is velocity of water movement over the element. We conservatively

picked a value of 0.05 m/s as the velocity and 0.02 m as the flow depth of  $y$ , then estimated that  $\Delta t$  should be less than 101 seconds. A  $\Delta t$  of one minute was used in actual simulation for both Imnavait Creek and the Upper Kuparuk basin. Roughness coefficient values  $n'$  for overland flow in Manning's equation are typically greater than that for channel flow  $n$ . *Bedient and Huber* [1992] summarized some  $n'$  values based on field and laboratory data. For the watersheds studied here, we used the roughness parameter  $n'$  equals 0.3 for overland flow routing, which is typical for grass covered ground.

After each time step of  $\Delta t$ , a mass balance is conducted for each element by considering all mass components going into or leaving the element. Then the new flow depth of  $y$  is determined for the next time step. The mass component contributed from subsurface flow was evenly distributed in each  $\Delta t$ .

#### **6.3.3.C. Channel Flow Routing**

The kinematic wave equation was used to conduct channel flow. A triangular cross section was assumed

for all channels. Similar to the analysis in overland flow, the time step  $\Delta\tau$  for channel flow was adopted as about 2 seconds, assuming that the flow velocity is less than 1.0 m/s and the depth is less than 2 m. *Bedient and Huber* [1992] and *Chaudhry* [1993] also compiled similar tables for channel flow showing a range of values of Manning's coefficient  $n$  for different conditions. A value of 0.03 has been used in this model for channel flow routing; this is comparable to a relatively straight channel with moderate roughness. Mass balance is also conducted in each time step of  $\Delta\tau$  for each channel segment and new water depth is obtained for the next time step. The amount of water contributed by overland flow is evenly distributed over  $\Delta t$  for each  $\Delta\tau$ . Since hourly measured hydrograph data were available at the gauging stations for Imnavait Creek and Upper Kupaaruk River, hourly hydrograph data from MATH model was retained for comparison.

## 6.4: Discussions

### 6.4.1. Moisture Distribution and Hydrographs

Prediction of spatially distributed moisture over a watershed is one of the most important uses of this type of model, in our case it is important because of the role soil moisture plays in greenhouse gas generation. In our model, moisture distribution results can be generated for each time step of  $\Delta T$  through the whole simulation period. Figure 6-6a shows the simulated moisture content distribution over Imnavait watershed on August 2, 1993. These results are qualitatively correct since they show ridges to be the driest, the valley bottoms to be wettest, with hillslope values in between. In order to verify the distributed model results, spatially derived soil moisture data from SAR images at the same location and time were used (Figure 6-6b) [Goering *et al.*, 1995; Kane *et al.*, 1996]. Modeled soil moisture contents by volume represent average values for the upper 10 cm of the active layer, whereas the SAR results are from the top 3 to 5 cm. Therefore, it is reasonable to expect as the porous organic soils

drain vertically that the modeled results would be higher than the SAR results as shown in Figure 6-6. Moisture distribution for the Upper Kupa-ruk River basin is shown in Figure 6-7a with SAR imagery of soil moisture distribution at the same time in Figure 6-7b. Again, it is quite easy to locate the drier ridges, wet valley bottom and the intermediate wet slopes, with both figures being qualitatively similar. The simulated soil moisture distribution and SAR imagery of soil moisture distribution at the east side of Upper Kupa-ruk River are not exactly comparable (Figure 6-7). The reason is that the SAR imagery was based on a 50 m DEM scale, and some small ridges exist at the east side of Upper Kupa-ruk River which block the water from flowing toward the main stream, shunting it northward. Whereas in the model simulation, 300 m DEM was used and those small features could not be captured.

The spatially distributed, physically based hydrologic models currently in use have seldom been evaluated by comparing predicted results with spatially measured data. Using remotely sensed data for a watershed of

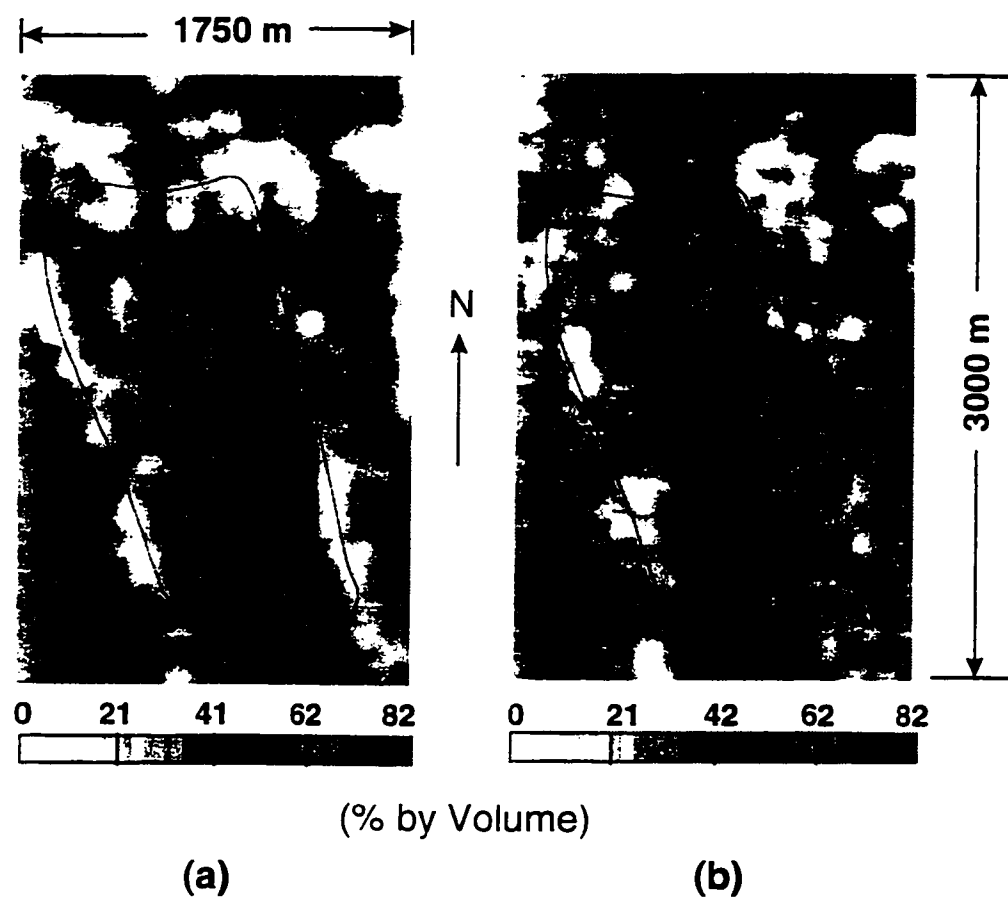


Figure 6-6. Modeled soil moisture content distribution (a) and SAR imagery of soil moisture content distribution (b) of Imnavait watershed at noon, August 2, 1993.



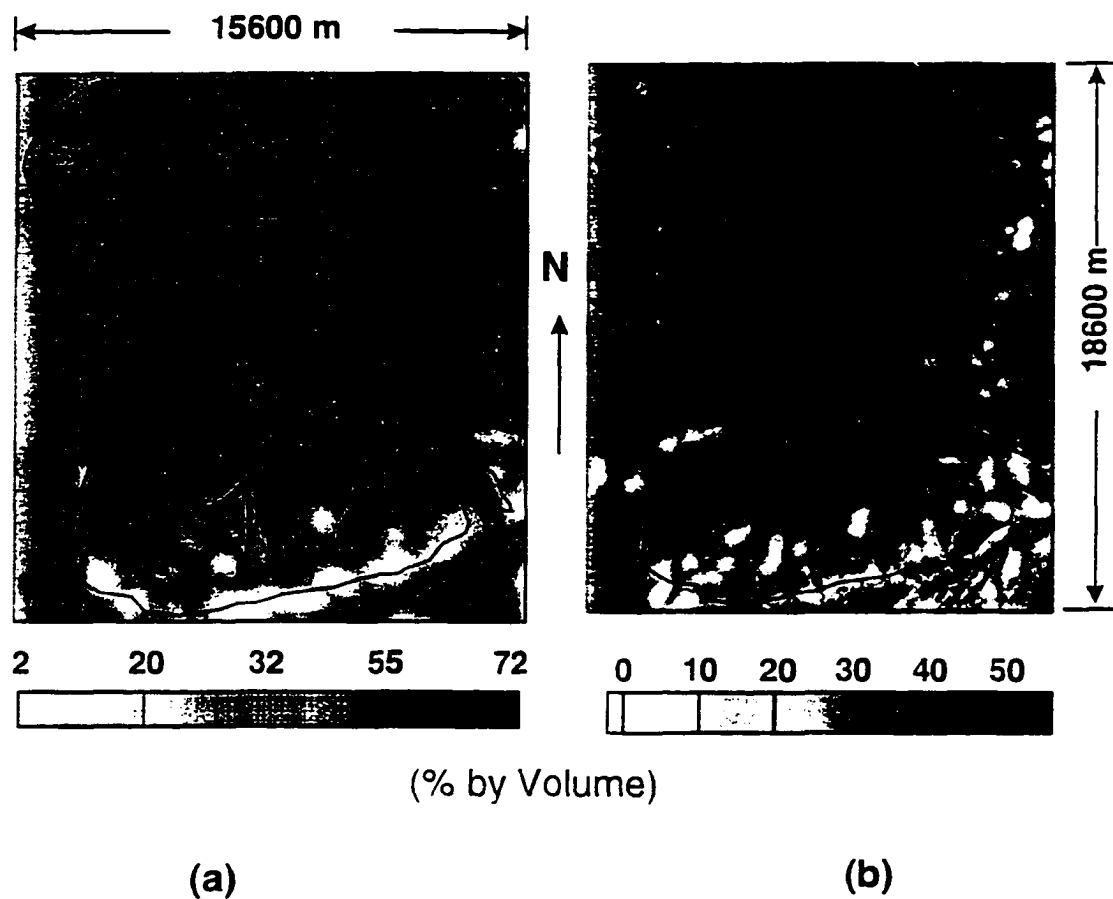


Figure 6-7. Modeled soil moisture content distribution (a) and SAR imagery of soil moisture content distribution (b) of Upper Kugaruk basin at 13:00, August 15, 1996.

appreciable size is the only way to have an independent check on model performance spatially. Remotely sensed snow ablation and soil moisture data are two spatially distributed data sets that can be used based on present technology. We have used results of soil moisture derived from SAR imagery in our comparisons here. *Wigmosta et al.* [1994] used advanced very high resolution radiometer (AVHRR) data for snowcover verification.

The classic verification of model performance is the comparison of measured and modeled hydrograph data. Figures 6-8 and 6-9 show the comparison of simulated and measured hydrograph data for Imnavait Creek in 1993 and 1994. Figure 6-10 shows the similar results for the Upper Kuparuk River basin in 1996. There are some discrepancies between simulated results and observed data. For instance, our model predicts snowmelt runoff is initiated a few days before it actually occurs. This is because an algorithm for snow damming has not been incorporated in the model. Snow damming occurs when melt water flows off the hillslopes into the valley bottoms [*Hinzman and Kane, 1991a*]. The valley bottoms

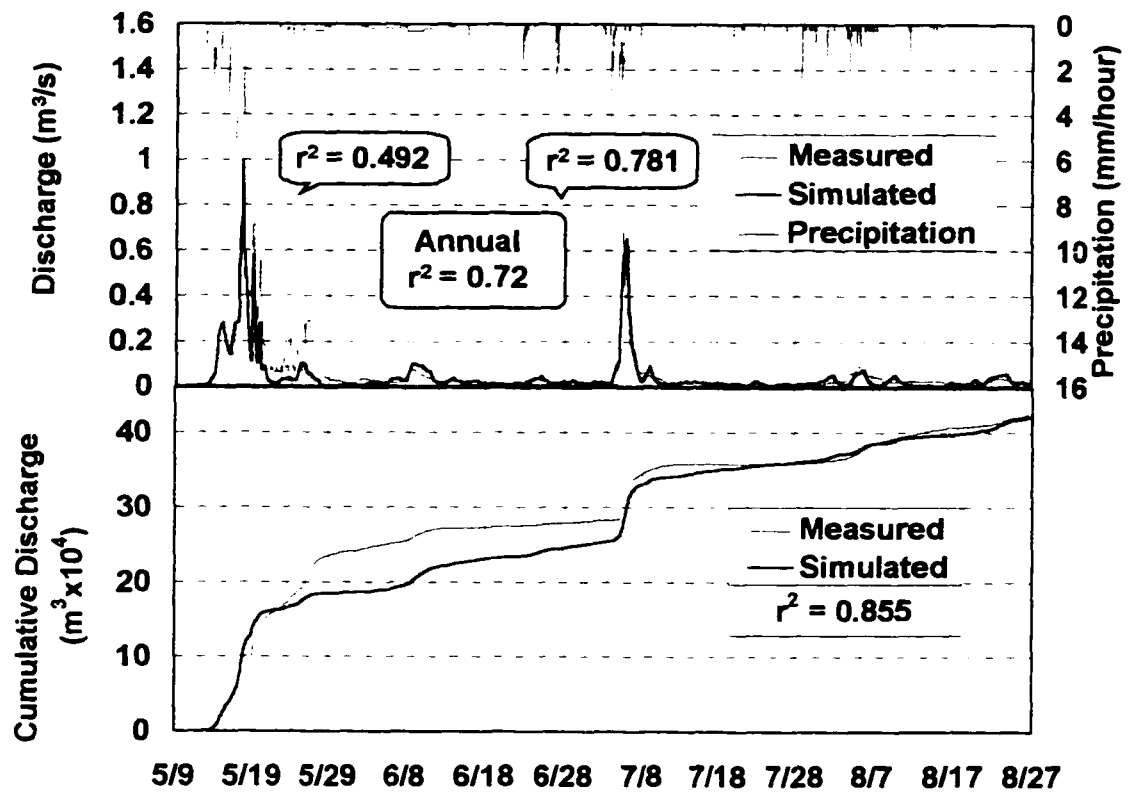


Figure 6-8. Comparison of modeled and measured discharges and cumulative volume of simulated and measured discharges at Innavait Creek, Alaska, 1993.

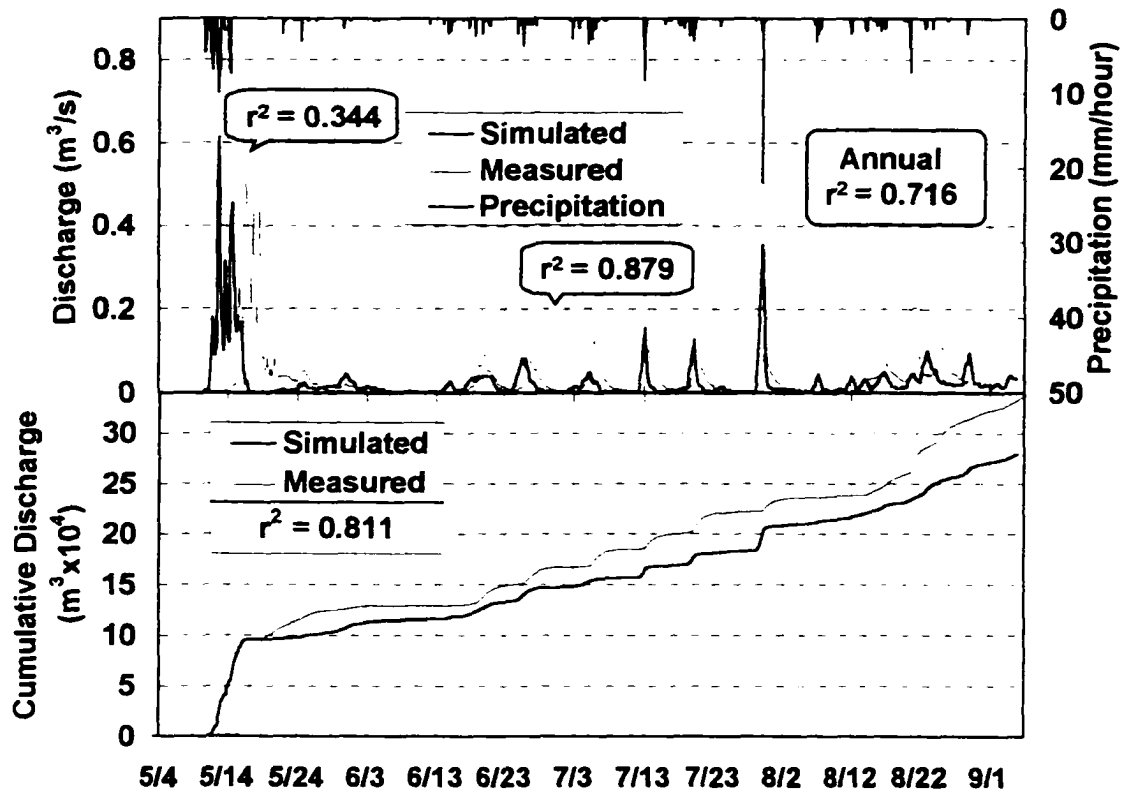


Figure 6-9. Comparison of modeled and measured discharges and cumulative volume of simulated and measured discharges at Innavait Creek, Alaska, 1994.

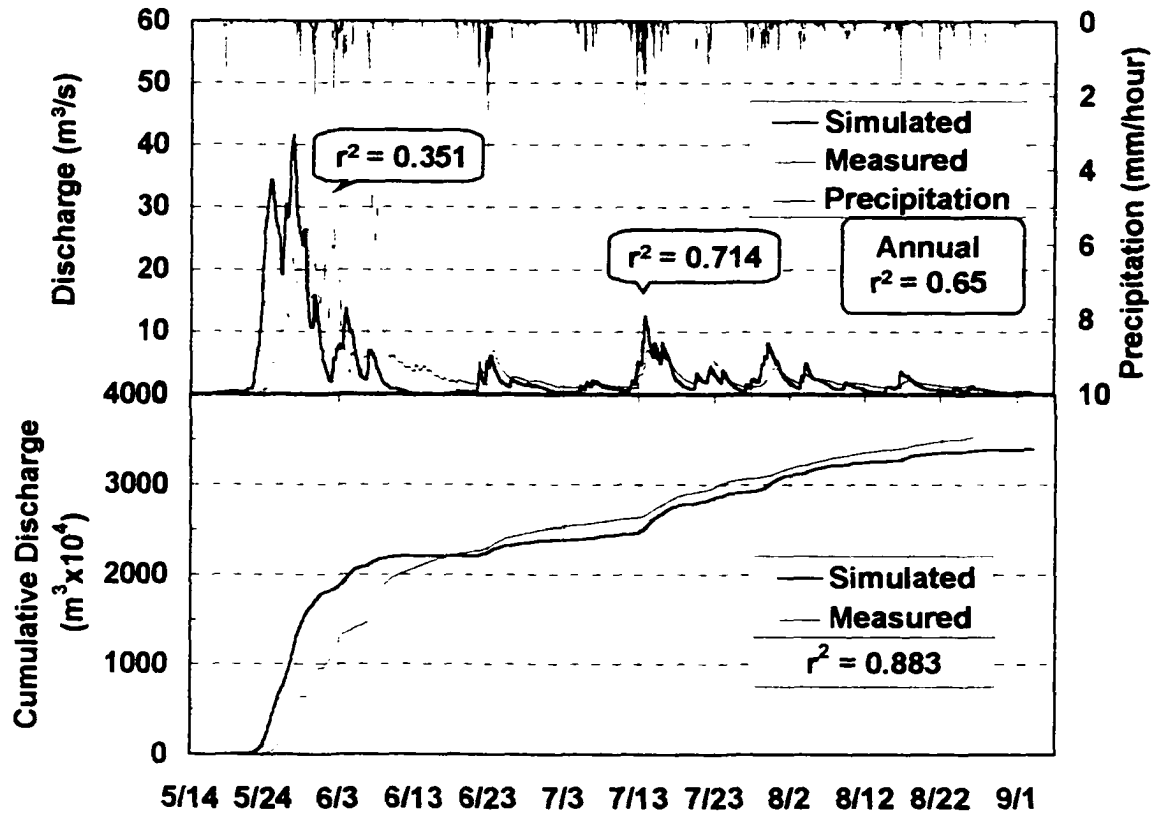


Figure 6-10. Comparison of modeled and measured discharges and cumulative volume of simulated and measured discharges at Upper Kuparuk River, Alaska, 1996.

and stream channels accumulate excessive amounts of wind packed snow, so this water collects in the dense snowpack in the valley bottom until the snowpack is structurally weakened and a slush flow occurs [Kane et al., 1997].

Other model calculations involved in various processes like snowmelt and flow routing can also contribute errors to the results. When the simulated cumulative discharge volume of water is compared to the measured cumulative discharge volume, they compare quite closely (Figures 8, 9 and 10). The model performance generally relies upon three criteria; visual inspection of simulated and measured hydrographs, a continuous plot of the accumulated discharge between simulated and measured hydrographs, and a variance,  $r^2$ , Nash-Sutcliffe coefficient. The validity of using the Nash-Sutcliffe coefficient as a comparative index of performance of the model was discussed by *Martinec and Rango* [1989]. It is calculated as:

$$r^2 = 1 - \frac{\sum_{t=1}^n [Q_{sim}(t) - Q_{meas}(t)]^2}{\sum_{t=1}^n [Q_{meas}(t) - \bar{Q}_{meas}]^2} \quad (6-3)$$

$Q_{sim}$  = simulated accumulative discharge (m<sup>3</sup>/s),

$Q_{meas}$  = measured accumulative discharge (m<sup>3</sup>/s),

$t$  = time variable (days or hours),

$n$  = number of time steps,

$$\bar{Q}_{meas} = \frac{1}{n} \sum_{t=1}^n Q_{meas}(t) \quad (\text{m}^3/\text{s}).$$

In addition to the above criteria, plots of simulated ET (Figures 6-4 and 6-5), snowmelt (Figures 6-1, 6-2 and 6-3) and soil moisture (Figures 6-6 and 6-7) aid in the model evaluation. Also, water balance analyses were conducted for Imnavit Creek watershed (1993 and 1994) and for Upper Kuparuk River basin (1996) using cumulative amount over the summer flow period (Figure 6-11). Simulated components compared favorably to measured values. Model results have been compared with both point and distributed measured data, and generally good agreement exists for both watersheds.

## **NOTE TO USERS**

**The original manuscript filmed by the school contained missing page(s).**

**176**

**This reproduction is the best available copy.**

**UMI**



#### 6.4.2. Data Input

One requirement for correctly utilizing a distributed model is the availability of distributed input data. In this model, hourly meteorological data were used. Distributed input data included net radiation, incoming shortwave radiation, reflected longwave radiation, air temperature, wind speed, relative humidity, atmospheric pressure, maximum snow water equivalent and summer precipitation (mostly rain). For Imnavait Creek, hourly uniform data measured at a point within the watershed were used because it is a relatively small watershed (2.2 km<sup>2</sup>) where the most important input variable, precipitation, can be approximately treated as uniformly distributed. In reality, non-uniform distribution exists during convective storms in early summer. This is reflected in the difference between predicted and measured hydrographs. Analyses by *Lilly et al.* [1998] showed that the average precipitation in Imnavait is greater than what is reported at the gage.

For the Upper Kuparuk basin, the assumption of uniformly distributed data is no longer appropriate.

Having seven meteorological stations (two major and five micro stations) installed across the 146 km<sup>2</sup> basin (Figure 3-2), we are able to generate hourly distributed data input for use in the model. Using spatial distributed data improves the model performance over earlier simulations assuming uniform distribution based on the one major meteorological station in that catchment. Simulations start a few days before snow starts melting and continues until the next snow accumulation season. The pattern of snow distribution is complex. Because of the redistribution by the wind, it is difficult to quantify this spatial variability without numerous field measurements for incorporation into the model. Based on several years of observed snow data at the selected sites, simple but distributed initial snow index maps were compiled, and distributed initial snow water equivalents were used in the model. The index map represents the ratios of actual snow depths over a basin averaged snow depth.

The soil layers in the active layer are initially completely frozen and are assumed to have zero moisture content in liquid state; the ice in the soil is

transformed to a liquid once the soil starts thawing. Most parameters related to soil hydraulic and thermal properties were adopted from other independent studies in this region. However, since there are no soil maps (only maps of vegetation), it is difficult to spatially distribute soil properties accurately. This is not as critical here as in non-permafrost watersheds, because of the limited storage involved in the active layer above the permafrost and the fact that it is a natural area that is undisturbed. No adjustment of parameters was done to optimize the model output. Because of the data limitation, some parameters were not distributed, such as roughness, for overland flow and channel flow. Also in these simulations, the depth of thaw was not predicted spatially. We have developed a physically based model to spatially predict the depth of thaw; however, it has not been incorporated into the hydrologic model yet [Hinzman et al., 1998]. This model encompasses all of the equations from the surface energy balance to derive the surface temperature by solving them simultaneously. This calculated surface temperature is then used in a subsurface finite element

formulation to solve for the temperature profile and depth of thaw.

#### **6.4.3. Other Issues**

Due the existence of permafrost, the subsurface flow system is physically limited to the thin active layer. This makes it relatively easy to measure the moisture regime and determine hydraulic properties for use in our model. In most other watershed studies, modeling of subsurface processes is difficult because of anisotropic and heterogeneous properties of soils and bedrock and the deep groundwater aquifers with large storage reservoirs. Within the active layer, the top organic soils are highly porous and infiltration rates are very high. In our model, the travel time from the ground surface to the water table in the active layer during infiltration by water is neglected, as it is quite short compared to the travel time of flow down the hillslopes.

Because vegetation in the Arctic is relatively small, many of the problems associated with precipitation and radiation distributions at various levels in the canopy are eliminated. In our energy budget algorithms for

evapotranspiration and snowmelt, we use measured values of net radiation from radiometers installed at each major meteorological site.

Channel networks are created based on the DEM data. The amount of detail generated by the DEM algorithm depends upon the size of the elements used and the format of the digital elevation data. For Imnavait Creek, the triangular elements were 50 m by 50 m and for the Upper Kuparuk River they were 300 m by 300 m. For larger elements, the likelihood of capturing water tracks is reduced. This is confirmed by comparing the results of the number of water tracks per unit area in Figures 4-5 and 4-6.

In our model, a simple triangular cross section was assumed for channels and water tracks and one value of channel roughness was used. Using other cross sectional geometries and other values for channel roughness should help improve model performance.

Simulated results could be improved by an examination of the parameter values used. In the example shown here, there was never any attempt to improve modeling results by adjusting parameters values. There are

probably many cases where we have not selected the optimum value for a parameter.

#### **6.4.4. Model Weaknesses**

The three areas where the model could be improved are: include a modeling component for snow damming, use smaller elements so that more water tracks are generated in the drainage network, and improve our data collection network to measure spatial variability.

A good physical explanation for the snow damming process does not exist; from field observations, it is quite apparent that snow damming retards snowmelt runoff for several days and results in higher peak flows than would occur without this process. From Figures 6-8, 6-9, and 6-10, the variances,  $r^2$ , are smaller during snowmelt than the rest of summer.

As the watershed size to be modeled increases, it becomes a computational necessity to increase element size. This results in the more subtle water tracks not being depicted in the simulated drainage network. We plan to examine this aspect more carefully in future studies.

Finally, some of the discrepancies between simulated and measured results are due to the quality of the input data. With the exception of one gauging station operated by the U. S. Geological Survey and three Wyoming snow gauges run by U. S. Department of Agriculture, we collected all of the data used in this study. Financial constraints and the lack of data generally available, such as soil maps, restricted the amount of input data available for model use.

#### **6.5: Conclusions**

A process based, spatially distributed hydrologic model (MATH model) has been tested and applied against the data obtained at two watersheds located at the North Slope of Alaska. Most hydrologic and thermal processes important in the Arctic are included in the model and the algorithms used are physically-based. MATH model has the capacity to accept spatially distributed data or uniform data, depending on the availability of data. The simulated results were compared with available measured data both at selected points and spatially. Since these results were produced from the coupled

processes, we can conclude that this physically based, spatially distributed hydrologic model can be used to study the arctic hydrologic regime. With the ability to simulate spatial soil storage, flow and evapotranspiration characteristics, this model can also be combined with other models such as those used to describe biogeochemical processes, for example, trace gas fluxes.

Because of the existence of continuous permafrost in the Alaskan Arctic, subsurface flow is limited within a thin active layer above the permafrost. The limited subsurface storage makes it easier to deal with subsurface flow in the model. On the other hand, since this is the first attempt to develop a spatially distributed hydrologic model for the Arctic, there are still needed improvements. For example, because the snow damming effect was not considered in the model, the predicted snowmelt runoff begins and ends sooner than actual discharge at gage. Some of the assumptions made in this model result from the lack of data or physical understanding; in addition, not all parameters and processes are totally distributed.



Spatially distributed precipitation, wind speed and air temperature data were available for the Upper Kugaruk River basin, and the results from the model yielded good agreement with measured data despite using larger elements. For the Imnavait watershed, uniform rainfall data, which was measured at a point within the watershed, was used, whereas in reality, non-uniform distribution exists during convective storms. In Imnavait Creek watershed we have one gauge for 2.2 km<sup>2</sup> and for the Upper Kugaruk catchment, where the data is distributed, we have seven gauges for 146 km<sup>2</sup>.

Some results can not be verified now due to a lack of measured data, such as distributed evapotranspiration and snow distribution after progression of snow melt. Based on the available data and results produced by the model, the distributed hydrologic model for arctic regions described in this paper performs adequately and the simulation results can be used or coupled with other models of arctic ecosystem processes.

## Chapter VII. Summary

### 7.1: About the Model

Since the development of the Stanford Watershed Model in 1966 by Crawford and Linsley [1966], there has been a proliferation of watershed models [Renard et al., 1982; James et al., 1982; Singh, 1989]. The models are of different types and were developed for different purposes. They can be classified according to different criteria that may encompass process related descriptions, spatial and temporal scales, and solution techniques as shown in Figures 7-1, 7-2 and 7-3 [from Singh, 1995]. Nevertheless, a hydrologic model usually contains components such as an input file, an algorithm of watershed characteristics and hydrologic processes, initial and boundary condition files, and output data.

The development of hydrologic models has kept pace with the development of computers. Due to the computational and data storage limitations of computers, the hydrologic models developed during 1960s and 1970s were mostly conceptually formulated lumped models

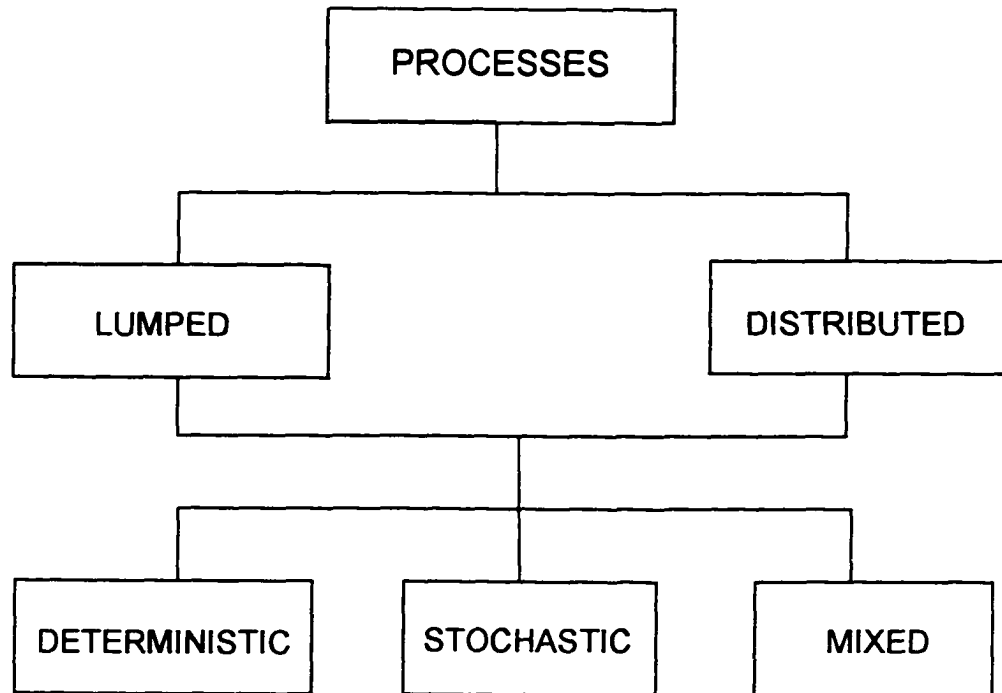


Figure 7-1: Classification of watershed models [Singh, 1995].

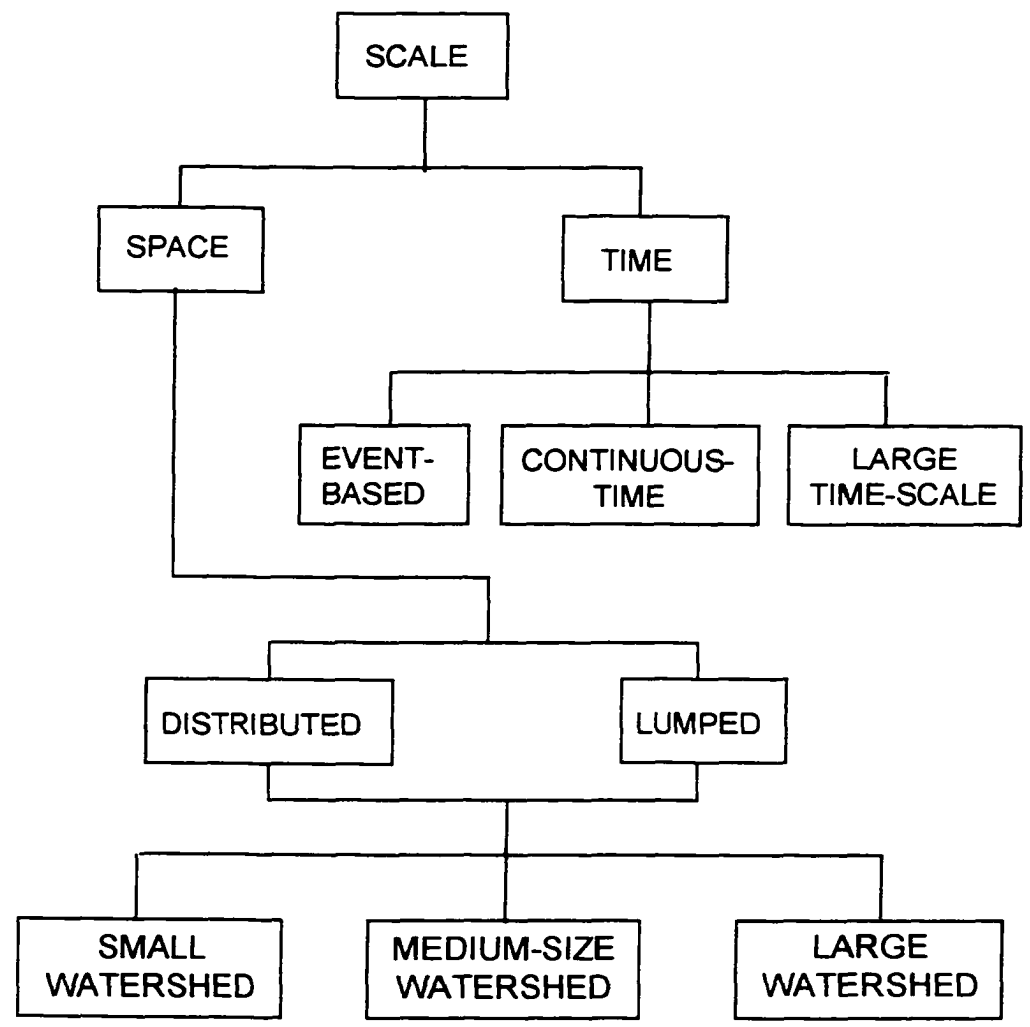


Figure 7-2: Classification of models based on space and time scales [Singh, 1995].

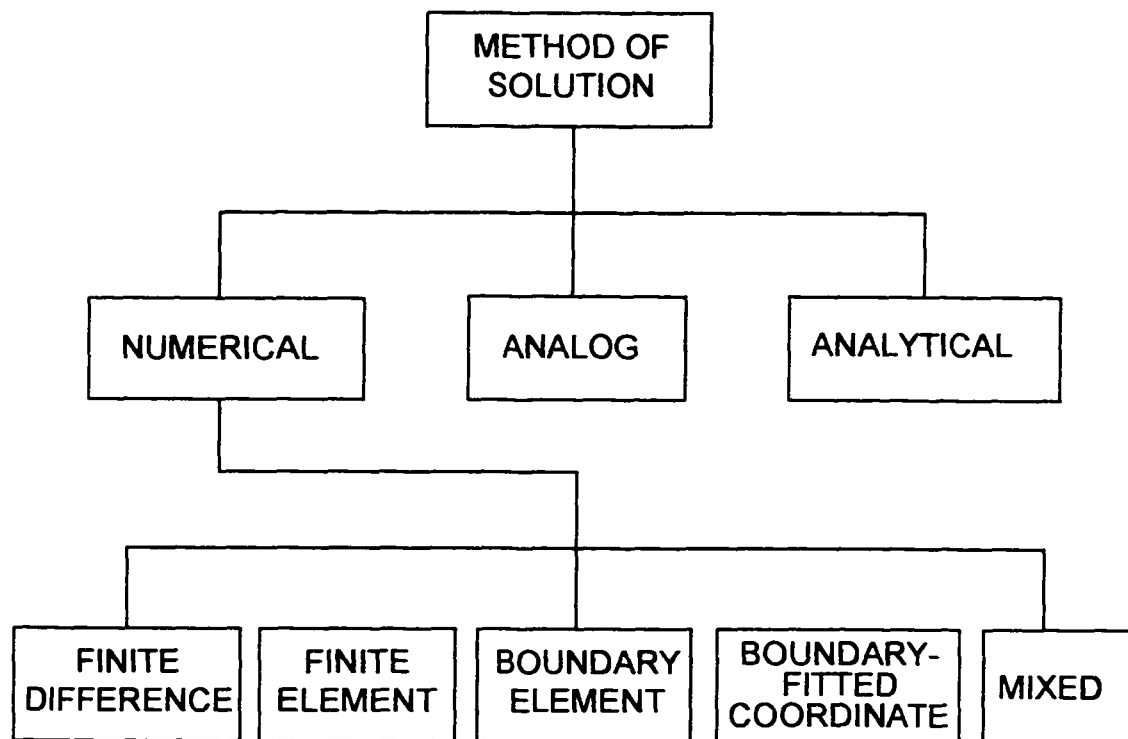


Figure 7-3: Classification of models based on solution techniques [Singh, 1995].

[Crawford *et al.*, 1966; Bergström, 1976] which required less computing resources and data storage facilities. Starting in the early 1980s, more complex hydrologic models have been developed. Most of them are spatially distributed [Abbott *et al.*, 1986; Beven, 1986a and 1986b; Ostendorf *et al.*, 1996; Grayson *et al.*, 1992; Wigmosta *et al.*, 1994]. These computationally intense models need substantially more input data and can provide more detailed results on desired hydrologic processes.

Lumped models predict hydrologic results at selected point in a watershed. However, the single most important attribute of spatially distributed models is that they make spatial predictions of numerous variables such as evapotranspiration, soil moisture, groundwater and snow cover. The main virtue of physically based models is that they attempt to mathematically represent all of the pertinent hydrologic processes. Development and application of spatially distributed, physically based models will continue at a fairly high level because these models lend themselves to the coupling with models of other processes such as sediment, gas and

dissolved chemical fluxes. As shown in many studies [Ostendorf et al., 1996; Reynolds et al., 1996; Oechel et al., 1993; Leadley and Reynolds, 1992; Shaver et al., 1990; Jorgenson, 1984; Peterson and Billings, 1980; Webber, 1978], the moisture gradients and patterns have a great impact on vegetation dynamics, chemical and biological variables, and gas flux exchange between the terrestrial and atmospheric systems.

The model that has been developed in this thesis is spatially distributed and it accommodates the characteristics of the unique arctic environment. Figure 7-4 shows the flow chart of the water flow processes in the hydrologic model. For each time step, the model reads in precipitation data as 'RAINFALL' or 'SNOWFALL'. If it is snowfall, then 'SNOWMELT' subroutine is needed. Water from precipitation goes to each element as 'WATER STORAGE' which will be compared with soil water capacity in 'STORAGE VS. CAPACITY'. Then it performs calculations of 'SUBSURFACE FLOW' and 'EVAPOTRANSPIRATION'. If the storage exceeds the capacity then 'OVERLAND FLOW' will be called. Next 'CHANNEL FLOW' subroutine will collect water from

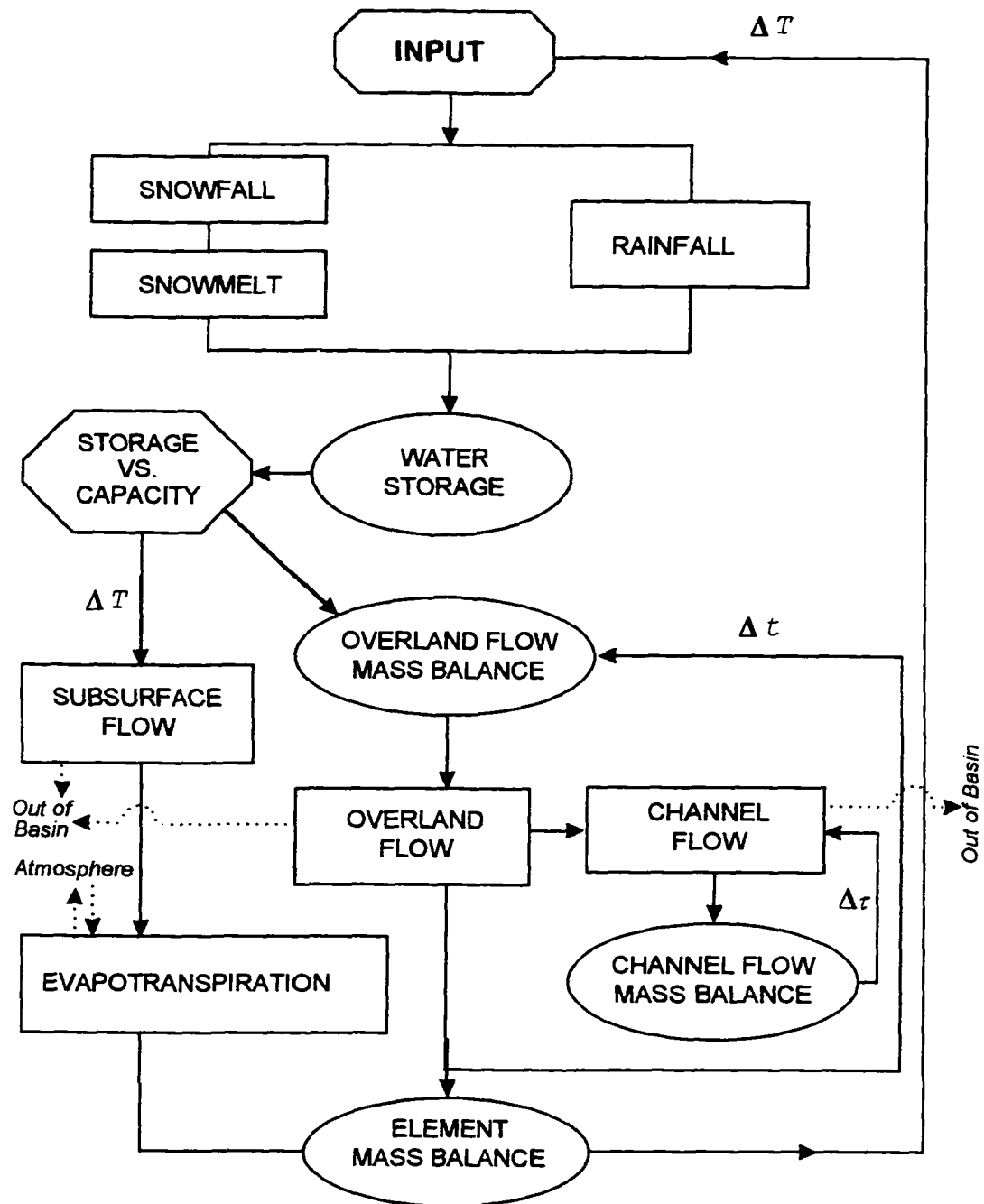


Figure 7-4. Flow chart of the water flow computations in the hydrologic model.



'OVERLAND FLOW" and water will be routed through channel segments to the outlet of a watershed. Mass balances for each element or channel segment are conducted within 'ELEMENT MASS BALANCE', 'OVERLAND FLOW MASS BALANCE' and 'CHANNEL FLOW MASS BALANCE'. For the three flow routing routines in the model, subsurface ( $\Delta T$ ), overland ( $\Delta t$ ) and channel ( $\Delta \tau$ ) flow, calculations were performed using different time steps with subsurface flow having the longest time period and channel flow the shortest time period. Parameter values used in this model were taken from complementary field research and related published papers. There was no attempt to vary parameter values to optimize simulated output.

## 7.2: About the Results

Prediction of spatially distributed hydrologic processes over a watershed is one of the most important uses of this type of model, in our case it is important because of the role soil moisture plays in greenhouse gas generation of carbon dioxide and methane in the Arctic. In our model, moisture distribution results can

be generated for each time step of  $\Delta T$  through the whole simulation period for each element.

One of the challenges in distributed hydrologic modeling is that we lack independent data sets that are distributed to verify the model-produced distributed results. In this study, we were able to compare spatial soil moisture from the hydrologic model to the data from SAR imagery at the same location and time (Figures 6-6 and 6-7). General patterns compared well. The results from SAR imagery, generally have lower soil moisture values than the ones from the model. This is because modeled soil moisture contents by volume represent average values for the upper 10 cm of the active layer, whereas the SAR results are from the top 3 to 5 cm (because of the microwave penetration ability is related to wave length) depending upon wetness. In MATH model we used 300 m DEM data for Upper Kuparuk River basin simulations. Some local drainage features, such as smaller water tracks, were not captured at this scale. SAR imagery results (Figure 6-7) are based on 50 m pixel values and therefore capture more detail.

For Imnavait watershed, field measured moisture data were available along a transect, their comparison with simulated and SAR data are shown in Figures 7-5 and 7-6. Simulated results were compiled every 50 meters (because it was based on 50 m DEM data) whereas field soil samples and SAR pixels were 25 meters apart. Although general variations are comparable, the simulated results are usually higher than the other two. The reason for SAR data being generally lower was explained before. For the field-measured data, the samples were collected as the average moisture content of the top 5 cm of organic matter. It is generally less than simulated results for the same reason as SAR data. Also, during the soil sampling and transporting, it is inevitable that some of water be lost, particularly for soils near saturation. This contributes to lower measured values also.

In the valley bottom where soil is near saturation, the three data sets tend to agree better. This is because when the soil is saturated at the surface it is saturated at all depths.

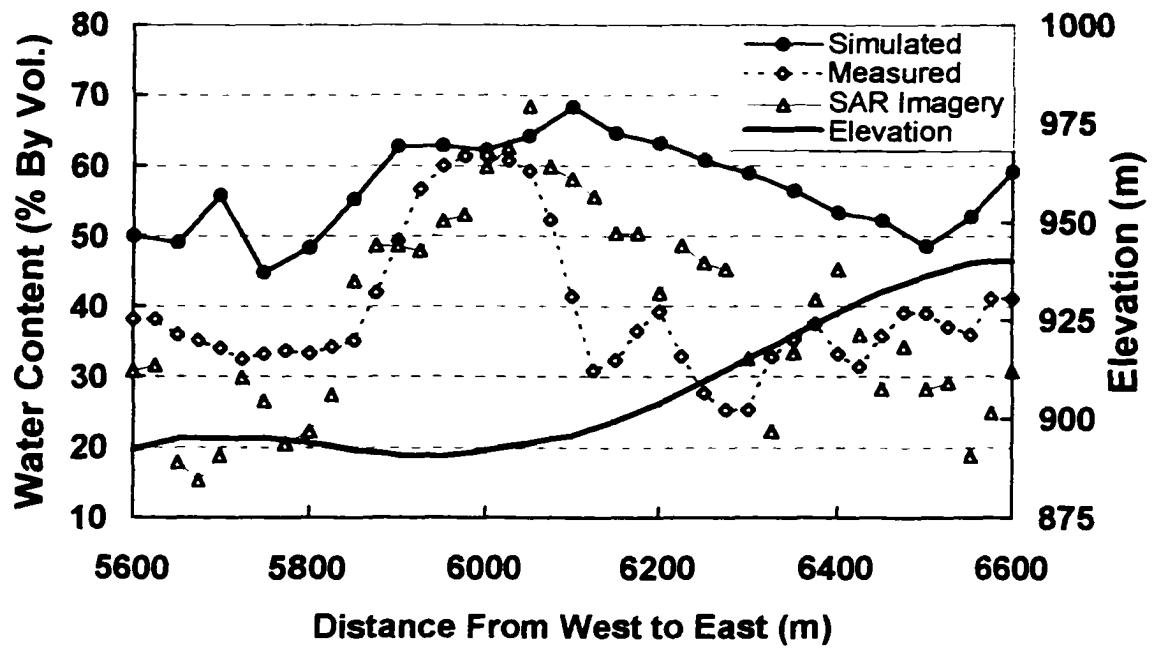


Figure 7-5. Comparison of soil moisture distribution along a transect within Imnavait watershed, Alaska, June 12, 1993.

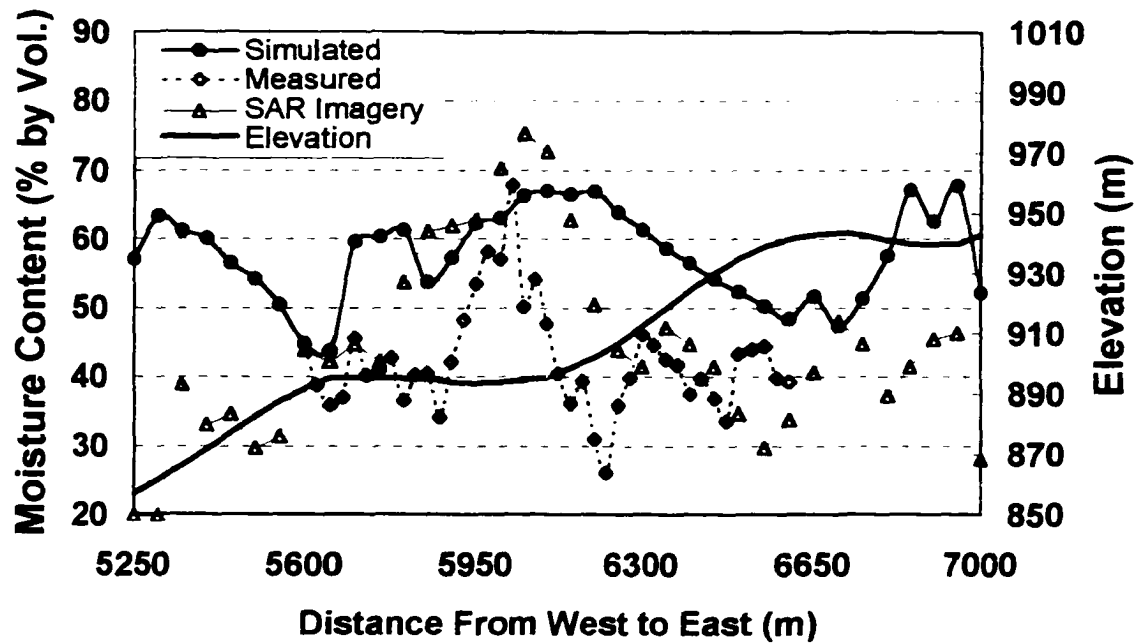


Figure 7-6. Comparison of soil moisture distribution along a transect within Imnavait watershed, Alaska, July 25, 1994.

This model also predicted distributed snowmelt patterns as shown in Figures 6-2 and 6-3. Even though they are reasonably correct when compared with field observations, they remain to be verified by spatially distributed data at watershed scale. But by comparing average simulated snowmelt result with average measured data as shown in Figure 6-1, the good comparison encouraged us that the snowmelt simulation algorithms are valid. This snowmelt algorithm is quite similar to Kane et al. [1997], which performed well for a wide range of conditions over a three year verification period.

The distributed information on evapotranspiration can also be produced by the model (Figure 6-5) but needs to be verified by distributed measured data in the future. The basin-wide average evapotranspiration rates, compare favorably for Priestley-Taylor and energy balance methods (Figure 6-4). When compared with field water balance data, the simulated results including ET by this model generally compare favorably. (Figure 6-11).

The classic verification of model performance is the comparison of measured and modeled hydrograph data. In

this paper, hydrographs obtained at specific gauging stations were used for comparison against model results (Figures 6-8, 6-9, and 6-10). The hydrographs compare favorably most of the summer; during snowmelt our model predicts that snowmelt runoff should start a few days before it actually occurs. The reason is because an algorithm for snow damming has not been incorporated into the model. From Figures 6-1, 6-8, 6-9 and 6-10, it can be seen the snowmelt is reasonably modeled, but the routing in the channel is not. When the simulated cumulative discharge volume of water is compared to the measured cumulative discharge volume, they compare quite closely (Figures 6-8, 6-9, and 6-10). Thus, simulated results from the hydrologic model compare favorably with both point and distributed measured data.

Reliable simulations depend upon a correct topographic delineation. The details of geometric information in turn rely are a function of the DEM scale. For Imnavait Creek and the Upper Kuparuk River, 50 m DEM data and 300 m DEM data were used respectively. For the larger grid, the likelihood of capturing water tracks is reduced. This is confirmed by the results in

Figures 4-5 and 4-6. On the other hand, smaller scale of DEM will require more computing resources and efforts in preparing input data.

Some of the discrepancies between simulated and measured results are due to the quality of the input data. Financial constraints, accessibility, and limited measurements restricted the amount of input data available for model use. Further improvements of model performance could be made by including a modeling component for snow damming, coupling with distributed thermal model, and using smaller elements to catch detailed topographic features. More spatially distributed data to feed into the model and to evaluate model performance would be beneficial. For example, more distributed meteorological data would be helpful for improving model performance and distributed evapotranspiration data would be useful to verify the simulated results. Good quality field data, such as precipitation data and radiation data, is crucial for correctly simulations of physical processes since these data are main factors in conducting mass and energy analyses.



### 7.3: Conclusions

A process based, spatially distributed hydrologic model has been developed for the Arctic, the first of this kind for this environment. The acronym for this model is MATH from Modeling of Arctic Thermal and Hydrologic Processes.

Existence of permafrost in the Arctic limits the subsurface flow within a relative shallow active layer simplifying subsurface routing. With the high porosity of organic soils in this region, the infiltration is assumed to be instantaneous compared to the lateral flow along the slope.

The model has been tested and applied against data obtained at two watersheds located at the North Slope of Alaska. First a watershed drainage simulation based on the DEM data is performed. By dividing the watershed into many smaller triangular elements, the area, aspect, and slope of each element can be determined. Subsequently, the drainage area and the channel network for a watershed can also be obtained. The model also

has the ability to analyze the stream orders based on a given scale of DEM data.

The second part of the model deals with hydrologic processes and their interactions. The model is capable of simulating distributed processes such as snowmelt, subsurface flow, overland flow, channel flow, and evapotranspiration. Spatial results on soil moisture content, snow distribution, and evapotranspiration can be generated for each time step. Most hydrologic and thermal processes important in the Arctic are included in the model. The model has the capacity to accept spatially distributed data or uniform data, depending on the availability of data.

The simulated results were compared with available measured data both at selected points and spatially distributed across the watershed. Spatially distributed data such as precipitation, wind speed and air temperature were available for the Upper Kuparuk River basin; the results from the model yielded good agreement with measured data when distributed data was utilized. This was true for both the watersheds used despite the fact that larger elements were used for the Upper

Kuparuk basin. For the Imnavait watershed, uniform rainfall data was assumed. Precipitation was measured at a point within the watershed and uniformly distributed over the basin. In reality, non-uniform distributions exist, especially during convective storms. Some results can not be verified now due to a lack of measured data, such as distributed evapotranspiration and snow distribution after progression of snow melt.

Since this is the first attempt to develop a spatially distributed hydrologic model for the Arctic, some processes discussed in this model have room for improvement in the future. Some of the assumptions made in this model result from the lack of data or physical understanding; in addition, not all parameters and processes are totally distributed. The soil thawing/freezing process is not fully incorporated as a physically based, spatially distributed subroutine. The snow damming process which impacts both overland and channel flow has not been incorporated in this model yet, causing the predicted snowmelt runoff to be initiated, peak and recede sooner than measured

discharge at gauge. Energy exchange and redistribution of water within the snowpack was not considered because the snowpack is quite shallow and this detail is not warranted for a watershed scale model. Some input data were not distributed. This will cause inaccuracy in simulating processes of large watershed where spatial variation of both data and physical processes cannot be neglected.

In conclusion, this research has proven the two hypotheses originally stated in Chapter I. The first hypothesis was, "a process-based, spatially distributed hydrologic model can be developed that will accurately predict Arctic hydrologic and thermal processes and their interactions." We have developed such a model (MATH model) and compared simulated results with field measurements for different processes such as snowmelt, evapotranspiration, soil moisture distribution, and runoff. Simulated results compared well with measured data and other independently derived data such as SAR imagery. The second hypothesis was, "this spatially distributed model can be used to simulate hydrologic and thermal processes in watersheds at vary watershed

scales." We have demonstrated that this hypothesis is true by applying MATH model to two different watershed scales, Imanvait Creek and Upper Kuparuk River basins located on the North Slope of Alaska. Again, good agreement between simulated results and measured data has been shown for both watersheds.

## References

- Abbott, M. B., J. C. Bathurst, J. A. Counge, P. E. O'Connell, and J. Rasmussen, An introduction to the European Hydrological System - Système Hydrologique Européen "SHE": 2. Structure of the physically based, distributed modeling system, *J. Hydrol.*, 87, 61-77, 1986.
- Alley, R. B., Resolved: The Arctic controls global climate change, *Arctic Oceanography: Marginal Ice Zones and Continental Shelves Coastal and Estuarian Studies*, 49, pp. 263-283, 1995.
- Ambler, D. C., Runoff simulation, Falls River watershed near d'Iberville Fiord, Ellesmere Island, In: *Cold Climate Hydrology*, Proceedings of N.W.T. Canadian Hydrology Symposium, Vancouver, B.C., pp. 277-289, May 1979.
- Ambroise, B., J. Freer, and K. Beven, Application of a generalised TOPMODEL to the small Ringelbach catchment, Vosges, France, *Water Resources Research*, 32(7), 2147-2159, 1996.

- Anderson, E. A., A point energy and mass balance model of a snow cover, *NOAA Technical Report NWS 19*, U. S. Dept. of Commerce, National Weather Service, 1976.
- Anderson, M. G., and T. P. Burt, *Process studies in hillslope hydrology*, John Wiley & Sons Ltd, 1990.
- Ashton, W. S., and R. F. Carlson, Predicting fish passage design discharges for Alaska, In: *Proceedings of Fourth International Conference on Permafrost*, 17-22 July 1983, Fairbanks, Alaska, National Academy Press, Washington, D.C., pp. 29-33, 1983.
- Band, L. E., P. Patterson, R. Nemani, and S. W. Running, Forest ecosystem processes at the watershed scale: incorporating hillslope hydrology, *Agric. for Ecol.* 7, 111-118, 1993.
- Baracos, P. C., K. W. Hipel, and A. I. McLeod, Modeling hydrologic time series from the arctic, *Water Resources Bulletin*, 17(3), 414-422, 1981.
- Bathurst, J. C., 1. Physically based distributed modelling of an upland catchment using the Systéme

Hydrologique Europeen, 2. Sensitivity analysis of the Système Hydrologique Europeen for an upland catchment, *Journal of Hydrology*, Vol. 87, 79-123, 1986.

Becker, A., Applied principles of catchment simulation, *Proceedings, IASH/UNESCO Symp. on Mathematical Models in Hydrology*, Warsaw, Poland, International Association of Hydrological Sciences Publication 101, pp. 762-774, 1973.

Bedient, P. B., and W. C. Huber, *Hydrology and floodplain analysis*, Addison-Wesley Publishing Company, 1992.

Bengtsson, L., The importance of refreezing on the diurnal snowmelt cycle with application to a northern Swedish catchment, *Nordic Hydrology*, 13, 1-12, 1982.

Benson, C. S., Reassessment of winter precipitation on Alaska's Arctic slope and measurements on flux of wind blown snow, *Geophys. Inst., Res. Rep., UAG R-288*, Univ. of Alaska Fairbanks, 1982.



- Bergström, S., Development and application of a conceptual runoff model for Scandinavian catchments, Swed. Meteorol. and Hydrol. Inst., Rep. RH07, Norrköping, 1976.
- Bergström, S., M. Persson, and B. Sundquist, Operational hydrological forecasting by conceptual models, Swedish Meteorological and Hydrological Institute, Norrköping, HB Report No. 1978.
- Bergström, S., Recent development in snowmelt-runoff simulation, In: *Proceedings: Cold Region Hydrology*, edited by D. L. Kane, Fairbanks, Alaska, pp. 461-468, 1986.
- Beven, K. J., and M. J. Kirkby, A physically based, variable contributing area model of basin hydrology, *Hydrol. Sci. Bull.*, 24(1), 43-69, 1979.
- Beven, K. J., and P. E. O'Connell, Physically based models in hydrology, *Inst. of Hydrology Rep. 81*, Wallingford, Oxon, England, 1982.
- Beven, K. J., and E. F. Wood, Catchment geomorphology and the dynamics of runoff contributing areas, *J. of Hydrol.*, 65, 139-158, 1983.

- Beven, K. J., Runoff production and flood frequency in catchments of order  $n$ : an alternative approach, In: *Scale Problems in Hydrology*, edited by V. K. Gupta, I. Rodriguez-Irtube, and E. F. Wood, pp. 191-219, Reidel, Dordrecht, 1986a.
- Beven, K. J., Hillslope runoff processes and flood frequency characteristics, In: *Hillslope Processes*, edited by A. D. Abrahams, Allen and Unwin, Boston, pp. 187-202, 1986b.
- Beven, K. J., A. Calver, and E. M. Morris, The Institute of Hydrology distributed model, *Inst. of Hydrology Rep. 98*, Wallingford, UK, 1987.
- Beven, K. J., Changing ideas in hydrology -- the case of the physically-based models, *J. of Hydrol.*, 105, 157-172, 1989.
- Beven, K. J., A discussion of distributed hydrological modeling, in *Distributed Hydrological Modeling*, edited by M. B. Abbott and J. C. Refsgaard, *Water Science and Technology Library*, 22, pp. 255-278, 1996.

Bhatia, P. K., S. Bergström, and M. Persson, Application of the distributed HBV-6 model to the Upper Narmada basin in India, Swedish Meteorological and Hydrological Institute, Norrköping, *Report No. RH035*, Sweden, 1984.

Bliss, L. C., North American and Scandinavian tundra and polar deserts, In: *Tundra ecosystems: a comparative analysis*, edited by L. C. Bliss, O. W. Heal, and J. J. Moore, pp. 8-24, Cambridge University Press, Cambridge, 1981.

Bliss, L. C., J. Svoboda, and D. I. Bliss, Polar deserts, their plant cover and plant production in the Canadian High Arctic, *Holarct. Ecol.* 7, pp. 305-324, 1984.

Bliss L. C., and N. V. Matveyeva, Circumpolar arctic vegetation, In: *Arctic Ecosystems in a Changing Climate: an ecophysiological perspective*, edited by F. S. III. Chapin, R. L. Jefferies, J. F. Reynolds, G. R. Shaver, J. Svoboda, and E. W. Chu, Academic Press, San Diego, pp. 59-89, 1992.

Bowen, I. S., The ratio of heat losses by conduction and by evaporation from any water surface, *Physics Review*, 11, 779-787, 1926.

Braun, L. N., Simulation of snowmelt-runoff in lowland and lower alpine regions of Switzerland, *Zücher Geographische Schriften*, Geographische Institut, Eidgenössische Technische Hochschule, Zürich, Switzerland, Heft 21, 166 pp., 1985.

Burton, K. L., W. R. Rouse, and L. D. Boudreau, Factors affecting the summer carbon dioxide budget of subarctic wetland tundra, *Climate Research*, 6, 203-213, 1996.

Campbell, G. S., An introduction to environmental biophysics, *Springer-Verlag.*, New York, 159 pp., 1977.

Cermak, R. J., Continuous hydrologic simulation of the West Branch DuPage River above west Chicago: an application of HYDROCOMP's HSP, U.S. Army Corps of Engineers, Research Note no. 6, The Hydrologic Engineering Center, Davis, Calif., 1979.

- Chapin, F. S. III, K. Van Cleve, and M. C. Chapin, Soil temperature and nutrient cycling in the tussock growth form of *Eriophorum vaginatum*, *J. Ecol.*, 67, 169-189, 1979.
- Chapin, F. S. III, G. R. Shaver, A. E. Giblin, K. J. Nadelhoffer, and J. A. Laundre, Responses of arctic tundra to experimental and observed changes in climate, *Ecology*, 76, 694-711, 1995.
- Charbonneau, R., J. P. Fortin, and G. Morin, The CEQUEAU model: description and examples of its use in problems related to water resource management, *Hydrological Science Bulletin*, 22(1/3), 193-202, 1977.
- Chaudhry, M. H., *Open-Channel Flow*, Prentice-Hall, 1993.
- Chow, V. T., D. R. Maidment, and L. W. Mays, *Applied Hydrology*, McGraw-Hill, New York, 1988.
- Ciriani, T. A., U. Maione, and J. R. Wallis, Mathematical methods for surface water hydrology, *Workshop on Mathematical Models in Hydrology*, Pisa, Italy, 1974, Proceedings, by John Wiley & Sons, Ltd., 1977.

- Claborn, B. J., and W. L. Moore, Numerical simulation of watershed hydrology, *Technical Report HYD4-7001*, Hydraulic Engineering Lab., Dept. of Civil Engineering, University of Texas Austin, 1970.
- Claggett, G. P., The Wyoming windshield—An evaluation after 12 years of use in Alaska, In: *Proceedings, Western Snow Conference*, Vol. 56, pp. 113-123, Western Snow Conference, Beaverton, Ore., 1988.
- Clark, C. O., Storage and unit hydrograph, *Transactions, ASCE*, Vol. 110, 1419-1446, 1945.
- Clarke, K. D., Application of Stanford watershed model concepts to predict flood peaks for small drainage areas, Kentucky Dept. of Highways, Lexington, Ky., *Research Report*, 1968.
- Coulson, K. L., *Solar and terrestrial radiation*, New York, Academic Press, 1975.
- Crawford, N. H., and R. K. Linsley, Digital simulation in hydrology, Stanford Watershed Model IV, *Tech. Rep. 39*, Civil Engineering Dept., Stanford University, Stanford, California, 1966.

- Dawdy, D. R., and T. O'Donnell, Mathematical models of catchment behavior, *ASCE, Journal of Hydraulic Engineering*, 91(4), 123-137, 1965.
- Dawdy, D. R., R. W. Litchy, and J. M. Bergmann, A rainfall-runoff simulation model for estimation of flood peaks for small drainage basin, *U.S. Geological Survey Professional Paper 506-B*, Washington, D.C., 1972.
- Dawdy, D. R., J. C. Schaake, and W. M. Alley, Users guide for distributed routing rainfall-runoff model, *Water Resources Investigations 78-90*, U.S. Geological Survey, NSTL Station, Mississippi, 1978.
- Dingman, S. L., Hydrologic effects of frozen ground: literature review and synthesis, U.S. Army Corps of Engineers, Cold Regions Research and Engineering Laboratory, Hanover, New Hampshire, *CRREL Special Report No. 218*, March, 1975.
- Doyle, W. H. and J. E. Miller, Calibration of a distributed routing rainfall-runoff model at four urban sites near Miami, Florida, U.S. Geological

Survey, NSTL Station, Mississippi, *Water Resources Investigations* 80-1, 1980.

Doyle, W. H., Using a distributed routing rainfall-runoff model, *Water Resources Bulletin* 17(2), 225-232, 1981.

Eagleson, P. S., *Dynamic hydrology*, McGraw-Hill, New York, 1970.

Farouki, O.T., Thermal properties of soils, *USACRREL, Monogr.*, 81-1, 1981.

Feddes, R. A., P. Kowalik, S. P. Neuman, and E. Bresler, Finite difference and finite element simulation of field water uptake by plants, *Hydrological Sciences Bulletin* 21, 81-98, 1976.

Feldman, A. D., HEC models for water resources system simulation: theory and experience, *Advances in Hydroscience*, 12, pp. 297-423, Academic Press, New York, 1981.

Fleming, G., *Computer Simulation Techniques in Hydrology*, Elsevier, 333 pp., 1975.

Flerchinger, G. N., C. L. Hanson, and J. R. Wight, Modeling evapotranspiration and surface energy



- budgets across a watershed, *Water Resources Research*, 32(8), 2539-2548, 1996.
- Foroud, N. and R. S. Broughton, Flood hydrograph simulation model, *Journal of Hydrology*, Vol. 49, 139-172, 1981.
- Gary, N. K., and D. J. Sen, Determination of watershed features for surface runoff models, *J. of Hydraulic Engineering*, ASCE, 120(4), 427-447, 1994.
- Goering, D. J., and J. P. Zarling, Geotechnical thermal analysis with a microcomputer, In: *Civil Engineering in the Arctic Offshore*, ASCE, pp. 604-616, New York, 1985.
- Goering, D. J., H. Chen, L. D. Hinzman, and D. L. Kane, Removal of terrain effects from SAR satellite imagery of arctic tundra, *IEEE Transactions on Geoscience and Remote Sensing*, 33(1), 185-194, 1995.
- Goodrich, D. C., Geometric simplification of a distributed rainfall-runoff model over a range of basin scales, Ph.D. dissertation, Dept. of Hydro. and Water Resour., Univ. of Arizona, Tucson, 1990.

- Grayson, R. B., I. D. Moore, and T. A. McMahon,  
Physically based hydrologic modeling: 1. A terrain-  
based model for investigative purposes, *Water  
Resources Research*, 28(10), 2639-2666, 1992.
- Gupta, V. P., Computer models of watershed hydrology,  
*Water Resources Publication*, Highlands Ranch,  
Colorado, 1995.
- Hamilton, T. D., Late Cenozoic glaciation of the Central  
Brooks Range, In: *Glaciation in Alaska: Geologic  
Record*, edited by T. D. Hamilton, K. M. Reed, and  
R. M. Thorson, Alaska Geological Society, pp. 9-49,  
1986.
- Harlan, R. L., Analysis of coupled heat-fluid transport  
in partially frozen soil, *Water Resources Research*,  
9(5), 1314-1323, 1973.
- Hastings, S. J., S. A. Luchessa, W. C. Oechel, and J. D.  
Tenhunen, Standing biomass and production in water  
drainages of the foothills of the Phillip Smith  
Mountains, *Holarctic Ecology*, 12(3), 304-311, 1989.
- Hinzman, L. D., D. L. Kane, and R. E. Gieck, Regional  
snow ablation in the Alaskan Arctic, In: Northern

Hydrology, Selected Perspectives, NHRI Symposium No. 6, pp. 121-140, edited by T. D. Prowse, and C. S. L. Ommanney, National Hydrology Research Institute, Saskatoon, Saskatchewan, 1991a.

Hinzman, L.D., D. L. Kane, R. E. Gieck, and K. R. Everett, Hydrologic and thermal properties of the active layer in the Alaskan arctic, *Cold Regions Science and Technology*, 19, pp. 95-110, 1991b.

Hinzman, L. D., and D. L. Kane, Snow hydrology of a headwater arctic basin: 2. Conceptual analysis and computer modeling, *Water Resources Research*, 27(6), 1111-1121, 1991.

Hinzman, L.D. and D. L. Kane, Potential response of an arctic watershed during a period of global warming, *J. of Geophysical Research*, 97(D3), 2811-2820, 1992.

Hinzman, L. D., G. Wendler, R. E. Gieck, and D. L. Kane, Snowmelt at a small Alaskan arctic watershed: 1. Energy related processes, In: Proc. of the 9th International Northern Research Basins Symposium/Workshop, Canada, 1992, edited by T. D.

Prowse, C. S. L. Ommanney and K. Ulmer, *NHRI Symposium*, No. 10, Vol. 1, pp. 171-226, 1993.

Hinzman, L. D., D. L. Kane, C. S. Benson, and K. R. Everett, Energy balance and hydrological processes in an Arctic watershed, In: *Landscape Function and Disturbance in Arctic Tundra*, edited by J. F. Reynolds and J. D. Tenhunen, *Ecological Studies*, Vol. 120, pp. 131-154, Springer-Verlag Berlin Heidelberg, 1996.

Hinzman, L. D., D. J. Goering, and D. L. Kane, A Distributed thermal model for calculating temperature profiles and depth of thaw in permafrost regions, *Journal of Geophysical Research - Atmospheres*, in review, 1998.

Hirschi, M. C., and B. J. Barfield, Kyermo--A physically based research erosion model, 1. Model development, *Trans. ASAE*, 31(3), 804-813, 1988a.

Hirschi, M. C., and B. J. Barfield, Kyermo--A physically based research erosion model, 2. Model sensitivity analysis and testing, *Trans. ASAE*, 31(3), 814-820, 1988b.

- Holtan, H. N., G. F. Stiltner, W. H. Henson, and N. C. Lopez, USDA-74 revised model of watershed hydrology, U.S. Dept. of Agriculture, Washington, D. C., Agriculture Research Service, *Technical Bulletin No. 1518*, 1975.
- Huggins, L. F., and E. J. Monke, The mathematical simulation of the hydrology of the small watersheds, *Water Resources Research*, 4(3), 529-539, 1968.
- Huggins, L. F., and E. J. Monke, Mathematical simulation of the hydrologic events of ungaged watersheds, Purdue University, West Lafayette, Ind., Water Resources Research Center, *Technical Report 14*, 1970.
- Huggins, L. F., T. H. Podmore, and C. F. Hood, Hydrologic simulation using distributed parameters, *Technical Report no. 82*, Water Resources Research Center, Purdue University, West Lafayette, Ind., 1975.
- Hydrologic Engineering Center, HEC-1, *Flood Hydrograph Package—Users Manual*, U.S. Army Corps of Engineers, Davis, Calif., 1981.

- Hydrologic Engineering Center, Hydrologic analysis of ungaged watersheds using HEC-1, *Training Document no. 15*, U.S. Army Corps of Engineers, Davis, Calif., 1982.
- IPCC (International Panel on Climate Change), *Climate change 1992, The Supplement Report to the IPCC Scientific Assessment*, Cambridge University Press, Cambridge, 1992.
- Iorgulescu, I., and J. P. Jordan, Validation of TOPMODEL on a small Swiss catchment, *J. Hydrol.*, 159, 255-273, 1994.
- Jackson, T. H., D. G. Tarboton, and K. R. Cooley, A spatially-distributed hydrologic model for a small arid mountain watershed, Utah Water Research Laboratory, Working Paper WP-96-HWR-DGT/002, May 1996.
- James, L.D., D. S. Bowles, and R. H. Hawkins, A taxonomy for evaluating surface water quantity model reliability, in *Applied Modeling in Catchment Hydrology*, edited by V. P. Singh, pp. 189-229, Water Resources Publication, Fort Collins, Colorado, 1982.

- James, W. P., and K. W. Kim, A distributed dynamic watershed model, *Water Resources Bulletin*, 26(4), 587-596, 1990.
- Jasieniuk, M. A., and E. A. Johnson, Peatland vegetation organization and dynamics in the western subarctic, Northwest Territories, Canada, *Canadian J. Bot.* 60, 2581-2593, 1982.
- Johansen, R. C., J. C. Imhoff, and H. H. Davis, Users manual for hydrological simulation program-FORTRAN (HSPF), *EPA-600/9-80-015*, Environmental Research Lab., U.S. EPA, Athens, Georgia, 1980.
- Johansen, R. C., J. C. Imhoff, J. L. Kittle, and A. S. Donigian, Jr., Hydrological simulation program--FORTRAN (HSPF): users manual for release 8.0 *EPA-6-13-84-066*, Environmental Research Lab., U.S. EPA, Athens, Georgia, 1984.
- Jonch-Clausen, T., SHE, Système Hydrologique Européen, a short description, Danish Hydraulic Institute, 1979.
- Jones, N. L., S. G. Wright, and D. R. Maidment, Watershed delineation with triangle-based terrain

models, *J. of Hydraulic Engineering*, ASCE, 116(10), 1232-1251, 1990.

Jorgenson, T., The response of vegetation to landscape evolution on glacial till near Toolik Lake, Alaska, In: Proc. Int. Symp., *Inventorizing Forest and Other Vegetation of the High Latitude and High Altitude Regions*, Soc. Am. Forest Regional Tech. Conf., Fairbanks, Alaska, pp. 134-141, 1984.

Sand, K. and D. L. Kane, Effect of seasonal frozen ground in snowmelt modeling, In: Proc. of the Symposium: *Cold Regions Hydrology*, edited by Douglas L. Kane, pp. 321-327, Fairbanks, Alaska, July, 1986.

Kane, D. L., L. D. Hinzman, C. S. Benson, and K. R. Everett, Hydrology of Imnavait Creek, an arctic watershed, *Holarctic Ecology*, 12, 262-269, Copenhagen, 1989.

Kane, D. L., R. E. Gieck, and L. D. Hinzman, Evapotranspiration from a small Alaskan arctic watershed, *Nordic Hydrology*, 21, 253-272, 1990.



- Kane, D. L., L. D. Hinzman, C. S. Benson, and G. E. Liston, Snow hydrology of a headwater arctic basin: 1. Physical measurements and process studies, *Water Resources Research*, 27(6), 1099-1109, 1991a.
- Kane, D. L., L. D. Hinzman, and J. P. Zarling, Thermal response of the active layer to climatic warming in a permafrost environment, *Cold Regions Science and Technology*, 19, 111-122, 1991b.
- Kane, D. L., and L. D. Hinzman, Use of spatially distributed data to model arctic hydrologic processes, In: Proc. of Sixth International Conference on Permafrost, Beijing, China, pp. 326-331, 1993.
- Kane, D.L., R. E. Gieck, G. Wendler, and L. D. Hinzman, Snowmelt at a small Alaskan arctic watershed: 2. Energy related modeling results, In: Proc. of the 9th International Northern Research Basins Symposium/Workshop, Canada, 1992, edited by T. D. Prowse, C. S. L. Ommanney and K. Ulmer, *NHRI Symposium No. 10*, Vol. 1, pp. 227-247, 1993.
- Kane, D. L., L. D. Hinzman, H. Yu, and D. J. Goering, The use of SAR satellite imagery to measure Arctic

layer moisture contents in Arctic Alaska, *Nordic Hydrology*, 27, 25-38, 1996.

Kane, D. L., R. E. Gieck, and L. D. Hinzman, Snowmelt modeling at small Alaskan Arctic watershed, *J. of Hydrol. Engr.*, ASCE, 2(4), 204-210, 1997.

Keckler, D., SURFER for Windows, Version 6, User's Guide, Golden Software, Inc., July 1995.

Kent, K. M., Hydraulic predictions of downstream floods, *Transactions of the American Society of Agricultural Engineers* 9, 347-351, 1966.

Kite, G. W., Development of a hydrologic model for a Canadian watershed, *Can. J. Civ. Eng.*, 5, 126-134, 1978.

Kite, G. W., Hydrologic modelling with remotely sensed data, In: *Proceedings of the 57<sup>th</sup> Annual Western Snow Conference*, pp. 1-8, Ft. Collins, Col., April 18-20, 1989.

Kite, G. W. and N. Kouwen, Watershed modeling using land classifications, *Water Resources Research*, 28(12), 3193-3200, 1992.

- Kite, G. W., A. Dalton, and K. Dion, Simulation of streamflow in a macroscale watershed using general circulation model data, *Water Resources Research*, 30(5), 1547-1559, 1994.
- Kreig, R. A., and R. D. Reger, Air-photo analysis and summary of landform and soil properties along the route of the trans-Alaska pipeline system, *Geol. Rep. 66*, Division of Geological and Geophysical Surveys, State of Alaska, 1982.
- Kreit, K., B. J. Peterson, and T. L. Corliss, Water and sediment export of the upper Kuparuk River drainage of the North Slope of Alaska, *Hydrobiologica*, 240, 71-81, 1992.
- Laramie, R. L., and J. C. Schaake, Jr., Simulation of the continuous snowmelt process, *Rep. 143*, Ralph M. Parsons Lab., Mass. Inst. of Tech., Cambridge, 1972.
- Lee, D. T., and B. J. Schactor, Two algorithms for constructing a Delauney triangulation, *Int. J. Comput. and Information Sci.*, 9(3), 219-242, 1980.

Laurenson, E. M., and R. G. Mein, RORB-version 3: Runoff routing program-user manual, 2<sup>nd</sup> ed., Dept. of Civil Engineering, Monash University, Monash, Australia, 1983.

Leadley, P. W., and J. F. Reynolds, Long-term response of an arctic sedge to climate change: a simulation study, *Ecol. Appl.*, 2, 323-340, 1992.

Lilly, E. K., D. L. Kane, L. D. Hinzman, and R. E. Gieck, Annual water balance for three nested watersheds on the North Slope of Alaska, In: Proc. 7th International Permafrost Conference, Yellowknife, NWT, Canada, in press, 1998.

Liou, E. Y., OPSET: Program for computerized selection of watershed parameter values for the Stanford watershed model, *Research Report No. 34*, Water Resources Institute, University of Kentucky, Lexington, Kentucky, 1970.

Llamas, J., A. P. Plamondon, and S. M. U. Ahmed, Adaptation of the Stanford watershed model to Canadian conditions, *Proceedings of International Conference on Water Development*, pp. 419-437, Taipei, Taiwan, 1980.

- Maddaus, W. O., and P. S. Eagleson, A distributed linear representation of surface runoff, Mass. Inst. of Tech., Cambridge, Dept. of Civil Engineering Hydrodynamics Lab., Report No. 115, 1969.
- Manabe, S., and R. J. Stouffer, Sensitivity of a global climate model in the atmosphere, *J. Geophysical Research*, 85, 5529-5554, 1980.
- Marsh, P., and M. K. Woo, Annual water balance of small high arctic basins, In: *Canadian Hydrology Symposium: 79*, Proceedings, National Research Council of Canada, Vancouver, British Columbia, Associate Committee on Hydrology, pp. 536-546, Ottawa, Ontario, 1979.
- Martinec, J., and A. Rango, Merits of statistical criteria for the performance of hydrologic models, *Water Resources Bulletin*, 25(2), 412-432, 1989.
- Mein, R. G., E. M. Laurenson, and T. A. McMahon, Simple nonlinear model for flood estimation, *Journal of the Hydraulics Division*, ASCE, 100(11), 1507-1518, 1974.

McNamara, J. P., A nested watershed study in the Kuparuk River basin, arctic Alaska: Streamflow, scaling, and drainage basin structure, Ph.D. dissertation, University of Alaska Fairbanks, 1997.

Metcalf & Eddy, Inc., University of Florida, Gainesville, and Water Resources Engineers, Inc., Storm water management model, for environmental protection agency, EPA Rep., 4 Volumes, Nos. 11024DOC07/71, 11024DOC08/71, 11024DOC09/71, and 11024DOC10/71, 1971.

Miller, P. C., W. D. Billings, and W. C. Oechel, A modeling approach to understanding plant adaptation to low temperatures, In: *Comparative mechanism of cold adaptation*, edited by L. S. Underwood, L. L. Tieszen, A. B. Callahan, and G. E. Folk, pp. 181-214, Academic Press, New York, 1979.

Miller, P. C., P. M. Miller, M. Blake-Johnson, F. S. III Chapin, K. R. Everett, D. W. Hilbert, J. Kummerow, A. E. Linkins, G. M. Marion, W. C. Oechel, S. W. Roberts, and L. Stuart, Plant-soil processes in *Eriophorum vaginatum* tussock tundra in Alaska: a

- systems modeling approach, *Ecol. Monogr.*, 54, 361-405, 1984.
- Monteith, J. L., Principles of environmental physics, American Elsevier, New York, 1973.
- Moore, I. D., E. M. O'Loughlin, and G. J. Burch, A contour-based topographic model for hydrological and ecological applications, *Earth Surf. Processes Landforms*, 13, 305-320, 1988.
- Moore, I. D., and R. B. Grayson, Terrain-based prediction of runoff with vector elevation data, *Water Resources Research*, 27(6), 1177-1191, 1991.
- Morris, E. M., Forecasting flood flows in grassy and forested basins using a deterministic distributed mathematical model, *International Association of Scientific Hydrology Publication* 129, pp. 247-255, 1980.
- Morris, E. M., and R. T. Clarke, Watershed and river channel characteristics and their use in a mathematical model to predict flood hydrographs, In: *Remote Sensing Applications in Agriculture and*

*Hydrology*, edited by G. Fraysee. Rotterdam, The Netherlands: Balkema Publishers, 1980.

Nash, J. E., The form of the instantaneous unit hydrograph, *IASH Pub.* 45(3), 114-121, 1957.

Oechel, W. C., S. J. Hastings, G. Vourlitis, M. Jenkins, G. Richers, and N. Grulke, Recent changes of arctic tundra ecosystems from a net carbon dioxide sink to a source, *Nature*, 361, 520-532, 1993.

Ohmura, A., Evaporation from the surface of the Arctic tundra on Axel Heiberg Island, *Water Resources Research*, 18(2), 291-305, 1982.

Ostendorf, B., and J. F. Reynolds, Relationships between a terrain-based hydrologic model and patch-scale vegetation patterns in an arctic tundra landscape, *Landscape Ecol.* 8, pp. 229-237, 1993.

Ostendorf, B., P. Quinn, K. Beven, and J. D. Tenhunen, Hydrological controls on ecosystem gas exchange in an arctic landscape, In: *Ecological Studies*, Vol. 120, Landscape Function and Disturbance in Arctic Tundra, 370 pp., edited by J. F. Reynolds, and J.



D. Tenhunen, Springer-Verlag Berlin Heidelberg,  
1996.

Osterkamp, T. E., and M. W. Payne, Estimates of  
permafrost thickness from well logs in northern  
Alaska, *Cold Reg. Sci. and Technol.*, 5(1), 13-27,  
1981.

Osterkamp, T. E., J. K. Peterson, and T. S. Collet,  
Permafrost thickness in the Oliktok Point, Prudhoe  
Bay and Mikkelson Bay area of Alaska, *Cold Regions  
Sci. Tech.*, 11, 99-105, 1985.

Oswood, M. W., J. G. Irons III, and D. M. Schell,  
Dynamics of dissolved and particulate carbon in an  
arctic stream, In: *Ecological Studies*, Vol. 120,  
Landscape Function and Disturbance in Arctic  
Tundra, edited by J. F. Reynolds and J. D.  
Tenhunen, pp. 275-289, 1996.

Outcalt, S. I., C. Goodwin, G. Weller, and J. Brown,  
Computer simulation of the snowmelt and soil  
thermal regime at Barrow, Alaska, *Water Resources  
Research*, 11(5), 709-715, 1975.

- Palacios, O., and B. Cuevas, Automated river course, ridge and basin delineation from digital elevation data, *J. Hydrol.*, 86, 299-314, 1986.
- Paniconi, C., and E. F. Wood, A detailed model for simulation of catchment scale subsurface hydrologic processes, *Water Resources Research*, 29(6), 1601-1620, 1993.
- Peck, E. L., Catchment modeling and initial parameter estimation for the National Weather Service river forecast system, U.S. Dept. of Commerce, National Weather Service, Silver Springs, Maryland, NOAA Technical Memo NWS HYDRO-31, 1976.
- Peterson, K. M., and W. D. Billings, Tundra vegetational patterns and succession in relation to microtopography near Atkasook, Alaska, *Arctic and Alpine Res.* 16, 331-335, 1980.
- Petrie, G., and T. J. M. Kennie, Terrain modeling in surveying and civil engineering, *Comput. Aided Design*, 19(4), 171-187, 1987.

- Price, A. G., and T. Dunne, Energy balance computations of snowmelt in a subarctic area, *Water Resources Research*, 12(4), 686-694, 1976.
- Priestley, C. H. B., and R. J. Taylor, On the assessment of surface heat flux and evaporation using large-scale parameters, *Monthly Weather Review*, 100, 81-92, 1972.
- Quinn, P., K. Beven, P. Chevallier, and O. Planchon, The prediction of hillslope flow paths for distributed hydrological modeling using digital terrain model, *International Journal of Hydrol. Processes* 5, 59-79, 1991.
- Refsgaard, J. C., The surface component of an integrated hydrological model, Technical University of Denmark, Lyngby, Denmark, *Susa Hydrology Report* 12, 1981.
- Refsgaard, J. C., and O. Stang, An integrated groundwater/surface water hydrological model, Technical University of Denmark, Lyngby, Denmark, *Susa Hydrology Report* 13, 1981.

- Refsgaard, J. C., and E. Hansen, A distributed groundwater/surface water model for the Susa-catchment, Part I-model description, Part II-simulations of streamflow depletions due to groundwater abstraction, *Nordic Hydrology* 13, 299-322, 1982.
- Refsgaard, J. C., and B. Storm, MIKE SHE, in *Computer Models in Watershed Hydrology*, edited by V. J. Singh, pp. 809-846, *Water Resources Publications*, 1995.
- Refsgaard, J. C., and B. Storm, Construction, calibration and validation of hydrological models, in *Distributed Hydrological Modeling*, edited by M. B. Abbott and J. C. Refsgaard, *Water Science and Technology Library* 22, pp. 41-54, 1996.
- Renard, K. G., W. J. Rawls, and M. M. Fogel, Currently available models, Chapter 13 in *Hydrologic Modeling of Small Watersheds*, ASAE No. 5, pp. 507-522, edited by C.T. Haan, H. P. Johnson, and D. L. Brakensiek, *American Society of Agricultural Engineers*, ST. Joseph, Michigan, 1982.

Reynolds, J. F., J. D. Tenhunen, P. W. Leadley, H. Li, D. L. Moorhead, B. Ostendorf, and F. S. Chapin III, Patch and landscape models of arctic tundra: Potentials and limitations, In: *Ecological Studies*, Vol. 120, Landscape Function and Disturbance in Arctic Tundra, edited by J. F. Reynolds and J. D. Tenhunen, pp. 293-324, Springer-Verlag Berlin Heidelberg, 1996.

Ricca, V. T., The Ohio State University version of the Stanford streamflow simulation model, part I- technical aspects, Ohio State University, Columbus, OH, 1972.

Rogers, C. C. M., K. J. Beven, E. M. Morris, and M. G. Anderson, Sensitivity analysis, calibration and predictive uncertainty of the Institute of Hydrology distributed model, *Journal of Hydrology*, 81, 179-191, 1985.

Roots, E. F., Climate change: high-latitude regions, *Climate Change*, 15, 223-253, 1989.

Rouse, W. R., and R. B. Stewart, A simple model for determining the evaporation from high latitude

upland sites, *J. of Applied Meteorology*, 11, 1063-1070, 1972.

Rouse, W. R., P. F. Mills, and R. B. Stewart,  
Evaporation in high latitudes, *Water Resources Research*, 13(6), 909-914, 1977.

Rovansek, R. J., L. D. Hinzman, and D. L. Kane,  
Hydrology of a tundra wetland complex on the  
Alaskan Arctic Coastal Plain, *Arctic and Alpine Research*, 28(3), 1996.

Running, S. W., Computer simulation of regional  
evapotranspiration by integrating landscape  
biophysical attributes with satellite data, In:  
*Land Surface Evaporation Measurement and  
Parameterization*, pp. 359-370, Springer-Verlag, New  
York, 1991.

Schlesinger, M. E., and J. F. B. Mitchell, Model  
projections of the equilibrium climatic response to  
climate effects of increasing carbon dioxide, U. S.  
Dept. of Energy, Wash. D. C., *Report DOE/ER 0237*,  
pp. 81-147, 1985.

- Shaver, G. R., and F. S. III Chapin, Effect of fertilizer on production and biomass of tussock tundra, Alaska, USA, *Arctic and Alpine Res.*, 18, 261-268, 1986.
- Shaver, G. R., F. S. III Chapin, and B. L. Gartner, Factors limiting seasonal growth and peak biomass accumulation in *Eriophorum vaginatum* in Alaska tussock tundra, *J. Ecol.*, 74, 257-278, 1986.
- Shaver, G. R., K. H. Nadelhoffer, and A. E. Giblin, Biogeochemical diversity and element transport in a heterogeneous landscape, the north slope of Alaska, In: *Quantitative methods in landscape ecology*, edited by M. G. Turner, and R. H. Gardner, *Ecological Studies* 82, pp. 105-125, Springer, Berlin Heidelberg, New York, 1990.
- Shaw, E. M., *Hydrology in Practice*, Third edition, Chapman & Hall, 1994.
- Singh, V. P., A geomorphic approach to hydrograph synthesis with potential for application to ungaged watersheds, Louisiana State University, Louisiana

Water Resources Research Institute, Baton Rouge, La., *Technical Completion Report*, 1983.

Singh, V. P., A quasi-linear conceptual model for synthesis of direct runoff, with potential for application to ungaged basins, U.S. Army Corps of Engineer Waterways Experiment Station, Environmental Lab., Vicksburg, Miss., *Military Hydrology Report*, 1987.

Singh, V. P., *Hydrologic systems*, Volume II, Watershed modeling, Prentice-Hall, Inc., Englewood Cliffs, New Jersey, 1989.

Singh, V. P., Watershed modeling, in *Computer Models of Watershed Hydrology*, edited by V. P. Singh, pp. 1-22, *Water Resources Publication*, Highlands Ranch, Colorado, 1995.

Smith, R. L., and A. M. Lumb, Derivation of basin hydrographs, Kansas State University, Kansas Water Resources Research Institute, Manhattan, Kansas, *Contribution No. 19*, 1966.



- Soil Conservation Service, Computer program for project formulation hydrology, U.S. Dept. of Agriculture, Washington, D.C., *Technical Release no. 20*, 1973.
- Stang, O., A regional groundwater model for the Susa area, Technical University of Denmark, Lyngby, Denmark, *Susa Hydrology Report 9*, 1981.
- Stewart, R. B., and W. R. Rouse, Simple models for calculating evaporation from dry and wet tundra surfaces, *Arctic and Alpine Research*, 8(3), 263-274, 1976.
- Storm, B. and K. H. Jensen, Experience with field testings of SHE on research catchments, *Nordic Hydrology* 15, 283-294, 1984.
- Tenhunen, J. D., O. L. Lange, S. Hahn, R. Siegwolf, and S. F. Oberbauer, The ecosystem role of poikilohydric tundra plants, In: *Arctic ecosystems in a changing climate: an ecophysiological perspective*, edited by F. S. III Chapin, R. L. Jefferies, J. F. Reynolds, G. R. Shaver, and J. Svoboda, pp. 213-238, Academic Press, San Diego, 1992.

- Tenhunen, J. D., R. Siegwolf, and S. F. Oberbauer,  
Effects of phenology, physiology, and gradients in  
community composition, structure, and microclimate  
on tundra ecosystem CO<sub>2</sub> exchange, In: *Ecophysiology  
of photosynthesis*, edited by E-D Shulze, and M.  
Caldwell, pp. 431-460, Springer, Berlin Heidelberg,  
New York, 1994.
- van Everdingen, R. O., The importance of permafrost in  
the hydrological regime, Chapter 9 in *Canadian  
Aquatic Resources*, edited by Healey, M.C. and R. R.  
Wallace, Canadian Bulletin of Fisheries and Aquatic  
Science No. 215, pp. 243-276, 1987.
- Waelbroeck, C., Climate-soil processes in the presence  
of permafrost: a system modelling approach,  
*Ecological Modelling*, 69: 185-225, 1993.
- Walker, M. D., D. A. Walker, and K. R. Everett, Wetland  
soils and vegetation, Arctic foothills, Alaska,  
*U.S. Department of the Interior Biological Report*,  
89(7), 1989a.
- Walker, D. A., E. Binnian, B. E. Evans, N. D. Lederer,  
E. Nordstrand, and P. J. Webber, Terrain,  
vegetation, and landscape evolution of the R4D

research site, Brooks Range Foothills, Alaska,  
*Holarct. Ecol.* 12, 238-261, 1989b.

Walker, D. A., and M. D. Walker, Terrain and vegetation of the Imnavait Creek watershed, In: *Ecological Studies*, 120, Landscape Function and Disturbance in Arctic Tundra, edited by J. F. Reynolds and J. D. Tenhunen, pp. 73-108, 1996.

Washburn, A. L., *Geocryology: a survey of periglacial processes and environments*, Halsted Press, Wiley, New York, 1980.

Webber, P. J., Spatial and temporal variation of the vegetation and its productivity, In: *Vegetation and production ecology of an Alaskan arctic tundra*, edited by Tieszen L. L., *Ecological Studies Series* 29, pp. 37-112, Springer, Berlin Heidelberg, New York, 1978.

Weller, G., and B. Holmgren, The microclimates of the arctic tundra, *J. Appl. Meteorol.* 13, 854-862, 1974.

Weller, G., F. S. Chapin, K. R. Everett, J. E. Hobbie, D. L. Kane, W. C. Oechel, C. L. Ping, W. S.

- Reeburgh, D. Walker, and J. Walsh, The Arctic flux study: a regional view of trace gas release, *J. of Biogeography*, 22, 365-374, 1995.
- Wigmosta, M. S., L. W. Vail, and D. P. Lettenmaier, A distributed hydrology-vegetation model for complex terrain, *Water Resources Research*, 30(6), 1665-1679, 1994.
- Williams, J. R., and R. W. Hann, Jr., HYMO, a problem-oriented computer language for building hydrologic models, *Water Resources Research*, 8(1), 79-86, 1972.
- Wolock, D. M., and C. V. Price, Effects of digital elevation model map scale and data resolution on a topography-based watershed model terrain, *Water Resources Research*, 30(11), 3041-3052, 1994.
- Woo, M. K., and J. Sauriol, Channel development in snow-filled valleys, Resolute, Northwest Territories, Canada, *Geografiska Annaler*, 62A(1-2), 37-56, 1980.
- Woo, M. K., Snow hydrology of the High Arctic, In: *Western Snow Conference*, Reno, Nevada, April 20-23, 1982.

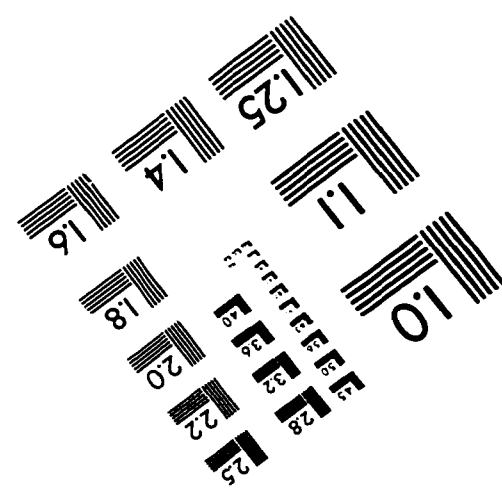
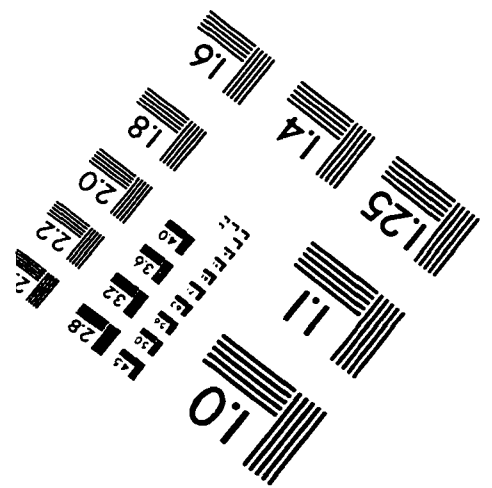
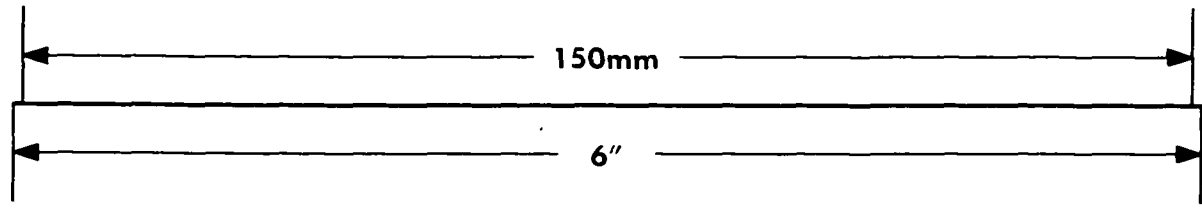
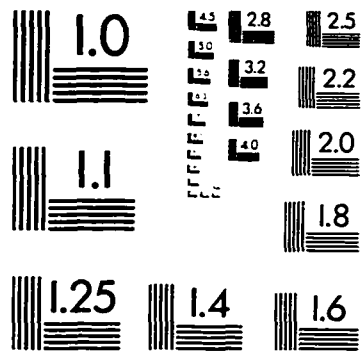
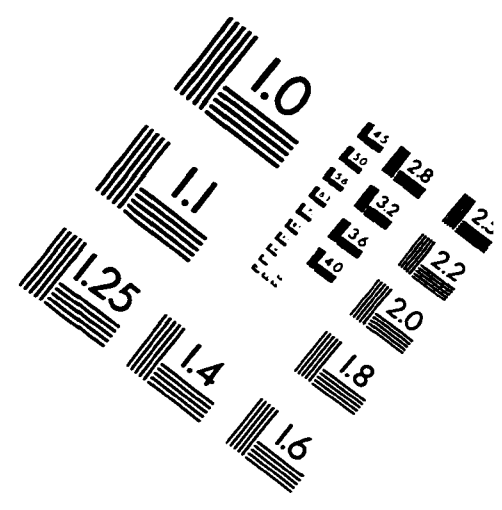
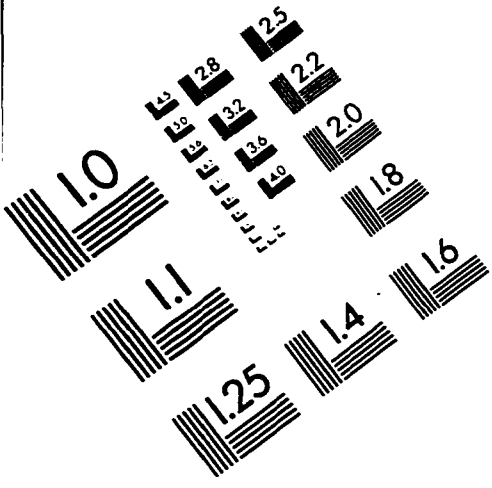
- Woo, M. K., Hydrology of a drainage basin in the Canadian High Arctic, *Ann. Assoc. Am. Geogr.*, 73(4), 577-596, 1983.
- Woo, M. K., Permafrost hydrology in North America, *Atmos. Ocean*, 24(3), 201-234, 1986.
- Woo, M. K., and R. Heron, Breakup of small rivers in the subarctic, *Can. J. Earth Sci.*, 24(4), 784-795, 1987.
- Woo, M. K., and J. J. Drake, A study to model the effects of uranium mine on a permafrost environment, Northern Affairs Program, Indian and Northern Affairs Canada, *Environmental Studies* No. 53, Ottawa, Ontario, 41 pp., March, 1988.
- Woo, M. K., Permafrost hydrology, In: Northern Hydrology: Canadian Perspectives, *NHRI Science Report* No. 1, edited by T. D. Prowse and C. S. L. Ommanney, 63 pp., 1990.
- Woolhiser, D. A., R. E. Smith, and D. C. Goodrich, KINEROS, A kinematic runoff and erosion model: Documentation and User Manual, ARS-77, Agric. Res.

Serv., U. S. Dep. of Agric., Washington, D. C.,  
1990.

Zarling, J. P., W. A. Braley, and C. Pelz, The modified  
Berggren method—a review, In: Proc. of Fifth  
International Conference on Cold Regions  
Engineering, ASCE, pp. 263-273, New York, 1989.

Zhao, R. J., Y. L. Zhang, L. R. Fang, X. R. Liu, and Q.  
S. Zhang, The Xinanjiang model, *International  
Association of Hydrological Sciences Publication*  
no. 129, Proc. of the Oxford Symp. on Hydrological  
Forecasting, pp. 351-356, 1980.

# IMAGE EVALUATION TEST TARGET (QA-3)



**APPLIED IMAGE . Inc**  
 1653 East Main Street  
 Rochester, NY 14609 USA  
 Phone: 716/482-0300  
 Fax: 716/288-5989

© 1993, Applied Image, Inc., All Rights Reserved